Report 021779-2-T

SIGNAL DETECTION AND PARAMETER IDENTIFICATION WITH APPLICATION TO UNDERWATER ACOUSTICS

Fuad Imran Khan

COMMUNICATIONS AND SIGNAL PROCESSING LABORATORY
Department of Electrical Engineering and Computer Science
The University of Michigan
Ann Arbor, Michigan 48109

February 1986

Technical Report No. 233
Approved for public release; distribution unlimited.

Prepared for
OFFICE OF NAVAL RESEARCH
Department of the Navy
Arlington, Virginia 22217

REPORT DOCUMENTATION PAGE

1a. REPORT SECURITY CLASSIFICATION Unclassified	1b. RESTRICTIVE MARKINGS None
2a. SECURITY CLASSIFICATION AUTHORITY	3. DISTRIBUTION/AVAILABILITY OF REPORT Approved for public release; distribution unlimited.
2b. DECLASSIFICATION/DOWNGRADING SCHEDULE	
4. PERFORMING ORGANIZATION REPORT NUMBER(S) 021779-2-T	5. MONITORING ORGANIZATION REPORT NUMBER(S)
6a. NAME OF PERFORMING ORGANIZATION Communications and Signal Processing Laboratory 6b. OFFICE SYMBOL (If applicable)	7a. NAME OF MONITORING ORGANIZATION Office of Naval Research Code 425UA
6c. ADDRESS (City, State, and ZIP Code) The University of Michigan Ann Arbor, Michigan 48109	7b. ADDRESS (City, State, and ZIP Code) 800 North Quincy Street Arlington, Virginia 22217
8a. NAME OF FUNDING/SPONSORING ORGANIZATION 8b. OFFICE SYMBOL (If applicable)	9. PROCUREMENT INSTRUMENT IDENTIFICATION NUMBER Contract No. N00014-84-K-0066
8c. ADDRESS (City, State, and ZIP Code)	10. SOURCE OF FUNDING NUMBERS PROGRAM ELEMENT NO. / PROJECT NO. / TASK NO. NR 386-941 / WORK UNIT ACCESSION NO.

11. TITLE (Include Security Classification)
SIGNAL DETECTION AND PARAMETER IDENTIFICATION WITH APPLICATION TO UNDERWATER ACOUSTICS

12. PERSONAL AUTHOR(S)
Khan, Fuad Imran

13a. TYPE OF REPORT	13b. TIME COVERED	14. DATE OF REPORT (Year, Month, Day)	15. PAGE COUNT
Technical Report	FROM 5/84 TO 2/86	February 1986	168

16. SUPPLEMENTARY NOTATION

17. COSATI CODES		
FIELD	GROUP	SUB-GROUP

18. SUBJECT TERMS (Continue on reverse if necessary and identify by block number)
Passive Detection
Multipath Acoustic Propagation
Underwater Acoustics

19. ABSTRACT (Continue on reverse if necessary and identify by block number)

A problem of passive detection of underwater moving acoustic sources is formulated. It is found that solving the exact problem, when a multipath acoustic propagation environment is assumed, is fairly difficult. Keeping the multipath assumption intact, we develop two abstract problems that are solvable and yet are sufficiently related to reality to allow us to form guidelines and rules of thumb for the passive detection problem. Multipath propagation from a moving acoustic source is characterized by doppler and delay parameters on each path. We assume that sound is received at two remote receivers. If there are M paths to one receiver and N paths to the other receiver, the normalized crosscorrelation of the receptions will exhibit M.N peaks.

We use the concept of Extended M-orthogonal signals to unify the information on the ambiguity plane and to find how many of the peaks on the ambiguity plane need to be localized for acceptable detector performance.

The M.N peaks are generated by M+N independent sets of doppler and delay parameters.

(over)

20. DISTRIBUTION/AVAILABILITY OF ABSTRACT ☐ UNCLASSIFIED/UNLIMITED ☒ SAME AS RPT. ☐ DTIC USERS	21. ABSTRACT SECURITY CLASSIFICATION Unclassified
22a. NAME OF RESPONSIBLE INDIVIDUAL Carol S. Van Aken	22b. TELEPHONE (Include Area Code) (313) 764-5220 22c. OFFICE SYMBOL

DD FORM 1473, 84 MAR 83 APR edition may be used until exhausted. All other editions are obsolete.

SECURITY CLASSIFICATION OF THIS PAGE
UNCLASSIFIED

19. Abstract (cont).

Periodic Random Sequences are used to address the question:
Should the detector treat the M.N peaks as independent entities or as being generated from M+N independent parameter sets? i.e. Should the detector have M.N degrees of freedom or M+N degrees of freedom?

ACKNOWLEDGEMENTS

I would like to thank the members of my dissertation committee, Profs. Neuhoff, Perakis, Root and Stark. Their suggestions and guidance made this a better thesis. In particular I would like to thank Prof. Birdsall, who over the years has been both a teacher and a friend. Without his guidance, insight and inspiration my graduate studies would have been incomplete.

I would like to thank the staff of Cooley Electronics Lab. for their support, in particular I would like to mention Dr. Kurt Metzger for several useful discussions and for help with the word processor. Ms. Linda Russell for her help with FORM and the word processor. Mr. John Campbell for his help with programming. Ms. Carol Van Aken for her administrative assistance. Mr. Wayne V. Wald for his assistance with the figures. I am grateful to my colleagues and friends Matt and Deb for their encouragement and help.

My friends Babar, J.B., Naveed, Alan and Firdous encouraged and inspired me to excel, I would like to thank them for this and much more. I would like to thank Feisal for his help with the figures. I would like to thank Aliya for her encouragement and humor. Last but not least I wish to thank my dear friend Farzana for her encouragement, support and understanding in both good times and bad.

Finally I would like to thank my parents and my sister for providing me with the opportunity of studying in the United States and for their constant support, encouragement and love.

The support of the Office of Naval Research (Code 425UA) is gratefully acknowledged.

TABLE OF CONTENTS

LIST OF TABLES

LIST OF FIGURES

LIST OF APPENDICES

LIST OF SYMBOLS AND ABBREVIATIONS

A_i	Power level of Periodic Random Sequence with period P_i
BNC	Bivariate Normalized Crosscorrelation
CAED	Circulating Average Energy Detector
C_n	Generic nxn circulant matrix
c_n	Normalized complex attenuation coefficient of the nth path
DFT	Discrete Fourier Transform
D_0	Decision in favor of the noise alone hypothesis
D_1	Decision in favor of the signal+noise hypothesis
d	Normal detectability
d'	Square root of the normal detectability
dB	Decibel
ED	Energy Detector
EMOS	Extended M-Orthogonal signals
E(.)	Expected value
FSED	Frequency Selective Energy Detector
$f_x(.)$	Probability density function of random variable x
f(.|.)	Conditional Probability density function
H_0	Noise alone hypothesis
H_1	Signal+Noise hypothesis
I_L	LxL identity matrix
i.i.d.	independent and identically distributed
L	Number of samples in observation

L_i	Number of integer periods of PRS with period P_i in the observation
L.C.M.	Least Common Multiple
$\ell(.)$	Likelihood ratio
$\ell(.\|.)$	Conditional likelihood ratio
MOS	M-Orthogonal signals
$N(\mu,\sigma^2)$	Normal density with mean μ and variance σ^2
n(.)	Noise
$\underline{n}$	Noise vector
P_D	Probability of Detection
P_{FA}	Probability of False Alarm
PRS	Periodic Random Sequence
p.d.f.	probability density function
$p_i(.)$	PRS with period P_i
$\tilde{p}_i(.)$	One period of PRS $p_i(.)$
R	Autocorrelation matrix
R(.)	Autocorrelation function
R.O.C.	Receiver Operating Characteristic
r.v.	random variable
s(.)	Signal
$\underline{s}$	Signal vector
$\hat{\underline{s}}$	Estimate of $\underline{s}$
U_n	Unitary matrix of the eigenvectors of a nxn circulant matrix
U(0,1)	Uniform density over [0,1)
Y(.)	DFT of the sequence y(.)

$\underline{Y}$	Vector of the sequence Y(.)
$y(.)$	Observation
$\underline{y}$	Observation vector
$z(.)$	Log-likelihood ratio
$z(.\|.)$	Conditional log-likelihood ratio
$\tilde{z}(.)$	Quasi log-likelihood ratio
β	Differential doppler correction parameter
$\delta(.)$	Delta function
$\Phi(.)$	Normal distribution function
$\phi_x(.)$	Characteristic function of random variable x
$\Gamma(.)$	Gamma function
$\Gamma(.,.)$	Incomplete gamma function
$\gamma(.,.)$	Incomplete gamma function
$\gamma_T(.,.)$	Bivariate Normalized Crosscorrelation function with an observation interval of T seconds
$\gamma(.,.)$	Bivariate Normalized Crosscorrelation function with an infinite observation interval
$\tilde{\gamma}$	Observation pattern in the discrete ambiguity plane
$\underline{\chi}$	Vector associated with the observation pattern in the discrete ambiguity plane
σ_x^2	Variance of random variable x
τ	Differential time delay correction parameter
$\tau_n(t)$	Time delay on the nth path at time t
τ_n	Time delay on the nth path at time 0
τ_n'	Time delay derivative of the nth path
Ψ_n	Diagonal matrix of the eigenvalues of an

	n×n circulant matrix
$\psi_T(.,.)$	Ambiguity function with an observation interval of T seconds
$\psi(.,.)$	Ambiguity function with an infinite observation interval

CHAPTER I

INTRODUCTION

Passive Sonar Detection and the associated problems of doppler and time delay estimation are problems of continuing research interest in the underwater acoustics community [1,2,3,4]. While passive systems have the disadvantage that they can not control signal energy, their anonymity and overall cost dictate their feasibility especially in surveillance systems [2].

A passive sonar system utilizes an array of two or more receivers (hydrophones). Two receivers are sufficient to estimate the bearing angle of the source in the plane of the receivers [2]. However if more information is required about the source, such as localization in three dimensions and estimation of source velocity, more receivers are required. The accuracy of the estimates is a function of the receiver geometry in three dimensions as well as measurement accuracy. Throughout this thesis we will assume that we have two receivers. This is a common assumption made by several authors [1,2,5]. It is not too difficult to extend the analysis to more than two receivers if the receivers are considered in pairs.

We assume a multipath channel for sound propagation to each of the receivers. This is in contrast to the assumption usually made; i.e. there is only one path to each receiver [2,6]. Associated with each path in the channel is a complex attenuation (or gain) coefficient, a doppler parameter due to source motion and time delay in propagation from the source to the receiver. The details of the multipath channel are given in Chapter III. The

implications of the multipath channel assumption will become clear as we proceed.

We will use the Bivariate Normalized Crosscorrelation (BNC) function as the observable for our detector. Bivariate refers to the presence of two search variables. We define the BNC function, denoted by $\gamma_T(\beta,\tau)$, as follows

$$\gamma_T(\beta,\tau) \triangleq \frac{\frac{1}{T}\int_T y_1(\beta t)y_2^*(t-\tau)dt}{(\frac{1}{T}\int_T |y_1(t)|^2 dt)^{1/2}.(\frac{1}{T}\int_T |y_2(t)|^2 dt)^{1/2}} \quad (1.1)$$

where $y_1(t)$ and $y_2(t)$ denote the receptions at the two receivers, $\int_T$ signifies an integral over an interval of length T. We will be interested in the intervals [0,T) and [-T/2,T/2). In general $\gamma_T(\beta,\tau)$ is complex. A simple application of the Schwarz inequality shows that $|\gamma_T(\beta,\tau)| \leq 1$. We will also need to consider the ambiguity function $\psi_T(\beta,\tau)$ defined as

$$\psi_T(\beta,\tau) \triangleq |\gamma_T(\beta,\tau)|^2 \quad (1.2)$$

The properties of the BNC function and the ambigutiy function are extensively documented in the literature [7]. We will also have occasion to consider the BNC and the ambiguity functions in the limit $T \to \infty$. We define

$$\gamma(\beta,\tau) = \lim_{T\to\infty} \gamma_T(\beta,\tau) \quad (1.3a)$$

$$\psi(\beta,\tau) = \lim_{T\to\infty} \psi_T(\beta,\tau) \quad (1.3b)$$

The search variables β, τ seek to match differential doppler and differential delay between paths to the two receivers. Two input correlators, univariate and multvariate, have been used extensively in the detection

theory literature to form the observation statistic [1,8,9].

A detector that is based on the assumption that there is a single path to each receiver seeks to identify a single maximum in the ambiguity diagram. The maximum is related to the mean differential delay and the mean differential doppler. For detection purposes the height of the maxmimum is compared to a pre-selected threshold. Detection is indicated if the height of the maximum is greater than the threshold. However a detector that is based on a multipath channel model seeks to identify all the resolvable path pairs. So, if there are M paths to one receiver and N paths to the other receiver and all the path pairs are resolvable, the detector based on the multipath channel model will identify MN peaks (local maxima) in the ambiguity plane. To resolve the peaks (path pairs), we need integration times that are long [10,11,12]. More is said about integration times in Chapter III.

From the above it follows that if the sound propagation is by a multipath channel, then a detector based on the multipath channel model has more apriori information available to it as compared to a detector based on the single path channel model. When sound propagation is by a multipath channel, we expect the performance of the "multipath channel detector" to be superior to the performance of the "single path channel detector." In making a decision an optimum detector utilizes all the information available about the signal (or source) in the observation. The primary goal of this thesis is not to find exact analytical solutions but to establish guidelines and rules of thumb about how best to unify the information available in the ambiguity plane as a detection statistic.

Outline of the Thesis

Chapter II is a brief review of fixed time detection theory, it is included for completeness and for establishing

notation and convention.

Chapter III starts off with a description of the multipath channel model. After that the problem is formulated and developed analytically. It is found that analytical solutions are non-trivial and perhaps not possible. This lays the foundation for the abstract problems considered in Chapters IV and V.

The object of formulating abstract problems is to study problems that are sufficiently related to reality and yet are solvable. The information gained from the study of the abstract problems is then utilized to form guidelines and rules of thumb for the exact problem.

In Chapter IV we study the first of two abstractions. Here we assume a discrete ambiguity plane and use the "Extended M-Orthogonal Signals" approach to

1) Unify the information in the ambiguity plane

2) Find how many peaks (path pairs) need to be matched for good or acceptable performance.

The MN peaks in the ambiguity diagram are generated by M+N independent sets of doppler and delay parameters. Chapter V uses the notion of "Periodic Random Sequences" to address the following questions

1) Should the detector treat the MN peaks as independent entities or as being generated from M+N independent parameter sets, i.e. should the detector have MN degrees of freedom or M+N degrees of freedom?

2) Does one approach offer a significant improvement in performance over the other?

In Chapter VI we summarize and highlight the findings of the study. Some suggestions for future work are also made.

Some liberty has been taken with the notations, however

the notations are consistent and the author hopes they are clear from the context.

CHAPTER II

REVIEW OF DETECTION THEORY

The purpose of this chapter is to review some of the results of detection theory that will be used in later chapters. This will also serve to establish notation and convention. Since most of the results presented here are well known [13,14,15,16,17] detailed derivations are not emphasized. For the most part, we will follow a Bayesian approach throughout the thesis. By this we mean that signal and noise parameters that are not known exactly can be modelled as random variables with known probability density functions (p.d.f.'s). The p.d.f.'s are chosen to reflect the observer's state of objective and subjective knowledge about the unknown parameters.

2.1 The Basic Detection Problem

A block diagram of the basic problem in fixed time detection theory is given in fig. 2.1. The observation y(t) belongs either to the noise alone hypothesis denoted H_0 or to the signal+noise hypothesis denoted H_1.

$$H_0 : y(t) = n(t) \tag{2.1a}$$

$$H_1 : y(t) = n(t) + s(t) \tag{2.1b}$$

$$0 \leq t < T$$

Where s(t) is a known signal or a random process. It is assumed that the hypothesis in effect does not change over

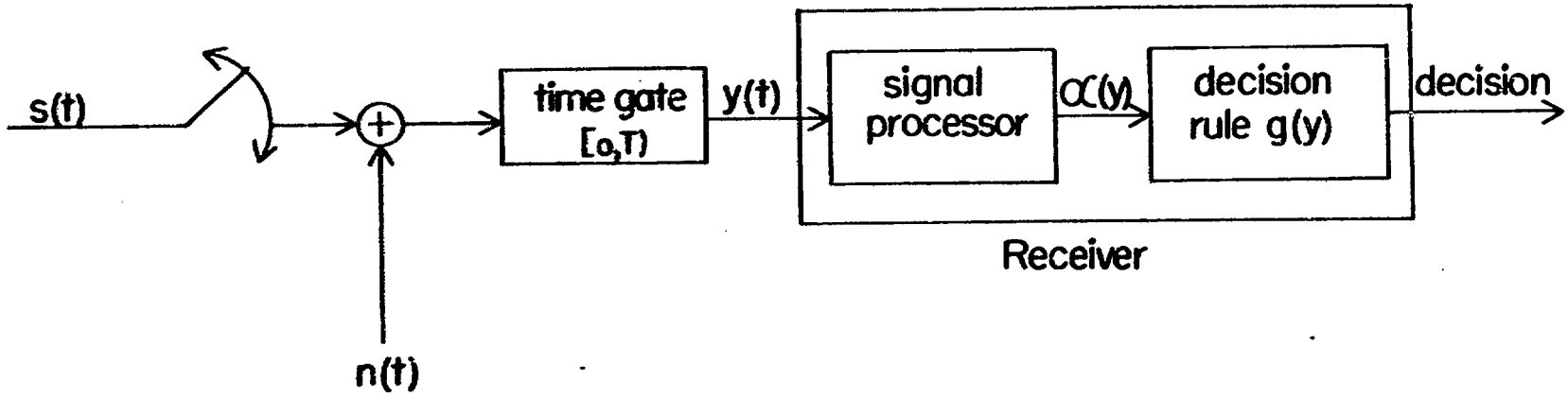

Fig. 2.1 Block diagram of the basic detection problem.

the observation interval. In other words the hypotheses H_0 and H_1 are mutually exclusive.

Often for analytical convenience random processes are expressed as random vectors. The elements of the random vector may be obtained using the Shannon sampling theorem [16, pp. 29-30] or by using a truncated form of some series expansion such as the Karhunen-Loeve expansion [16, pp. 54-74]. With vector notation the observation is written as

$$H_0 : \underline{y} = \underline{n} \tag{2.2a}$$

$$H_1 : \underline{y} = \underline{n} + \underline{s} \tag{2.2b}$$

where $\underline{y}$, $\underline{n}$ and $\underline{s}$ are column vectors with a fixed number of elements, say L. The observation under each hypothesis is then characterized by the joint p.d.f.'s $f_0(\underline{y})$ and $f_1(\underline{y})$ where

$$f_i(\underline{y}) \triangleq f(\underline{y}|H_i) = f(y_0, y_1, \ldots, y_{L-1}|H_i) \ , \ i=0,1 \tag{2.3}$$

and if given H_i the elements of $\underline{y}$ are independent and identically distributed (i.i.d.) we have

$$f_i(\underline{y}) = \prod_{k=0}^{L-1} f(y_k|H_i) \tag{2.4}$$

2.2 Optimum Receivers Detection Criteria and Decision Rules

Based on the observation and a detection criterion the processor computes a detection statistic $\alpha(\underline{y})$. The decision device makes a binary decision D_0 or D_1, according to a decision rule $g(y)$ and the value of $\alpha(\underline{y})$. D_0 implies a decision by the receiver that $\underline{y}$ is from H_0; D_1 implies a decision by the receiver that $\underline{y}$ is from H_1. There are four possible hypothesis-decision pairs

1) Decide D_0 when H_0 is true : Correct Rejection (CR)
2) Decide D_1 when H_0 is true : False Alarm (FA)
3) Decide D_0 when H_1 is true : Miss (M) (2.5)
4) Decide D_1 when H_1 is true : Detection (D)

The conditional probabilities associated with the hypothesis-decision pairs are

1) Probability of Correct Rejection $\triangleq P_{CR} = P(D_0|H_0)$
2) Probability of False Alarm $\triangleq P_{FA} = P(D_1|H_0)$
3) Probability of Miss $\triangleq P_M = P(D_0|H_1)$ (2.6)
4) Probability of Detection $\triangleq P_D = P(D_1|H_1)$

The design of the optimum receiver is based on the conditional probabilites associated with the hypothesis-decision pairs.

Commonly used detection criteria are the Bayes criterion, the Minimax criterion and the Neyman-Pearson criterion. Based on available knowledge all criteria seek to minimize the cost associated with making a decision. It has been shown by Birdsall [18] that for the above criteria and any other criteria that consider correct decisions "good" and incorrect decisions "bad" an optimum detection statistic is the likelihood ratio $\ell(\underline{y})$

$$\ell(\underline{y}) \triangleq f_1(\underline{y})/f_0(\underline{y}) \tag{2.7}$$

Upon making an observation the optimum receiver computes the likelihood ratio $\ell(\underline{y})$. The decision device then compares $\ell(\underline{y})$ with a pre-assigned threshold c ($0<c<\infty$) and decides D_1 if $\ell(\underline{y}) > c$ and D_0 if $\ell(\underline{y}) < c$. If $\ell(\underline{y}) = c$ then with probability β decision D_1 is made, this is called the randomized decision rule. The decision rule $g(\underline{y})$ can be summarized as follows

$$g(\underline{y}) \triangleq \text{Prob.}\{D_1|\underline{y}\} \tag{2.8}$$

$$= \begin{cases} 1 \text{ if } \ell(\underline{y}) > c \\ \beta \text{ if } \ell(\underline{y}) = c \\ 0 \text{ if } \ell(\underline{y}) < c \end{cases}$$

The operating values of c and β are chosen to satisfy the requirements of the detection criterion being used. If $\text{Prob.}\{\ell(\underline{y})=c\} = 0$ the value of β is of no significance. From now on we will not consider randomized decision rules and will assume $\beta = 1$. Any monotone increasing function of the likelihood ratio is an equivalent detection statistic. We will frequently use the log-likelihood ratio $z(\underline{y})$ defined below

$$z(\underline{y}) \triangleq \ln(\ell(\underline{y})) \tag{2.9}$$

2.3 Simple and Composite Signal Hypotheses

When both $f_1(\underline{y})$ and $f_0(\underline{y})$ are completely known the hypotheses, H_0 and H_1, are termed simple. In this case the optimum detection statistic $\ell(\underline{y})$ or $z(\underline{y})$ may readily be computed. However when the signal has some unknown parameters $\underline{\theta}$, the H_1 hypothesis is termed composite [15, p. 86]. If the noise has no unknown parameters the H_0 hypothesis remains simple. We will be interseted in the situation where the H_1 hypothesis is composite and the H_0 hypothesis is simple. When H_1 is composite it is assumed that the observer knows the conditional p.d.f. $f_1(\underline{y}|\underline{\theta})$. A Bayesian observer based on the state of his knowledge about $\underline{\theta}$, assigns $\underline{\theta}$ a prior p.d.f. $f(\underline{\theta})$. The marginal p.d.f. may now be computed

$$f_1(\underline{y}) = \int_{\underline{\theta}} f_1(\underline{y}|\underline{\theta}) f(\underline{\theta}) d\underline{\theta} \tag{2.10}$$

This reduces the composite signal hypothesis problem to a simple signal hypothesis problem. The optimum detection statistic $\ell(\underline{y})$ is now obtained as follows

$$\ell(\underline{y}) = \frac{f_1(\underline{y})}{f_0(\underline{y})} = \int_{\underline{\theta}} (f_1(\underline{y}|\underline{\theta})/f_0(\underline{y})).f(\underline{\theta})d\underline{\theta} \qquad (2.11)$$

$$= \int_{\underline{\theta}} \ell(\underline{y}|\underline{\theta})f(\underline{\theta})d\underline{\theta}$$

where

$$\ell(\underline{y}|\underline{\theta}) \triangleq f_1(\underline{y}|\underline{\theta})/f_0(\underline{y}) \qquad (2.12)$$

$\ell(\underline{y}|\underline{\theta})$ is the conditional likelihood ratio. $\ell(\underline{y})$ in this case is the average of the conditional likelihood ratios. Eq. 2.11 may be obtained in a different way, $f_1(\underline{y}|\underline{\theta})$ can be written as

$$f_1(\underline{y}|\underline{\theta}) = f_1(\underline{y})f(\underline{\theta}|\underline{y})/f(\underline{\theta}) \qquad (2.13)$$

Substituting eq. 2.13 in eq. 2.12 gives

$$\ell(\underline{y}|\underline{\theta}) = \frac{f_1(\underline{y})f(\underline{\theta}|\underline{y})}{f_0(\underline{y})f(\underline{\theta})} \qquad (2.14a)$$

or

$$\ell(\underline{y}|\underline{\theta})f(\underline{\theta}) = \ell(\underline{y})f(\underline{\theta}|\underline{y}) \qquad (2.14b)$$

Rewriting eq. 2.14b gives

$$\ell(\underline{y}) = \ell(\underline{y}|\underline{\theta})f(\underline{\theta})/f(\underline{\theta}|\underline{y}) \qquad (2.15)$$

Eq. 2.15 is the statement of the Bayes-Birdsall theorem. Integrating both sides of eq. 2.14b with respect to $\underline{\theta}$ gives

$$\ell(\underline{y}) = \int_{\underline{\theta}} \ell(\underline{y}|\underline{\theta}) f(\underline{\theta}) d\underline{\theta} \tag{2.16}$$

In certain situations, even for a Bayesian observer it might be unrealistic to assign a distribution to the unknown parameter vector $\underline{\theta}$. In such situations an approach that is often used is to fix some detector and then analyze the performance of the detector for various values of $\underline{\theta}$. The detector may or may not be based on the knowledge of the actual value of $\underline{\theta}$. In Chapter IV we will use this approach extensively.

2.4 Performance Evaluation

Given the decision rule $g(\underline{y})$, the probabilities of detection P_D and false alarm P_{FA} can be determined as follows

$$\begin{aligned} P_D &= E(g(\underline{y})|H_1) = \text{Prob.}\{\ell(\underline{y}) \geq c|H_1\} \\ &= \int_{\ell(\underline{y})\geq c} g(\underline{y}) f_1(\underline{y}) d\underline{y} \\ &= \int_{\ell(\underline{y})\geq c} f_1(\underline{y}) d\underline{y} \\ &= \int_c^\infty f(\ell|H_1) d\ell \end{aligned} \tag{2.17}$$

and

$$\begin{aligned} P_{FA} &= E(g(\underline{y})|H_0) = \text{Prob.}\{\ell(\underline{y}) \geq c|H_0\} \\ &= \int_{\ell(\underline{y})\geq c} g(\underline{y}) f_0(\underline{y}) d\underline{y} \\ &= \int_{\ell(\underline{y})\geq c} f_0(\underline{y}) d\underline{y} \\ &= \int_c^\infty f(\ell|H_0) d\ell \end{aligned} \tag{2.18}$$

where $f(\ell|H_i)$ is the conditional p.d.f. of the likelihood ratio under hypothesis H_i. Since given a hypothesis the decisions D_0 and D_1 are mutually exclusive and collectively exhaustive, we have the following

$$P_D + P_M = 1 \tag{2.19a}$$

$$P_{FA} + P_{CR} = 1 \tag{2.19b}$$

It follows that P_D and P_{FA} are sufficient to characterize receiver performance. From eqs. 2.17 & 2.18 we see that P_D and P_{FA} are parameterized by the single parameter c. A plot of P_D vs. P_{FA} for all possible operating values of c is called the Receiver Operating Characteristic (R.O.C.) curve. The R.O.C. curves completely determine performance for all operating values of c. R.O.C. curves have been extensively studied by Birdsall [18].

2.5 Two Examples

We briefly consider two examples of detection. The first, known signal in Gaussian noise, introduces the important family of normal R.O.C. curves and also introduces the concept of normal detectabilty. The second, Gaussian signal in Gaussian noise, is important because it occurs frequently in the later chapters.

2.5.1 Known Scalar Signal in Gaussian Noise

The observation under H_0 and H_1 is

$$H_0 : y = n \sim N(0,\sigma^2) \tag{2.20a}$$

$$H_1 : y = n + s \text{ , } s \text{ a known constant} \tag{2.20b}$$

Both hypotheses are simple; the p.d.f. of y under H_0 and H_1 is

$$f(y|H_0) = (2\pi\sigma^2)^{-1/2}\exp(-y^2/(2\sigma^2)) \tag{2.21a}$$

$$f(y|H_1) = (2\pi\sigma^2)^{-1/2}\exp(-(y-s)^2/(2\sigma^2)) \tag{2.21b}$$

the likelihood ratio and the log-likelihood ratio are

$$\ell(y) = \exp((2ys - s^2)/(2\sigma^2)) \tag{2.22a}$$

$$z(y) = (2ys - s^2)/(2\sigma^2) \tag{2.22b}$$

We define d, the normal detectability, as follows

$$d \triangleq \frac{[E(z|H_1) - E(z|H_0)]^2}{\text{var}_0(z)} \tag{2.23}$$

where $\text{var}_0(z)$ is the variance of z under H_0. For simple Gaussian hypotheses the expression for normal detectability simplifies to

$$d \triangleq E(z|H_1) - E(z|H_0) \tag{2.24}$$

We also define d' as follows

$$d' \triangleq d^{1/2} \tag{2.25}$$

Physically d is related to the output signal to noise ratio (SNR) and is used as a performance index. For a fixed value of P_{FA} larger values of d result in larger values of P_D. For the above problem $d = s^2/\sigma^2$ and the statistics of z under H_0 and H_1 are

$$H_0 : z \sim N(-d/2, d) \tag{2.26a}$$

$$H_1 : z \sim N(d/2, d) \tag{2.26b}$$

The probabilities of detection and false alarm are given by

$$P_D = \Phi(\lambda + d') \tag{2.27a}$$

and

$$P_{FA} = \Phi(\lambda) \tag{2.27b}$$

where

$$\Phi(x) = (2\pi)^{-1/2} \int_{-\infty}^{x} \exp(-t^2/2)dt \tag{2.28}$$

and λ is a function of the threshold. The R.O.C. curves so obtained are called the normal R.O.C. curves. They are usually plotted on normal-normal probability paper where they plot as straight lines with a slope of 1. Normal R.O.C curves are obtained when the hypotheses are simple and the log-likelihood ratio has a normal distribution under both hypotheses. For comparison purposes other R.O.C. curves are also plotted on normal-normal probability paper. In fig. 2.2 a family of normal R.O.C. curves is plotted for several d' values. In later chapters we will use d and d' to compare the performance of various detectors.

2.5.2 Gaussian Signal in Gaussian Noise

Now assume that the observation is a vector $\underline{y}$ of length L

$$H_0 : \underline{y} = \underline{n} \tag{2.29a}$$

$$H_1 : \underline{y} = \underline{n} + \underline{s} \text{ , } \underline{n} \text{ \& } \underline{s} \text{ independent} \tag{2.29b}$$

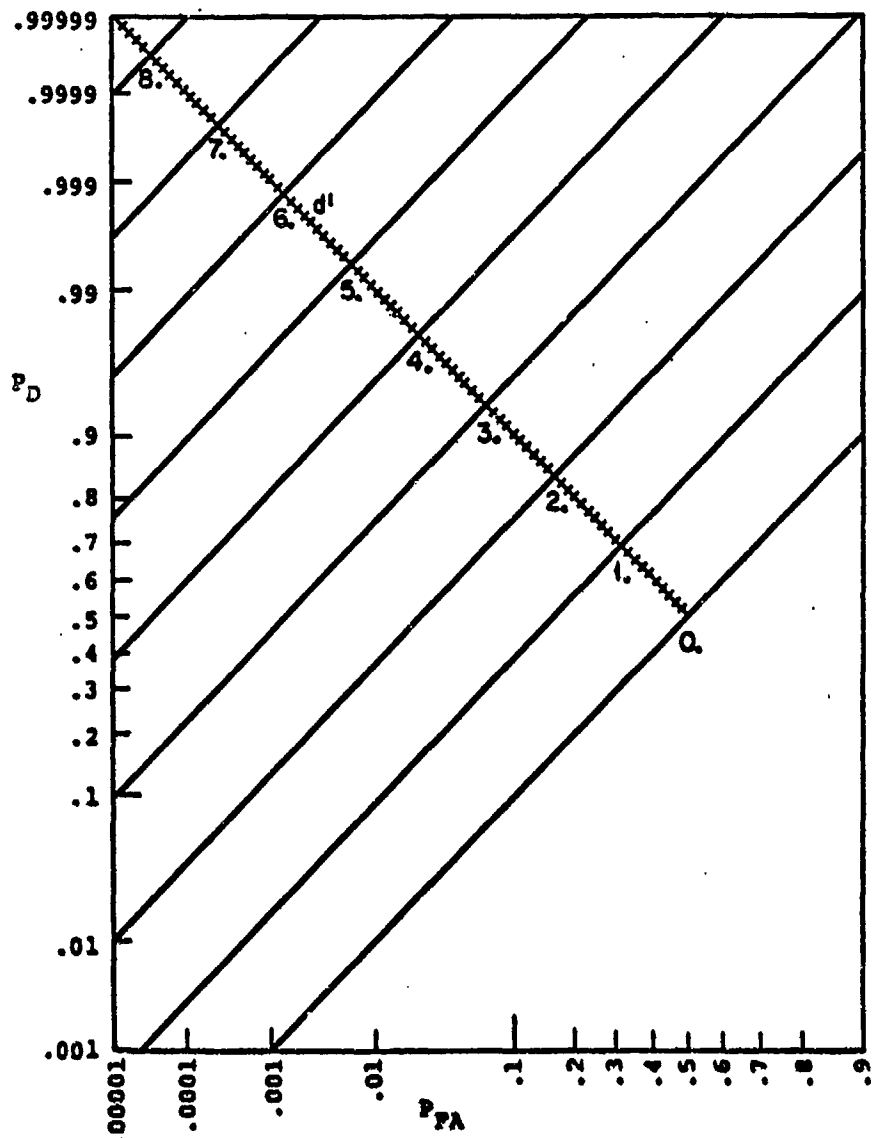

Fig. 2.2 Normal R.O.C. curves.

where bot $\underline{n}$ and $\underline{s}$ are zero mean Gaussian random vectors of length L. Let R_n and R_s denote the noise and signal autocorrelation matrices respectively

$$R_n = E(\underline{n}.\underline{n}^T) \tag{2.30a}$$

and

$$R_s = E(\underline{s}.\underline{s}^T) \tag{2.30b}$$

The density functions of the observation under the two hypotheses are

$$f(\underline{y}|H_0) = (2\pi)^{-L/2}|R_n|^{-1/2}\exp(-\underline{y}^T R_n^{-1}\underline{y}/2) \tag{2.31a}$$

and

$$f(\underline{y}|H_1) = (2\pi)^{-L/2}|R_n+R_s|^{-1/2}\exp(-\underline{y}^T(R_n+R_s)^{-1}\underline{y}/2) \tag{2.31b}$$

Where $|R|$ = determinant of R. We have assumed that the appropriate inverses exist. The likelihood ratio and the log-likelihood ratio are

$$\ell(\underline{y}) = |R_n|^{1/2}|R_n+R_s|^{-1/2}\exp(\underline{y}^T(R_n^{-1}-(R_n+R_s)^{-1})\underline{y}/2) \tag{2.32a}$$

$$z(\underline{y}) = \frac{1}{2}\,\underline{y}^T(R_n^{-1}-(R_n+R_s)^{-1})\underline{y} - \frac{1}{2}\ln(|R_n+R_s|/|R_n|) \tag{2.32b}$$

Since the second term in eq. 2.32b does not depend on the reception an equivalent detection statistic is

$$\eta(\underline{y}) = \underline{y}^T(R_n^{-1} - (R_n+R_s)^{-1})\underline{y} \tag{2.33}$$

the above may be written as follows

$$\eta(\underline{y}) = \underline{y}^T R_n^{-1} R_s (R_n+R_s)^{-1} \underline{y} \tag{2.34}$$

but $R_s(R_n+R_s)^{-1}\underline{y}$ is the linear minimum mean squared error (m.m.s.e.) estimate [15] of the signal vector, denote this by $\hat{\underline{s}}$, then

$$\eta(\underline{y}) = \underline{y}^T R_n^{-1} \hat{\underline{s}} \tag{2.35}$$

This result will be used extensively in Chapter V.

A commonly used sub-optimum detector for the Gaussian signal in Gaussian noise case is the Energy Detector. The energy detector uses the total energy in the observation as the detection statistic. Let $e(\underline{y})$ denote the detection statistic for the energy detector then

$$e(\underline{y}) = \underline{y}^T.\underline{y} \tag{2.36}$$

Note that the optimum detector simplifies to the energy detector when both signal and noise are white. In Chapter V we will often compare the performance of the optimum detector with that of the energy detector.

CHAPTER III

PROBLEM FORMULATION

In this chapter we first describe the underwater acoustic channel and the acoustic propagation model. This is followed by a description of the receiver geometry. Finally we discuss the analytic development of the detection problem. The analytic development is carried far enough to allow the formulation of the abstract problems discussed in Chapters IV and V.

3.1 The Underwater Acoustic Channel

Models similar to the model developed here for the underwater acoustic channel have been used by several authors [5,10,19,21]. The model incorporates a uniformly moving acoustic source, a fixed receiver and multipath propagation. The nth path in the channel is assumed to exhibit a real or complex gain c_n, where the path gain magnitudes, $|c_n|$, are assumed to be normalized. We assume a slowly varying ocean so that the c_n's and the number of paths, N, with significant gain remain essentially constant over the observation interval. The propagation delay of the nth path is denoted $\tau_n(t)$, where

$$\tau_n(t) = \tau_n + \tau_n' t \tag{3.1}$$

τ_n is the path delay at t=0, either the start or the middle of the observation interval. τ_n' is the path delay derivative or the doppler shift ratio. For receding sources $\tau_n'>0$ and for approaching sources $\tau_n'<0$. τ_n' is of the order

of v/c where v is the radial component of the source velocity and c is the speed of sound. The spread in τ_n and τ_n' is of the order of 0.5% to 1% of $\max_n \tau_n$ and $\max_n \tau_n'$ respectively [10]. We can view eq 3.1 as the truncated Taylor series expansion of $\tau_n(t)$. This models uniform source motion, to model more complicated source motion eq 3.1 would have to be augmented by including higher order terms from the Taylor series. Putting the above information together the underwater acoustic channel can be viewed as a linear filter with impulse response h(t), where

$$h(t) = \sum_{n=1}^{N} c_n \delta(t - \tau_n(t)) \qquad (3.2)$$

$$= \sum_{n=1}^{N} c_n \delta(\alpha_n t - \tau_n)$$

where

$$\alpha_n \triangleq 1 - \tau_n' \qquad (3.3)$$

According to the above model, if a source transmits a signal s(t), the receiver will receive a signal r(t) given by

$$r(t) = \sum_{n=1}^{N} c_n s(\alpha_n t - \tau_n) \qquad (3.3)$$

To complete the description of the acoustic channel we incorporate additive noise n(t) in the reception, so that

$$r(t) = \sum_{n=1}^{N} c_n s(\alpha_n t - \tau_n) + n(t) \qquad (3.4)$$

We assume that the noise is independent of the signal. We also assume that the noise is a zero mean, stationary, Gaussian process. The Gaussian assumption is widely used in the underwater acoustics literature [2,6,11].

3.2 Receiver Geometry and Hypothesis Formulation

The receiver geometry used is given in fig. 3.1. Two receivers RCVR1 and RCVR2 are placed a distance d apart. In a more general setting, where the interest is in localizing the acoustic source in three dimensions and estimating its velocity, more than two receivers are used. We will assume that the distance between the acoustic source and the receivers is of the order of 150 kilometers. Assuming that the speed of sound in the ocean is of the order of 1500 meters/second, the propagation delay from the source to the receiver will be of the order of 100 seconds and the differential path delays will be of the order of tenths of a second. We define T_d as the mean travel time of sound between the two receivers

$$T_d \triangleq d/\bar{c} \tag{3.5}$$

where $\bar{c}$ is the mean group speed of sound in the ocean. The difference in mean time delays to RCVR1 and RCVR2 is approximately T_d.

We assume that both the receivers have a finite observation interval of T seconds. We will assume that baseband signals are available to both the receivers. The complex demodulation that might be necessary to obtain the baseband signals will not be discussed. The receptions at RCVR1 and RCVR2 under H_0 are

$$H_0 : y_1(t) = n_1(t) , \quad -T/2 \leq t < T/2 \tag{3.6a}$$

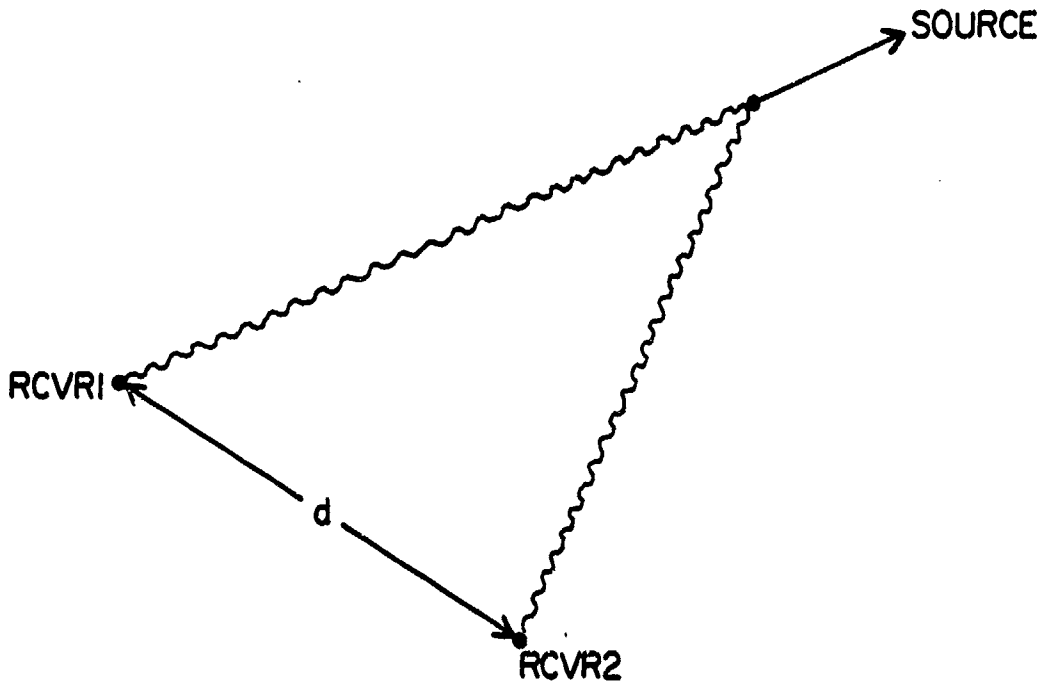

Fig. 3.1 Receiver geometry.

$$H_0 : y_2(t) = n_2(t) , \quad -T/2 \leq t < T/2 \tag{3.6b}$$

the $n_i(t)$ are stationary, complex, Gaussian and zero-mean processes. We assume that the receiver separation d is large enough so that $n_1(t)$ and $n_2(t)$ are independent, we also assume that $n_1(t)$ and $n_2(t)$ are identically distributed. The noise power in general is not known. Under the signal+noise hypothesis, H_1, we have the following situation

$$H_1 : y_1(t) = n_1(t) + \sum_{n=1}^{N} c_{1_n} s(\alpha_{1_n} t - \tau_{1_n}), -T/2 \leq t < T/2 \quad (3.7a)$$

$$H_1 : y_2(t) = n_2(t) + \sum_{m=1}^{M} c_{2_m} s(\alpha_{2_m} t - \tau_{2_m}), -T/2 \leq t < T/2 \quad (3.7b)$$

N and M are the number of paths to RCVR1 and RCVR2 respectively. c_{1_n} and c_{2_m} are the complex path gain coefficients, α_{1_n} and α_{2_m} are the doppler parameters (as defined in eq. 3.3). The signal s(t) is a zero mean, complex and stationary Gaussian random process on the infinite time interval. The autocorrelation of s(t) is denoted $R_s(\tau)$, where

$$R_s(\tau) = aR(\tau) \quad (3.8a)$$

and

$$|R(\tau)| \leq 1 \quad (3.8b)$$

We assume $R(\tau)$ is known, however "a" in general is unknown. We also assume that the stochastic signal and noise are independent and are individually and jointly ergodic [22]. The ergodic assumption allows us to approximate sample averages by long time averages and vice-versa. We assume the signal process is broadband, so that the signal autocorrelation is relatively narrow compared to the differential path delays. For our purposes a signal with a bandwidth of the order of 10 Hz or more is considered broadband.

3.3 Post Reception Processing for Detection

The usefulness of a correlator detector has already

been pointed out in the introduction. To reiterate; the correlation allows us the freedom to introduce independent delay and doppler search parameters. In our study we seek to match the differential dopplers and the differential path delays. As pointed out in the introduction we will use the Bivariate Normalized Crosscorrelation (BNC) functions $\gamma_T(\beta,\tau)$ as the observable for the detector.

$$\gamma_T(\beta,\tau) = \frac{\frac{1}{T}\int_{-T/2}^{T/2} y_1(\beta t)y_2^*(t-\tau)dt}{(\frac{1}{T}\int_{-T/2}^{T/2}|y_1(t)|^2dt)^{1/2}(\frac{1}{T}\int_{-T/2}^{T/2}|y_2(t)|^2dt)^{1/2}} \quad (3.9)$$

A plot of the magnitude of the BNC function for various values of β and τ is termed the ambiguity diagram. Peaks are obtained in the ambiguity diagram when the search values of β and τ match the actual values of differential doppler and delay for a path pair. Our goal is to combine the information contained in the peaks in a manner that allows us to make inferences about the presence or absence of the source. A block diagram of the post reception processing is given in fig. 3.2.

We now look at the BNC function in more detail. As in [10] we assume that the integration or observation times T are long enough for the denominator of $\gamma_T(\beta,\tau)$ to stabilize. That is, we assume T is long enough for the individual power measurements to stabilize. Once the power measurements stabilize it is enough to consider the numerator of $\gamma_T(\beta,\tau)$, denoted by $\gamma_{un_T}(\beta,\tau)$, as being representative of $\gamma_T(\beta,\tau)$.

We first examine the denominator terms of $\gamma_T(\beta,\tau)$. Under H_0 we obtain

$$\frac{1}{T}\int_{-T/2}^{T/2}|y_i(t)|^2dt = \frac{1}{T}\int_{-T/2}^{T/2}|n_i(t)|^2dt \quad (3.10)$$

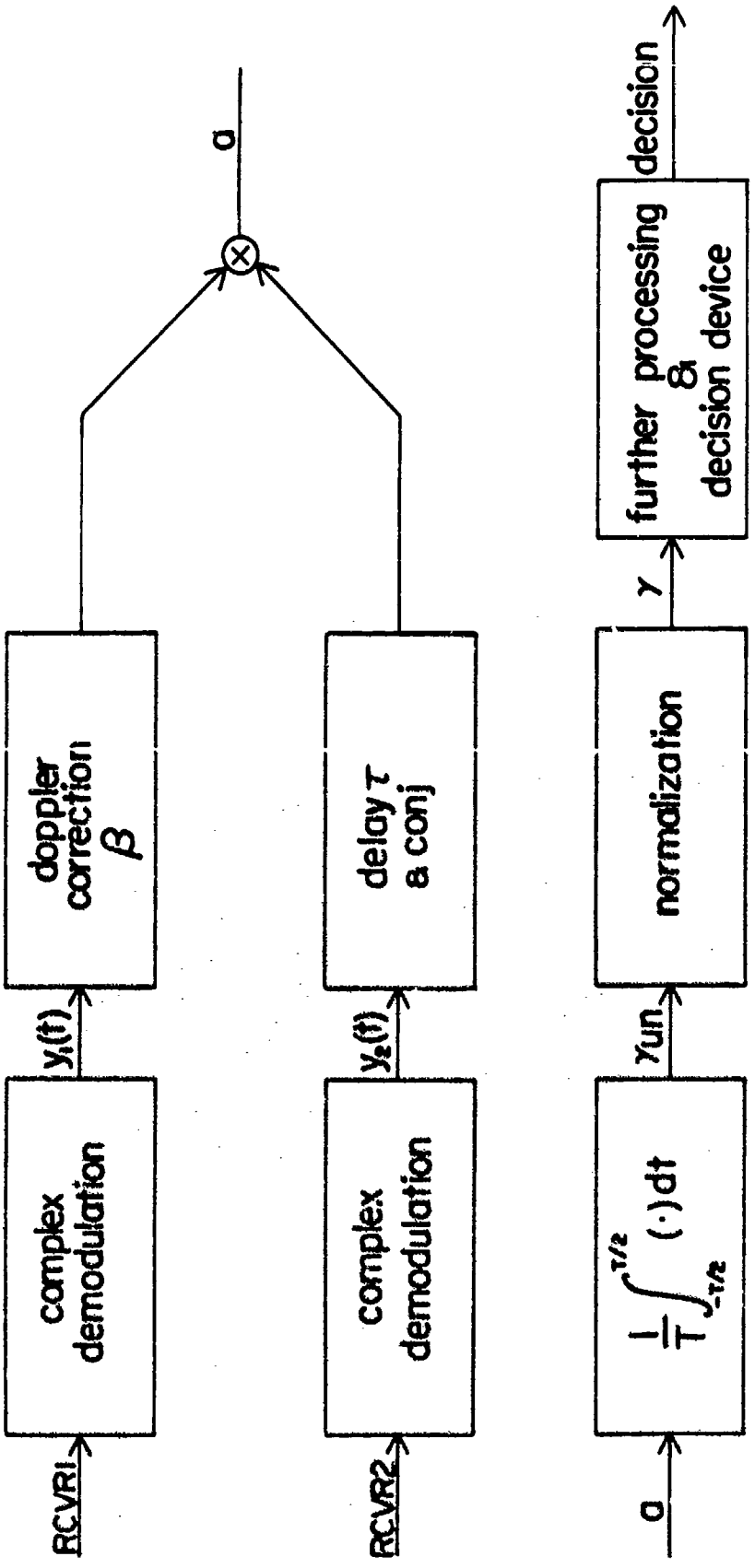

Fig. 3.2 Block diagram of the post reception processing.

using the ergodic assumption we obtain

$$\frac{1}{T}\int_{-T/2}^{T/2} |n_i(t)|^2 dt \approx R_{n_i}(0) \quad , \text{ T large} \tag{3.11}$$

Under H_1 we obtain

$$\frac{1}{T}\int_{-T/2}^{T/2} |y_i(t)|^2 dt = \frac{1}{T}\int_{-T/2}^{T/2} |n_i(t)|^2 dt$$

$$+ 2 \text{ Re} \sum_n c_{in} \frac{1}{T}\int_{-T/2}^{T/2} n_i^*(t) s(\alpha_{in} t - \tau_{in}) dt$$

$$+ \sum_n |c_{in}|^2 \frac{1}{T}\int_{-T/2}^{T/2} |s(\alpha_{in} t - \tau_{in})|^2 dt \tag{3.12}$$

$$+ \sum_n \sum_{m \neq n} c_{in} c_{im}^* \frac{1}{T}\int_{-T/2}^{T/2} s(\alpha_{in} t - \tau_{in}) s^*(\alpha_{im} t - \tau_{im}) dt$$

Since the source speeds are very small compared to the speed of sound, it is reasonable to approximate the α_{ij} by unity in the denominator integrals. This allows us to use the ergodic assumption in eq. 3.12. For large T consider the terms of eq. 3.12 individually

$$1) \quad \frac{1}{T}\int_{-T/2}^{T/2} |n_i(t)|^2 dt \approx R_{n_i}(0) \tag{3.13a}$$

$$2) \quad 2 \text{ Re} \sum_n c_{in} \frac{1}{T}\int_{-T/2}^{T/2} n_i^*(t) s(\alpha_{in} t - \tau_{in}) dt \approx 0 \tag{3.13b}$$

$$3) \sum_n |c_{in}|^2 \frac{1}{T} \int_{-T/2}^{T/2} |s(\alpha_{in}t - \tau_{in})|^2 dt \qquad (3.13c)$$

$$\simeq \sum_n |c_{in}|^2 R_s(0)$$

$$4) \sum_n \sum_{m\neq n} c_{in}c_{im}^* \frac{1}{T} \int_{-T/2}^{T/2} s(\alpha_{in}t - \tau_{in})s^*(\alpha_{im}t - \tau_{im})dt \qquad (3.13d)$$

$$\simeq \sum_n \sum_{m\neq n} c_{in}c_{im}^* R_s(\tau_{im} - \tau_{in})$$

From the broadband assumption we have $\min_{m\neq n} |\tau_{im} - \tau_{in}| > T_s$, where T_s is the signal correlation time, so that $R_s(\tau_{im} - \tau_{in}) \simeq 0$. Also given the different phases for the c_{ij}'s the terms in eq. 3.13d add up incoherently. Given the above it is reasonable to use the approximation

$$\sum_n \sum_{m\neq n} c_{in}c_{im}^* R_s(\tau_{im} - \tau_{in}) \simeq 0 \qquad (3.14)$$

Putting the approximations of eqs. 3.13 and 3.14 together we obtain

$$H_1 : \frac{1}{T} \int_{-T/2}^{T/2} |y_i(t)|^2 dt \simeq R_{n_i}(0) + \sum_n |c_{in}|^2 R_s(0) \qquad (3.15)$$

For the approximation to be valid we require the integration time T to be much larger than $\max(T_n, T_s)$, where T_n and T_s are the noise and signal correlation times respectively. In general $T_s > T_n$, so we require $T >> T_s$. For large but finite

T the right hand side of eq. 3.15 is the mean value of the integral on the left hand side. We expect a fluctuation about the mean, we assume that T is long enough so that the standard deviation is much smaller than the mean.

We now consider the numerator of the BNC function, $\gamma_{un_T}(\beta,\tau)$. In general $\gamma_{un_T}(\beta,\tau)$ is a function of the integration time T, the time delay correction τ, and the doppler correction β.

$$\gamma_{un_T}(\beta,\tau) \triangleq \frac{1}{T}\int_{-T/2}^{T/2} y_1(\beta t)y_2^*(t-\tau)dt \tag{3.16}$$

Under H_0 we obtain

$$H_0 : \gamma_{un_T}(\beta,\tau) = \frac{1}{T}\int_{-T/2}^{T/2} n_1(\beta t)n_2^*(t-\tau)dt \tag{3.17a}$$

since $n_1(t)$ and $n_2(t)$ are independent and zero mean we obtain

$$H_0 : \gamma_{un_T}(\beta,\tau) \simeq 0 \tag{3.17b}$$

Under H_1 eq. 3.16 has four terms, listed below individually

$$1)\ \frac{1}{T}\int_{-T/2}^{T/2} n_1(\beta t)n_2^*(t-\tau)dt \tag{3.18a}$$

$$2)\ \sum_{m=1}^{M} c_{2_m}^* \frac{1}{T}\int_{-T/2}^{T/2} n_1(\beta t)s^*(\alpha_{2_m}t - \tau_{2_m} - \tau)dt \tag{3.18b}$$

$$3)\ \sum_{n=1}^{N} c_{1_n} \frac{1}{T}\int_{-T/2}^{T/2} n_2^*(t-\tau)s(\beta\alpha_{1_n}t - \tau_{1_n})dt \tag{3.18c}$$

$$4) \sum_{n=1}^{N} \sum_{m=1}^{M} c_{1_n} c^*_{2_m} \frac{1}{T} \int_{-T/2}^{T/2} s(\beta\alpha_{1_n} t - \tau_{1_n}) \qquad (3.18d)$$

$$.s^*(\alpha_{2_m} t - \tau_{2_m} - \tau)dt$$

Long time integration, $T >> \max(T_n, T_s)$, results in eqs. 3.18a, 3.18b and 3.18c approaching zero in the mean squared sense. All three terms (3.18a, 3.18b & 3.18c) may be considered as additive "noise" in the observation, although the "noise" is no longer independent of the "signal." We need to examine the behavior of eq. 3.18d under long time integration. Consider the following value of β:

$$\beta = \beta_{ij} \triangleq \alpha_{2_j}/\alpha_{1_i} \qquad (3.19)$$

with this value of β eq. 3.18d can be written as follows

$$c_{1_i} c^*_{2_j} \frac{1}{T} \int_{-T/2}^{T/2} s(\alpha_{2_j} t - \tau_{1_i}) s^*(\alpha_{2_j} t - \tau_{2_j} - \tau)dt$$

$$+ \sum_{m \neq j}^{M} c_{1_i} c^*_{2_m} \frac{1}{T} \int_{-T/2}^{T/2} s(\alpha_{2_j} t - \tau_{1_i}) s^*(\alpha_{2_m} t - \tau_{2_m} - \tau)dt$$

$$+ \sum_{n \neq i}^{N} \sum_{m=1}^{M} c_{1_n} c^*_{2_m} \frac{1}{T} \int_{-T/2}^{T/2} s(\beta_{ij}\alpha_{1_n} t - \tau_{1_n}) s^*(\alpha_{2_m} t - \tau_{2_m} - \tau)dt$$

$$\simeq c_{1_i} c^*_{2_j} R_s(\tau - (\tau_{1_i} - \tau_{2_j})) \qquad (3.20)$$

$$+ \sum_{m \neq j}^{M} c_{1_i} c^*_{2_m} \frac{1}{T} \int_{-T/2}^{T/2} s(\alpha_{2_j} t - \tau_{1_i}) s^*(\alpha_{2_m} t - \tau_{2_m} - \tau)dt$$

$$+ \sum_{n\neq i}^{N} \sum_{m=1}^{M} c_{1n} c_{2m}^{*} \frac{1}{T} \int_{-T/2}^{T/2} s(\beta_{ij}\alpha_{1n}t - \tau_{1n}) s^{*}(\alpha_{2m}t - \tau_{2m} - \tau)dt$$

When $\tau = \tau_{1i} - \tau_{2j}$ the $c_{1i}c_{2j}^{*}R_s(\tau - (\tau_{1i} - \tau_{2j}))$ term peaks. Similarly we can define a total of MN β values for which expression like eq. 3.20 are obtained. Since we know the functional form of $R_s(\tau)$, terms similar to the first term in eq. 3.20 can be considered the "signal term" and the rest can be considered a part of the additive noise. Here we again use the broadband assumption, that is, the range of τ for which $R_s(\tau - (\tau_{1i} - \tau_{2j}))$ is significant, the other terms in eq. 3.20 are small. The problem then becomes similar to the set of problems called "signal known exactly except for specified parameters plus additive noise" [16]. The observation is two dimensional in that there are two search parameters, β & τ. This is a non-trivial problem to solve, to begin with we would have to determine the distribution function of the terms lumped together as noise.

Work has been done by several authors [23,24,25,26] in the area of determining the density function of the output of an analog crosscorrelator when the inputs are stochastic. However our formulation is complicated in that the received signal is the sum of several delayed and doppler shifted versions of the source signal. At this stage the custom is to remove the multipath assumption and solve a problem based on a single-path assumption. We choose to keep the multipath assumption intact and select solvable abstract problems, derived from the above problem, for further study. The results obtained from the study of the abstract problems will allow us to form rules of thumb and guidelines for an experimenter faced with the general problem formulated in this chapter.

CHAPTER IV

EXTENDED M-ORTHOGONAL SIGNALS AND THE FIRST ABSTRACTION

In Chapter III we saw that a solution to the exact problem as formulated was non-trivial and perhaps not possible. In this chapter we study the first of two abstractions of the problem formulated in Chapter III. The object of the abstraction in this chapter is to find out how many of the unknown β,τ parameter values have to be matched for good or acceptable performance.

4.1 Abstraction Formulation

In practise the ambiguity surface is usually quantized; being evaluated at discrete values of β and τ. The quantization is usually "fine", that is the steps in τ and β are chosen small enough to yield a continuous appearing surface, but large enough to make the computing job possible. For the purposes of analysis we will make the usual simplification that the quantization is coarser than used in practise and that the quantizations are "matched" in the sense that the response of a path-pair falls on one and only one point, and the value there is due to perfect alignment in time and frequency. We call the grid point a "cell" and the computed ambiguity value the "cell value". For simplicity the cells are integer indexed, $j=1,2,\ldots,L$ and the cell values are denoted by y_j. The total observation is thus a list or vector $\underline{y}=y_1,\ldots,y_L$ of length L.

The observation model will be intentionally oversimplified at the cell statistics level. Specifically

under H_0, the cell values are i.i.d. N(0,1). Under H_1, C of the cells are i.i.d. N(s,1) and the rest of the cells are i.i.d. N(0,1). C is the number of path pairs and in the notation of Chapter III C=M.N.

The complications arise from the composite nature of H_1. Let θ be the set of cells whose mean is s under H_1; θ is the "signal parameter", a set of cell indices. The number of possible θ is $n_\theta = L!/C!(L-C)!$. We refer to θ as a "pattern" or "signal" and n_θ as the number of possible patterns or signals.

Following the Bayesian philosophy we put a prior distribution on the signal parameter. If the prior is $p(\theta_i)$ where $i=1,2,\ldots,n_\theta$, then the likelihood ratio is

$$\ell(y) = \sum_{i=1}^{n_\theta} \exp(z(y|\theta_i))p(\theta_i) \qquad (4.1)$$

where

$$z(y|\theta_i) = s.\sum_{j\epsilon\theta_i} y_j - .5Cs^2 \qquad (4.2)$$

note $z(y|\theta_i)$ has a normal distribution and $\exp(z(y|\theta_i))$ has a log-normal distribution [29].

The first difficulty one would encounter if one were to try to base a receiver on $\ell(y)$ as given in eq. 4.1 is the size of the parameter space. For a well localized signal the ambiguity plane might be modelled by as small as a 100 by 100 square i.e. L=10,000. For a 4 path by 4 path propagation the value of C is 16; there are $n_\theta = 10^{50.67}$ possible signals and as such $10^{50.67}$ $z(y|\theta_i)$ have to be evaluated before the likelihood ratio can be calculated. The primary difficulty lies in the enormity of the number of

possible signals coupled with the fact that we lack a simple structure to reduce this to a sequence of smaller sub-hypotheses. Of course we do not want to build such a receiver, we only want to evaluate its performance. We immediately encounter the second type of difficulty; namely that the determination of the distribution of $\ell(y)$ is seemingly hopeless because the $z(y|\theta_i)$ are not independent over i.

Since we have no simple way of determining the performance of the optimum receiver we must consider an alternative approach that will allow us to make statements about the problem posed at the beginning of this chapter, i.e. how many of the β,τ parameter values have to be matched for good or acceptable performance. Now, out of the n_θ possible signal patterns, we could select at most L/C that do not have a cell in common. For the simple numerical example of the 100 by 100 square and a 4 path by 4 path propagation, such a partition of the ambiguity plane contains only 625 patterns. It is worthwhile to note that there are more than 10^{27334} such partitions.

In the following we consider a receiver based on such a partition, i.e. based on orthogonal signals. This is done primarily for mathematical convenience; however, it is realistic in that the receiver designer is also faced with the enormity of n_θ and is forced to simplify. For example a receiver designer may falsely believe that the doppler is the same on all the paths to a given receiver, in other words the designer overlooks differential doppler. This means that the source will affect only one narrow β band of the ambiguity plane (in our simplified ambiguity grid this band corresponds to one β index, that is, the doppler is centered and the frequency resolution sharp enough). To match our evaluation model exactly the designer would have to know all of the differential delays well enough to specify the C patterns without overlap. This is

unrealistic, so the following evaluation is optimistic and can be considered an upper bound on performance.

This chapter will consider a receiver based on orthogonal signals and examine its performance under several conditions; under the assumption that the partition was correctly chosen and the true signal is one of the patterns in the partition, and under two conditions where the true signal is not one of the patterns in the partition. These latter conditions are the ones of interest, for they may shed some light on how well one must match the true pattern to perform well.

4.2 The Orthogonal-Signal-Based Receiver

In this section we examine the orthogonal-signal-based receiver, introduced in the previous section, in more detail. Given a partition, we first reconfigure the observation y into a matrix so that each θ_i in the partition is one row of C columns. Without loss of generality we can re-index the patterns so that the receiver is based on the first L/C patterns (for simplicity in analysis we will assume that R=L/C is an integer). C is a mnemonic for both the number of cells in the signal pattern and for the number of columns in the reconfigured ambiguity diagram. R is the mnemonic for the number of rows in that reconfiguration. We also restrict ourselves to the simple case, where the receiver is based on the traditional worst case assumption that the R signals are equally likely. Formally we base the receiver on the following prior distribution

$$p(\theta_i) = \begin{cases} 1/R & , \text{ iff } i=1,2,\ldots,R \\ 0 & , \text{ iff } i=R+1,\ldots,n_\theta \end{cases} \qquad (4.3)$$

with the reminder that

$$\theta_i \cap \theta_j \text{ is empty for } 1 \leq i < j \leq R \tag{4.4}$$

The true signal pattern will be denoted by θ_J or simply by J. Also for the rest of this chapter H_i will mean H_{i,θ_J}.

4.2.1 The M-Orthogonal Signals Evaluation

Here we evaluate the above receiver under the assumption that the true signal is one of the patterns in the partition; that is, $J \leq R$. This case is known as "signal one of M-Orthogonal Signals" or simply M-Orthogonal Signals, abbreviated as MOS [13,18,27,28]. M is numerically equal to R here. The usual but optimistic normal detectability approximation is

$$d_{MOS} = Cs^2 - \ln(R) \tag{4.5}$$

4.2.2 The Extended M-Orthogonal Signals Evaluation

Here we evaluate the orthogonal-signal-based receiver under two conditions where the true signal is not one of the patterns in the partition. We call this Extended M-Orthogonal Signals (EMOS) as the receiver is designed for MOS, but the true signal is not one of the design signals. The true signal does have cells in common with the design signals. Let the number of cells that the true signal has in common with the ith design signal be denoted by K_i, then

$$K_i = \text{card}\{\theta_J \cap \theta_i\} \tag{4.6}$$

where card{ } is notation for the cardinality of the set.

For further analysis we make the following assumptions and restrictions

$$L = 2^b \tag{4.7a}$$

$$C = 2^a \tag{4.7b}$$

$$b \geq 2a \tag{4.7c}$$

$$\sum_{i=1}^{R} K_i = C \tag{4.7d}$$

Later, we will be interested in the situation where L=8192, C=64 and R=128 (this corresponds to an 8 path by 8 path propagation model).

Consider positive integers R and C, $R \geq C$, and any set κ of R non-negative integers K_i such that $\sum_{i=1}^{R} K_i = C$. Let $\#\{\kappa\}$ denote the number of decompositions of C into integer summands without regard to order [35 pg. 825]. For C=64 we obtain

$$\#\{\kappa\} = 1,741,630 \tag{4.8}$$

The receiver design was based on R orthogonal signals, each signal affecting C cells. For each signal strength, s, there are $\#\{\kappa\}$ possible conditional R.O.C. curves, one for each set κ. It is unrealistic to consider a distribution on $\{\kappa\}$ and seek an average R.O.C. An upper bound on these R.O.C.'s is given by the MOS evaluation, where $\kappa=(K_1,\ldots,K_R)$ is specified by

$$K_i = \begin{cases} C\ , & i=1 \\ 0\ , & i=2,3,\ldots,R \end{cases} \tag{4.9}$$

A lower bound on these R.O.C.'s is given by the sparse condition

$$K_i = \begin{cases} 1\ , & i=1,2,\ldots,C \\ 0\ , & i=C+1,\ldots,R \end{cases} \tag{4.10}$$

To shed light on the central question "how well does the receiver have to come to matching the actual signal?" two types of intersecting sets were selected and performance evaluated for C=64 and R=128. The first type which we call standard EMOS is given by the condition

$$K_i = \begin{cases} 2^C, & i=1,2,\ldots,2^{6-c} \\ 0, & \text{o.w.} \end{cases} \tag{4.11}$$

The second type which we call modified EMOS is given by the condition

$$K_i = \begin{cases} 2^C, & i=1 \\ 1, & i=2,3,\ldots,65-K_1 \\ 0, & \text{o.w.} \end{cases} \tag{4.12}$$

Intuitively performance for standard EMOS should be better than the performance for modified EMOS. We are also interested in determining how much the performances differ. That is, how much does it help performance if the largest K_i occurs several times?

4.3 Receiver Performance Evaluation

In the following we will discuss performance evaluation techniques for the standard EMOS in detail. Later when we discuss Monte-Carlo methods for performance evaluation we will also consider modified EMOS. Unless otherwise specified by EMOS we will mean standard EMOS.

Let S denote the number of rows that intersect the true signal θ_J and let K denote the value of K_i in the S rows. We can now write down the likelihood ratio for the EMOS evaluation

$$\ell(y) = \frac{1}{R}\left(\sum_{i=1}^{S} \exp(z_K(y|\theta_i)) + \sum_{i=S+1}^{R} \exp(z_0(y|\theta_i))\right) \qquad (4.13)$$

where the subscripts K and 0 are used to denote the number of cells the ith row has in common with the true signal. Now

$$z_K(y|\theta_i) = s.\sum_{j\epsilon\theta_i} y_j - .5Cs^2 \ , \ i=1,\ldots,S \qquad (4.14a)$$

and

$$z_0(y|\theta_i) = s.\sum_{j\epsilon\theta_i} y_j - .5Cs^2 \ , \ i=S+1,\ldots,R \qquad (4.14b)$$

We are interested in the statistics of $\sum_{j\epsilon\theta_i} y_j$ under H_0 and H_1

$$H_0 : \sum_{j\epsilon\theta_i} y_j = \Xi_i \sim N(0,C) \text{ i.i.d. } , \ i=1,\ldots,R \qquad (4.15a)$$

$$H_1 : \sum_{j\epsilon\theta_i} y_j = \begin{cases} sK + \Xi_i \ , & i=1,\ldots,S \\ \Xi_i \ , & i=S+1,\ldots,R \end{cases} \qquad (4.15b)$$

The distribution of $z_0(y|\theta_i)$ and $z_k(y|\theta_i)$ easily follow from the above

$$z_0(y|\theta_i) \sim N(-\frac{C}{2}s^2, Cs^2) \qquad (4.16a)$$

$$H_0 : z_K(y|\theta_i) \sim N(-\frac{C}{2}s^2, Cs^2) \tag{4.16b}$$

$$H_1 : z_K(y|\theta_i) \sim N((K - \frac{C}{2})s^2, Cs^2) \tag{4.16c}$$

Since $z_0(y|\theta_i)$ and $z_K(y|\theta_i)$ have a normal distribution $\exp(z_0(y|\theta_i))$ and $\exp(z_K(y|\theta_i))$ have a log-normal distribution and $\ell(y)$ has the distribution of the sum of independent log-normals. Before proceeding further we state a few pertinent facts about the log-normal distribution. A detailed discussion and further facts may be found in [29]. Let random variables X and Y be related as follows

$$X = \ln Y \tag{4.17}$$

with

$$X \sim N(\mu, \sigma^2) \tag{4.18}$$

then Y is said to be log-normally distributed. We denote this as $Y \sim \Lambda(\mu, \sigma^2)$. The density function of Y, f(y) is

$$f(y) = \begin{cases} (\frac{1}{2\pi})^{1/2}.(\sigma y)^{-1}.\exp(-\frac{1}{2}.(\frac{\ln y - \mu}{\sigma})^2) & , y>0 \\ 0 & , y\leq 0 \end{cases} \tag{4.19}$$

The kth moment of Y, $E(Y^k)$ is given by

$$E(Y^k) = \exp(k\mu + \frac{k^2.\sigma^2}{2}) \tag{4.20}$$

and the variance of Y, σ_Y^2 is

$$\sigma_Y^2 = \exp(2\mu + \sigma^2).(\exp(\sigma^2) - 1) \tag{4.21}$$

To evaluate the receiver performance we need to find the distribution of the sum of independent log-normal random variables. Since no closed form expression exists for the density function of the sum of independent log-normal random variables we must resort to other techniques, i.e. numerical or series approximation methods. We will discuss several ways for evaluating receiver performance.

4.3.1 Approximation to the Detectability Index

The normal detectability d or its square root d' are accurate measures of receiver performance when the R.O.C. is normal. In this case the R.O.C. is clearly not normal, however we will use normal detectability as an approximate measure of performance [16].

$$E(\ell(y)|H_1) = \frac{1}{R}\left(\sum_{i=1}^{S} E(\ell_K(y|\theta_i)|H_1) + \sum_{i=S+1}^{R} E(\ell_0(y|\theta_i)|H_1)\right) \quad (4.22)$$

Where $\ell_K(.)=\exp(z_K(.))$ and $\ell_0(.)=\exp(z_0(.))$. When the R.O.C. is normal we have [30]

$$E(\ell|H_1) = \exp(d) \quad (4.23a)$$

$$E(\ell|H_0) = 1 \quad (4.23b)$$

So assuming $\ell(y)$ results in a normal R.O.C. we obtain for eq 4.22

$$\exp(d_{EMOS}) = \frac{S}{R}.\exp(d_1(K)) + \frac{R-S}{R} \quad (4.24)$$

Where

$d_{EMOS} \triangleq$ detect. for Extended M-Orthog. signals (4.25a)

$d_1(K) \triangleq$ detect. for one row with K signal cells (4.25b)

eq. 4.24 simplifies to

$$\exp(d_{EMOS}) - 1 = \frac{S}{R}.(\exp(d_1(K)) - 1) \quad (4.26)$$

We will consider two cases:

1) Both $d_1(K)$ and d_{EMOS} are large.
2) Both $d_1(K)$ and d_{EMOS} are small.

With both $d_1(K)$ and d_{EMOS} large we obtain

$$\exp(d_{EMOS}) \approx \frac{S}{R}.\exp(d_1(K)) \quad (4.27a)$$

or taking the logarithm, we obtain

$$d_{EMOS} \approx d_1(K) - \ln(R/S) \quad (4.27b)$$

When both d_{EMOS} and $d_1(K)$ are small we can expand $\exp(d_1(K))$ and $\exp(d_{EMOS})$ in Taylor series and ignore the higher order terms. Thus we obtain

$$d_{EMOS} \approx \frac{S}{R}.d_1(K) \quad (4.28)$$

The results in eq. 4.27b and eq. 4.28 are similar to the results obtained for the M-Orthogonal signals case [30]. Now $d_1(K)$ may easily be calculated from the expression for d and the statistics for $z_K(y|\theta_i)$ given in eq. 4.16

$$d_1(K) \triangleq E(z_K(y|\theta_i)|H_1) - E(z_K(y|\theta_i)|H_0)$$

$$= (K - \frac{C}{2})s^2 - (-\frac{C}{2})s^2 \qquad (4.29)$$

$$= Ks^2$$

So for large d we have

$$d_{EMOS} = Ks^2 - \ln\frac{R}{S} \qquad (4.30)$$

We are interested in the situation where L=8192, C=64 and R=128. For the MOS evaluation (K=C) we desire that the detection be almost sure; we will use this to dictate our choice for s. From experience a d' ≈ 8 results in high detection probabilities for very small false alarm probabilities (also see fig. 2.2). Substituting in eq. 4.30 we obtain

$$s^2 = \frac{64 + 7.\ln 2}{64}$$

or

$$s \approx 1.03 \qquad (4.31)$$

In the following, for convenience we let s=1. With the above choice of variables we can find d_{EMOS} for several K. These values are tabulated in table 4.1.

4.3.2 Formal Evaluation of the p.d.f. of $\ell(y)$

Our interest is in deriving the density function for $\ell(y)$ (eq. 4.13) under both the signal+noise hypothesis and the noise alone hypothesis. Under the noise alone hypothesis eq. 4.13 simplifies to

K	$d_1(K)$	d_{EMOS}	d'_{EMOS}
1	1	.5	.707
2	2	.5	.707
4	4	1.92	1.39
8	8	5.23	2.29
16	16	12.53	3.54
32	32	27.84	5.28
64	64	59.15	7.69

Table 4.1 Table of normal detectability for several K values, for signal power s=1.

$$\ell(y) = \frac{1}{R} \sum_{i=1}^{R} \exp(z_0(y|\theta_i)) \tag{4.32}$$

Define

$$w_k = \frac{1}{R} \cdot \exp(z_K(y|\theta_i)) \tag{4.33}$$

then

$$f_{w_k}(\alpha) = \begin{cases} \frac{1}{\alpha} \cdot f_{z_k}(\ln R\alpha) & , \alpha > 0 \\ 0 & , \text{o.w.} \end{cases} \tag{4.34}$$

$$f_{w_k}(\alpha) = \begin{cases} (2\pi C\alpha^2)^{-1/2}.\exp(-\frac{1}{2C}(\ln\alpha-(K-\frac{C}{2}-\ln R))^2) & , \alpha>0 \\ 0 & , \text{ o.w.} \end{cases} \quad (4.35)$$

for C=64 and R=128 the above reduces to

$$f_{w_k}(\alpha) = \begin{cases} (\frac{1}{2\pi})^{1/2}.\frac{1}{8\alpha}.\exp(-\frac{1}{2}.(\frac{\ln\alpha-(K-36.852)}{8})^2) & , \alpha>0 \\ 0 & , \text{ ow.} \end{cases} \quad (4.36)$$

Since the w_k's are independent and identically distributed for fixed K, the density function for the likelihood ratio $\ell(y)$ is the convolution of the density functions of the w_k's. Or if we let $\phi_{w_k}(v)$ be the characteristic function of $f_{w_k}(\alpha)$ and $\phi_{l_k}(v)$ be the characteristic function of $f_{l_k}(\alpha)$ we have

$$\phi_{w_k}(v) = \int_0^\infty f_{w_k}(\alpha).\exp(jv\alpha)d\alpha \quad (4.37)$$

$$\phi_{l_k}(v) = (\phi_{w_k})^S.(\phi_{w_0}(v))^{R-S} \quad (4.38)$$

$$f_{l_k}(\alpha) = \begin{cases} \frac{1}{2\pi}\int_{-\infty}^{\infty} \phi_{l_k}(v).\exp(-jv\alpha)dv \\ 0 \quad , \text{ o.w.} \end{cases} \quad (4.39)$$

$$\phi_{l_0}(v) = (\phi_{w_0}(v))^R \quad (4.40)$$

and

$$f_{l_0}(\alpha) = \begin{cases} \frac{1}{2\pi}\int_{-\infty}^{\infty} \phi_{l_0}(v).\exp(-jv\alpha)dv \\ 0 \quad , \text{ o.w.} \end{cases} \quad (4.41)$$

Now if we choose λ as the threshold value for the purposes

of decision making, the probabilities of detection $P_D(\lambda|K)$ and false alarm $P_{FA}(\lambda)$ may be calculated as follows

$$P_D(\lambda|K) = \int_\lambda^\infty f_{l_k}(\alpha)d\alpha$$

$$= 1 - \int_0^\lambda f_{l_k}(\alpha)d\alpha \qquad (4.42)$$

$$P_{FA} = \int_\lambda^\infty f_{l_0}(\alpha)d\alpha$$

$$= 1 - \int_0^\lambda f_{l_0}(\alpha)d\alpha \qquad (4.43)$$

Formally the problem is solved. However to get the R.O.C. curves we need to do more because no closed form solutions to the above integrals(4.37 to 4.43) exist. We need to find suitable numerical or Monte-Carlo procedures for evaluating the R.O.C.'s. In the following, three procedures that were considered for evaluating the R.O.C. curves are described.

4.3.3 Discrete Fourier Transform Approach

The DFT approach for evaluating the density function for the sum of log-normal random variables is fairly natural. The procedure for evaluating the density function and the R.O.C. is briefly discussed.

First to calculate the characteristic functions $\phi_{w_k}(v)$ we need to find a value of α, say η such that for all K

$$\int_\eta^\infty f_{w_k}(\alpha)d\alpha < \varepsilon \qquad (4.44)$$

Where ε is chosen in accordance with how much error can be tolerated in the calculation. The next step is to sample $f_{w_k}(\alpha)$ and $f_{w_0}(\alpha)$ in the region $(0,\eta)$. The sampled

sequences are then padded with a sufficient number of zeros to avoid the wrap around effect in later calculation. This is followed by evaluating the DFT of the two sequences. The DFT of the sampled versions of $f_{w_k}(\alpha)$ and $f_{w_0}(\alpha)$ are raised to the Sth power and the (R-S)th power respectively. The sequences so obtained are then multiplied and the inverse DFT operation is performed; this results in a sampled version of $f_{l_k}(\alpha)$. A similar procedure yields the sampled version of $f_{l_0}(\alpha)$. A suitable numerical integration procedure (say Simpson's rule) then yields the probabilities of detection and false alarm.

In our problem, for the values selected for L, C, R and s, this procedure breaks down. From the values given in Table 4.2 for $E(w_k)$, $E(w_k^2)$, $\max f_{w_k}(\alpha)$ and the value of α at which the maximum occurs we see that the $f_{w_k}(\alpha)$'s are not well behaved. A suitable common sampling period can not be found. It is also not appropriate to model the densities as δ functions due to their long tails as evidenced by the huge variance.

4.3.4 Numerical Integration Methods for Evaluating the R.O.C.

This section is based on, and is an extension of the techniques developed by Nolte and Jaarsma [28] for evaluating the R.O.C. curves for the detection of one of M-Orthogonal signals.

We will only describe the calculation for $P_D(\lambda|K)$. The techniques for calculating $P_{FA}(\lambda)$ are the same except that S and K are both set to zero.

We can write the $\phi_{l_k}(v)$ the characteristic function for the density function of the likelihood ratio in terms of its real and imaginary parts

K	$E(w_k)$	$E(w_k^2)$	$\max f_{w_k}(\alpha)$	α_{max}	$f_{w_k}(1)$
0	0.0078	3.81×10^{23}	3.98×10^{28}	1.57×10^{-44}	1.23×10^{-6}
1	0.0212	2.81×10^{24}	1.46×10^{28}	4.31×10^{-44}	2.17×10^{-6}
2	0.0577	2.08×10^{25}	5.39×10^{27}	1.17×10^{-43}	3.77×10^{-6}
4	0.4266	1.13×10^{27}	7.29×10^{26}	8.66×10^{-43}	1.08×10^{-6}
8	2.33×10^{1}	3.38×10^{30}	1.33×10^{25}	4.73×10^{-41}	7.47×10^{-5}
16	6.94×10^{4}	3.01×10^{37}	4.48×10^{21}	1.41×10^{-37}	1.67×10^{-3}
32	6.17×10^{11}	2.37×10^{51}	5.04×10^{14}	1.25×10^{-30}	4.15×10^{-2}
64	4.87×10^{25}	1.48×10^{79}	6.38	9.89×10^{-17}	1.57×10^{-4}

Table 4.2 Statistics of the random variable w_k for K=0,1,2,4,8,16,32,64.

$$\phi_{1_k}(v) \triangleq \phi_{R_k}(v) + j\phi_{I_k}(v) \tag{4.45}$$

Substituting the above in eq. 4.39 gives

$$f_{1_k}(\alpha) = \begin{cases} \frac{1}{2\pi}\int_{-\infty}^{\infty}[\phi_{R_k}(v)+j\phi_{I_k}(v)][\cos(v\alpha)+j\sin(v\alpha)]dv\ ,\alpha>0 \\ 0\quad ,\quad \text{o.w.} \end{cases} \tag{4.46}$$

Since $f_{1_k}(\alpha)$ is real eq. 4.46 reduces to

$$f_{1_k}(\alpha) = \begin{cases} \frac{1}{2\pi}\int_{-\infty}^{\infty}[\phi_{R_k}(v)\cos(v\alpha)+\phi_{I_k}(v)\sin(v\alpha)]dv\ ,\alpha>0 \\ 0\quad ,\quad \text{o.w.} \end{cases} \tag{4.47}$$

Also since $f_{1_k}(\alpha)$ is the convolution of densities that are zero for $\alpha \leq 0$, $f_{1_k}(\alpha)$ must also be zero for $\alpha \leq 0$ i.e. for $\alpha > 0$, $f_{1_k}(-\alpha) = 0$. This implies that

$$\int_{-\infty}^{\infty}\phi_{R_k}(v)\cos(v\alpha)dv = \int_{-\infty}^{\infty}\phi_{I_k}(v)\sin(v\alpha)dv\ ,\ \alpha>0 \tag{4.48}$$

So

$$f_{1_k}(\alpha) = \begin{cases} \frac{1}{\pi}\int_{-\infty}^{\infty}\phi_{R_k}(v)\cos(v\alpha)dv\ ,\ \alpha>0 \\ 0\quad ,\quad \text{o.w.} \end{cases} \tag{4.49}$$

and since $\phi_{R_k}(v)$ is even

$$f_{1_k}(\alpha) = \begin{cases} \frac{2}{\pi}\int_{0}^{\infty}\phi_{R_k}(v)\cos(v\alpha)dv\ ,\ \alpha>0 \\ 0\quad ,\ \text{o.w.} \end{cases} \tag{4.50}$$

Now substituting eq. 4.50 in eq. 4.42 we obtain

$$P_D(\lambda|K) = 1 - \frac{2}{\pi}\int_0^{\lambda}\int_0^{\infty}\phi_{R_k}(v)\cos(v\alpha)\,dv\,d\alpha \qquad (4.51)$$

Changing the order of integration in eq. 4.51 gives

$$P_D(\lambda|K) = 1 - \frac{2}{\pi}\int_0^{\infty}\phi_{R_k}(v)\int_0^{\lambda}\cos(v\alpha)\,d\alpha\,dv \qquad (4.52a)$$

$$= 1 - \frac{2}{\pi}\int_0^{\infty}\phi_{R_k}(v).\frac{\sin(v\alpha)}{v}\Big|_0^{\lambda}\,dv \qquad (4.52b)$$

$$= 1 - \frac{2\lambda}{\pi}\int_0^{\infty}\phi_{R_k}(v)\frac{\sin(v\lambda)}{v\lambda}\,dv \qquad (4.52c)$$

For the time being assume that $\phi_{R_k}(v)$ is available, then the integral in eq. 4.52c can be calculated using Simpson's rule between the zeros of the function $\frac{\sin(v\lambda)}{v\lambda}$. The number of points chosen between the zeros depends on how fast $\phi_{R_k}(v)$ varies. The integration is carried out until successive approximations to the integral differ by less than 10^{-7}.

Now we develop the procedure for evaluating $\phi_{R_k}(v)$ at the selected v values. We can write the characteristic functions $\phi_{w_0}(v)$, $\phi_{w_k}(v)$, and $\phi_{l_k}(v)$ as follows

$$\phi_{w_0}(v) = |\phi_{w_0}(v)|.\exp(j\theta_0(s)) \qquad (4.53a)$$

$$\phi_{w_k}(v) = |\phi_{w_k}(v)|.\exp(j\theta_k(s)) \qquad (4.53b)$$

$$\phi_{l_k}(v) = |\phi_{l_k}(v)|.\exp(j\theta_l(s)) \qquad (4.53c)$$

Where $|\phi_{w_0}(v)|$, $\theta_0(v)$, $|\phi_{w_k}(v)|$, $\theta_k(v)$, and $|\phi_{l_k}(v)|$, $\theta_l(v)$ are the magnitude and phase of $\phi_{w_0}(v)$, $\phi_{w_k}(v)$ and $\phi_{l_k}(v)$ respectively. Substituting the above in eq. 4.38 gives

$$|\phi_{l_k}(v)|.\exp(j\theta_l(v) = |\phi_{w_k}(v)|^S.|\phi_{w_0}(v)|^{R-S} \qquad (4.54)$$

$$.\exp(j(S\theta_R(v) + (R-S)\theta_0(v)))$$

It follows that

$$\phi_{R_k}(v) = |\phi_{l_k}(v)|\cos(\theta_l(v)$$

$$= |\phi_{w_k}(v)|^S.|\phi_{w_0}(v)|^{R-S}.\cos(S\theta_k(v)+(R-S)\theta_0(v)) \qquad (4.55)$$

We need to calculate the magnitude and phase of $\phi_{w_k}(v)$ and $\phi_{w_0}(v)$ at the required v values. We will describe the procedure for obtaining $\phi_{w_k}(v)$; $\phi_{w_0}(v)$ is obtained using an identical procedure with K=0. Now $\phi_{w_k}(v)$ is given by

$$\phi_{w_k}(v) = (2\pi C)^{-1/2} \int_0^\infty \frac{1}{\alpha}.\exp(-\frac{1}{2C}(\ln\alpha - (K-\frac{C}{2}-\ln R))^2)$$

$$.\exp(jv\alpha)d\alpha \qquad (4.56)$$

Define

$$\mu_k \triangleq K - \frac{C}{2} - \ln R \qquad (4.57a)$$

and

$$\sigma^2 \triangleq C \qquad (4.57b)$$

Substituting the above in eq. 4.56 gives

$$\phi_{w_k}(v) = (2\pi)^{-1/2} \int_0^{\infty} (\sigma\alpha)^{-1}.\exp(-\frac{1}{2}(\frac{\ln\alpha - \mu_k}{\sigma})^2)$$

$$.\exp(jv\alpha)d\alpha \qquad (4.58)$$

Using the substitution $\beta = \ln\alpha$ gives

$$\phi_{w_k}(v) = (2\pi\sigma^2)^{-1/2} \int_{-\infty}^{\infty} \exp(-\frac{1}{2}(\frac{\beta - \mu_k}{\sigma})^2)$$

$$.\exp(jve^{\beta})d\beta \qquad (4.59)$$

Since we need to start the numerical integration at a finite lower limit a suitable lower limit which results in negligible error must be found. Let χ be the desired lower limit then

$$\phi_{w_k}(v) = (2\pi\sigma^2)^{-1/2} \int_{-\infty}^{\chi} \exp(-\frac{1}{2}(\frac{\beta - \mu_k}{\sigma})^2).\exp(jve^{\beta})d\beta$$

$$+ (2\pi\sigma^2)^{-1/2} \int_{\chi}^{\infty} \exp(-\frac{1}{2}(\frac{\beta - \mu_k}{\sigma})^2).\exp(jve^{\beta})d\beta \qquad (4.60)$$

Then the error E is

$$E = (2\pi\sigma^2)^{-1/2} \int_{-\infty}^{\chi} \exp(-\frac{1}{2}(\frac{\beta - \mu_k}{\sigma})^2).\exp(jve^{\beta})d\beta \qquad (4.61)$$

and

$$|E| \leq (2\pi\sigma^2)^{-1/2} \int_{-\infty}^{\chi} \exp(-\frac{1}{2}(\frac{\beta - \mu_k}{\sigma})^2)d\beta \qquad (4.62)$$

if we let $\chi = -6\sigma + \mu_k$, we obtain

$$|E| \leq (2\pi\sigma^2)^{-1/2} \int_{-\infty}^{-6\sigma+\mu_k} \exp(-\frac{1}{2}(\frac{\beta - \mu_k}{\sigma})^2)d\beta \qquad (4.63a)$$

using the substitution $x = \frac{\beta - \mu_k}{\sigma}$ we get

$$|E| \leq (2\pi)^{-1/2} \int_{-\infty}^{-6} \exp(-x^2/2)dx \approx 10^{-9} \qquad (4.63b)$$

This error is smaller than the quantization error introduced on the machine that was used for the calculation.

Let $\phi_{w_{kR}}(v)$ and $\phi_{w_{kI}}(v)$ be the real and imaginary parts of $\phi_{w_k}(v)$, from eq. 4.59 with χ substituted for $-\infty$, we obtain

$$\phi_{w_{kR}}(v) = (2\pi\sigma^2)^{-1/2} \int_{-6\sigma+\mu_k}^{\infty} \exp(-\frac{1}{2}(\frac{\beta - \mu_k}{\sigma})^2) \cdot \cos(ve^{\beta})d\beta \qquad (4.64a)$$

$$\phi_{w_{kI}}(v) = (2\pi\sigma^2)^{-1/2} \int_{-6\sigma+\mu_k}^{\infty} \exp(-\frac{1}{2}(\frac{\beta - \mu_k}{\sigma})^2) \cdot \sin(ve^{\beta})d\beta \qquad (4.64b)$$

Eqs. 4.64a & 4.64b were evaluated using a 5 point Gaussian integration procedure [35]. From $-6\sigma+\mu_k$ to the first zero of $\underset{\sin}{\cos}\{ve^{\beta}\}$ the 5 point gauss-quadrature procedure was applied over steps of $\sigma/4$. Thereafter the integration was performed between successive zeros of $\underset{\sin}{\cos}\{ve^{\beta}\}$. The integration was continued until the difference betweeen successive approximations to the integral became less than 10^{-7}. The R.O.C. curves so obtained are plotted in fig. 4.1.

4.3.5 Monte-Carlo Methods for Evaluating the R.O.C.

Monte Carlo simulation methods were used to confirm the

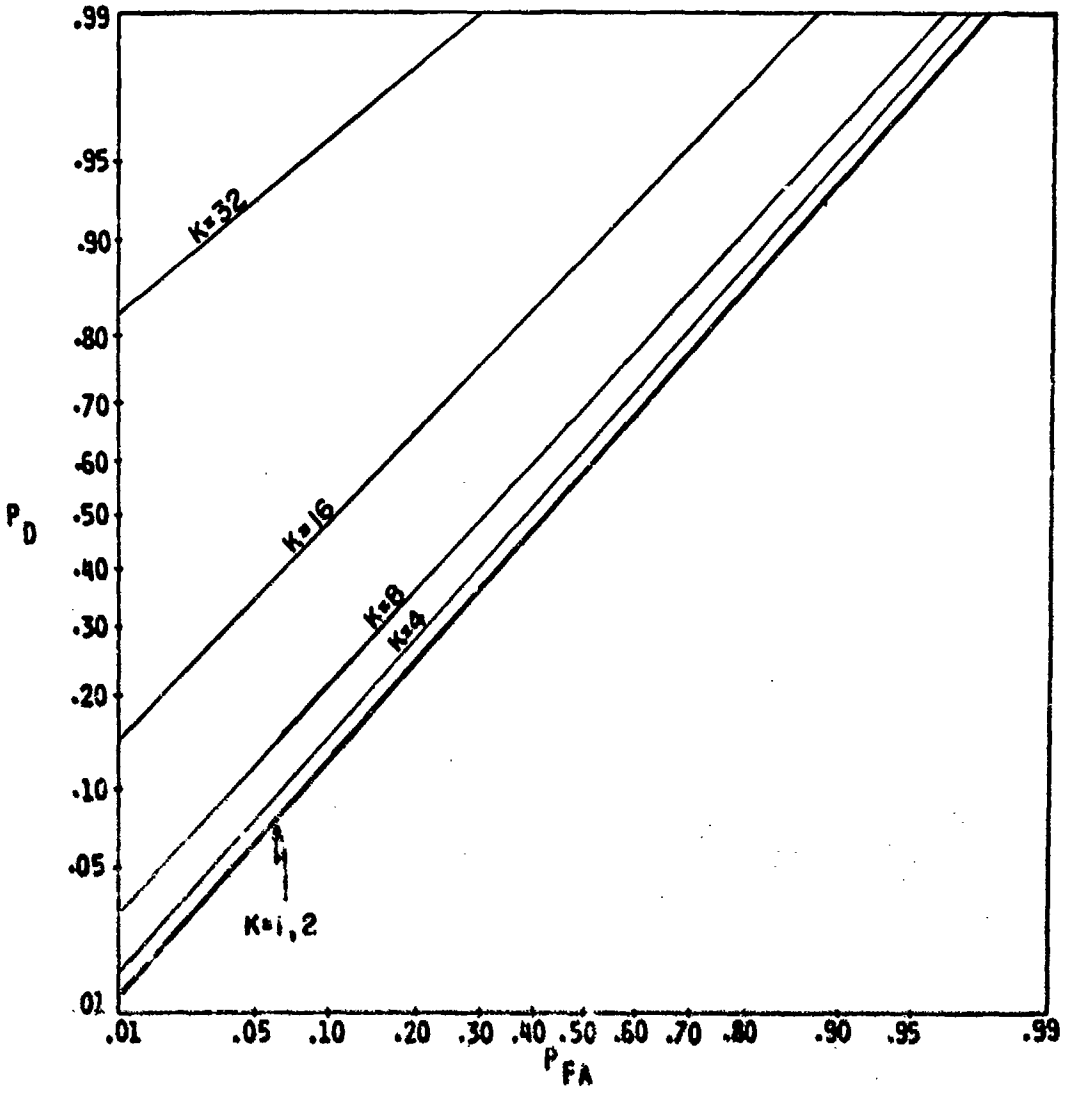

Fig. 4.1 R.O.C. curves for the Extended M-Orthogonal signals for K=1,2,4,8,16,32.

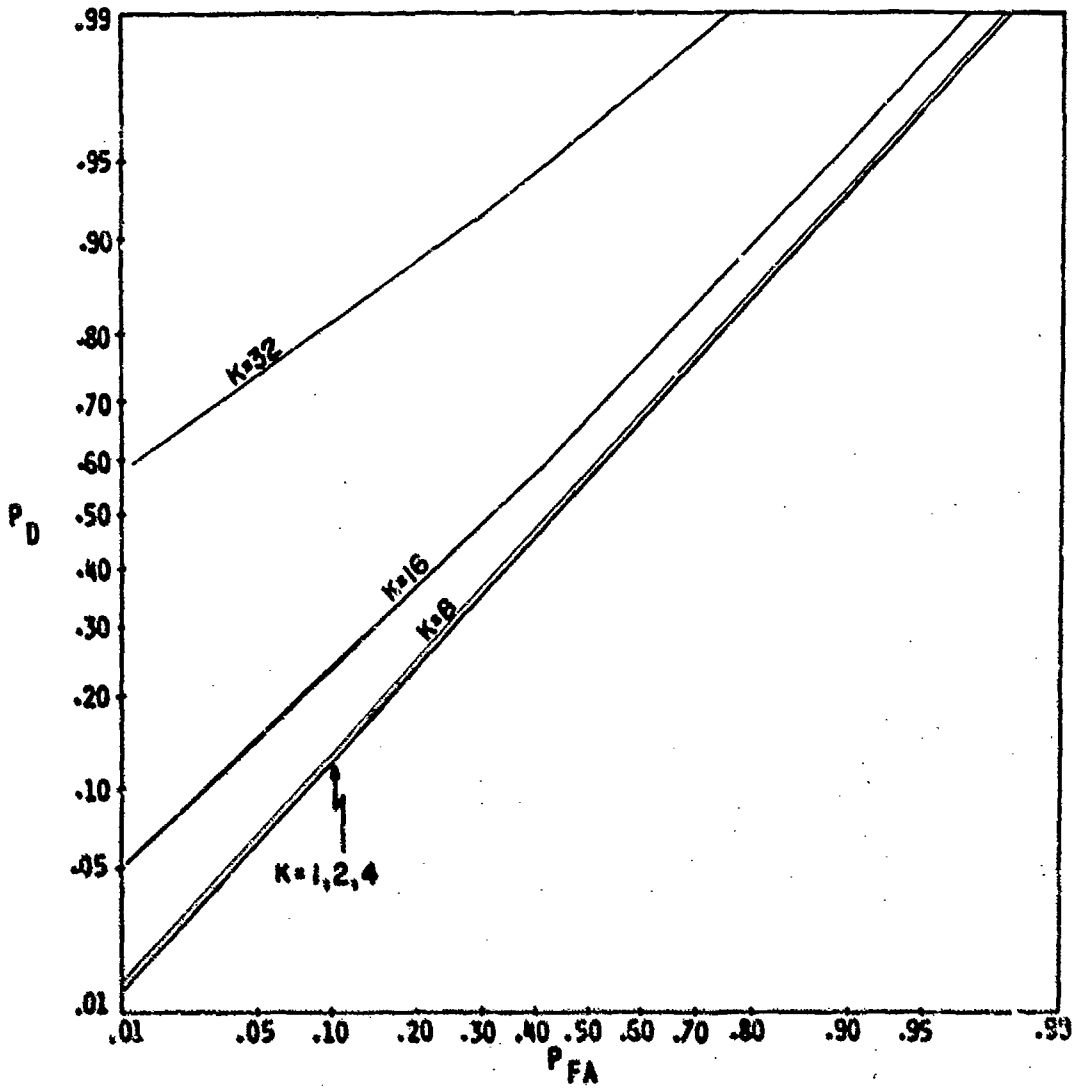

Fig. 4.2 R.O.C. curves for the modified Extended N-Orthogonal signals for K=1,2,4,8,16,32.

results obtained in fig. 4.1. The procedure is breifly discussed here. Basically a decision making device is simulated. The device sees random variables with the distribution of either $z(y|H_0)$ or $z(y|H_1)$. According to a predefined threshold the device either accepts or rejects the H_1 hypothesis. The probability of false alarm for a given threshold level is then estimated by dividing the number of $z(y|H_0)$ r.v.'s for which H_1 is accepted by the total number of $z(y|H_0)$ r.v.'s generated. A similar procedure using $z(y|H_1)$ r.v.'s gives the probability of detection. The procedure is repeated for as many threshold levels as points are desired on the R.O.C. curve. Our simulation evaluated 31 points on the R.O.C. curve based on 10,000 trials each.

The analysis in the previous was restricted to what we had termed standard EMOS. This was done primarily for analytic and computational simplicity. Monte-Carlo methods allow us to evaluate the R.O.C. curves for the modified EMOS. This was done for the following parameter values L=8192, C=64, R=128, s=1 and for K_1=1,2,4,8,16,32. The R.O.C. curves so obtained are given in fig. 4.2.

4.4 Summary

The R.O.C. curves obtained in figs. 4.1 & 4.2 suggest that when the design signals are such that the number of signal cells/row that are common to the true signal is small, the quality of detection is poor. The R.O.C. curves in fig. 4.2 in some sense provide a lower bound to perfomance in that we assume that localizing some of the signal bearing cells does not provide any information about the other signal bearing cells in the ambiguity plane. We see that in this case it is necessary to localize approximately half the signal bearing cells to obtain performance that is substantially better than chance. The R.O.C. curves in fig. 4.1 assume that localized signal

cells provide some information about the other signal cells in the ambiguity plane. We see that performance substantially better than chance is obtained when a quarter to a half of the signal cells have been localized. The above conclusions are based on the fact that no single signal bearing cell dominates the ambiguity diagram. The EMOS method also provides us with a technique for combining the information in the ambiguity diagram for detection purposes.

CHAPTER V

PERIODIC RANDOM SEQUENCES AND THE SECOND ABSTRACTION

As stated earlier, the MN peaks in the ambiguity diagram are generated by M+N independent sets of doppler and delay parameters. Two of the questions addressed in this chapter are

1) Should the receiver treat the MN peaks as independent entities or as being generated from M+N independent parameter sets? In other words should the receiver have MN degrees of freedom or M+N degrees of freedom?

2) Does one approach offer a significant improvement in performance over the other?

There is no simple or direct way of answering these questions. Our technique is to study a solvable abstraction that captures the essence of the above problem. To construct the abstraction we use the notion of Periodic Random Sequences. In Sect. 5.1 Periodic Random Sequences [PRS] are introduced and a framework for the abstract problem is established. The following sections deal with the theory of detection of Periodic Random Sequences in some detail. After this digression, the abstract problem is considerd in Sect. 5.4.

5.1 Periodic Random Sequences

We define a sequence p(n) to be periodic random with

period P if it satisfies the following two properties

$$1.\ p(n) \sim N(0,\sigma^2)\ \text{i.i.d.}\ 0 \le n \le P-1 \tag{5.1}$$

$$2.\ p(n) = p((n)\text{mod}P)\ \text{all}\ n. \tag{5.2}$$

Of course in general a PRS need not have independent or gaussian samples and the samples may not necessarily be zero mean. However, unless otherwise stated, by a PRS we will mean a sequence that satisfies the above properties. The autocorrelation function $R_p(k)=E\{p(n)p(n+k)\}$ of a PRS with period P is also periodic with period P

$$R_p(k)=\begin{cases}\sigma^2 & (k)\text{mod}P = 0\\ 0 & \text{o.w.}\end{cases} \tag{5.3}$$

Consider a signal s(n) made up of two independent PRS's, $p_1(n)$ and $p_2(n)$ with periods P_1 and P_2 respectively, that is $s(n)=p_1(n)+p_2(n)$. Assume that P_1 and P_2 are relatively prime and that our observation consists of $L=P_1.P_2$ samples and consider the detection problem in which s(n) is received in additive noise. Now the $P_1.P_2$ samples in the observation are really generated by P_1+P_2 independent samples. This situation is analogous to that of the M.N peaks in the ambiguity diagram being generated from M+N independent parameter sets. In Sect. 5.3 we will study the detection of s(n) (as described above) in noise based on two design hypotheses, one based on $P_1.P_2$ independent samples and the other based on P_1+P_2 independent samples. Now we study the detection of Periodic Random Sequences in noise.

5.2 Detection of one PRS of Known Period in Gaussian Noise

Let the observation be a vector $\underline{y}$ of length L, $\underline{y}=(y_0,y_1,\ldots,y_{L-1})^T$. The statistics of $\underline{y}$ under H_0 and the

H_1 hypotheses are

$$H_0 : y_i = n(i) \ , \ n(i) \sim N(0,1) \text{ i.i.d.} \tag{5.4a}$$

$$H_1 : y_i = p_1(i) + n(i) \ , \ \underline{p}_1 \text{ and } \underline{n} \text{ independent} \tag{5.4b}$$

where $p_1(i)$ is a PRS with period P_1 and $p_1(i) \sim N(0,A_1)$. We assume P_1 divides L, i.e. $L_1.P_1=L$, where L_1 is the number of periods of $p_1(i)$ in the observation. Let R be the autocorrelation matrix of the observation under the signal+noise hypothesis, $R=E(\underline{y}.\underline{y}^T|H_1)$. For now assume that R^{-1} exists, so we may write down the probability density function of the observation under the two hypotheses

$$f(\underline{y}|H_0) = (\frac{1}{2\pi})^{L/2}.\exp(-\underline{y}^T\underline{y}/2) \tag{5.5a}$$

$$f(\underline{y}|H_1) = (\frac{1}{2\pi})^{L/2}.(\frac{1}{|R|})^{1/2}.\exp(-\underline{y}^TR^{-1}\underline{y}/2) \tag{5.5b}$$

where $|R|$ is the determinant of R. From eq. 5.5 it follows that the likelihood ratio $\ell(\underline{y})$ and the log-likelihhod ratio $z(\underline{y})$ of the observation are given by

$$\ell(\underline{y}|\beta) = (\frac{1}{|R|})^{1/2}.\exp(\underline{y}^T(I-R^{-1})\underline{y}/2) \tag{5.6a}$$

$$z(y|\beta) = \tfrac{1}{2}\underline{y}^T(I-R^{-1})\underline{y} - \tfrac{1}{2}\ln(|R|) \tag{5.6b}$$

where $\beta = \{A_1,P_1\}$. The likelihood and log-likelihood ratios are conditional to the period and the signal power.

Before proceeding further we need to take a closer look at the autocorrelation matrix R

$$R = E(\underline{y}.\underline{y}^T|H_1) \tag{5.7}$$
$$= R_n + R_{p_1}$$

Where R_n is the noise autocorrelation matrix and R_{p_1} is the autocorrelation matrix of PRS p_1, the above decomposition follows from the independence of noise and PRS p_1. Now

$$R_n = I_L \text{ , the L×L identity} \tag{5.8a}$$

$$R_{p_1} = A_1\{\delta(|i-j| \bmod P_1)\} \quad i,j=0,1,\ldots,L-1 \tag{5.8b}$$

Of course R is Hermitian symmetric, and, as such is similar to a diagonal matrix [31 pp. 201-202]. Due to PRS p_1, R also has the interesting property that each row of R is a right circular shift by 1 of the row immediately above it. Matrices with this property are called circulant or cyclic matrices [32,33 pp. 133-139].

5.2.1 Properties of Circulant Matrices

Since the theory developed in this chapter relies heavily on the properties of circulant matrices, some of the useful properties are summarized here. Let C_n be a n×n circulant matrix, then

$$C_n = \begin{vmatrix} c_0 & c_1 & c_2 \ldots c_{n-1} \\ c_{n-1} & c_0 & c_1 \ldots c_{n-2} \\ c_{n-2} & c_{n-1} & c_0 \ldots c_{n-3} \\ \cdot & & \cdot \\ \cdot & & \cdot \\ \cdot & & \cdot \\ c_1 & c_2 & c_3 \ldots c_0 \end{vmatrix} \tag{5.9}$$

Circulant matrices are a special case of Toeplitz matrices. The matrix may easily be diagonalized. Let ψ_r be the rth eigenvalue and $\underline{u}_r$ the rth eigenvector, then ψ_r and $\underline{u}_r$ are the solutions of

$$C_n \cdot \underline{u}_r = \psi_r \cdot \underline{u}_r \tag{5.10a}$$

or equivalently of the following system of difference equations

$$\sum_{k=0}^{m-1} c_{n-m+k} u_{rk} + \sum_{k=m}^{n-1} c_{k-m} u_{rk} = \psi_r u_{rm} \quad , \quad \begin{matrix} m = 0,1,\ldots,n-1 \\ r = 0,1,\ldots,n-1 \end{matrix} \tag{5.10b}$$

where ψ_r is the rth eigenvalue and u_{rk} is the kth element of the rth eigenvector. It is easily verified [32,33 pp. 133-139] that

$$\psi_r = \sum_{k=0}^{n-1} c_k . \exp(-j2\pi rk/n) \quad , \quad r = 0,1\ldots,n-1 \tag{5.11a}$$

$$\underline{u}_r = (\tfrac{1}{n})^{1/2} . (1, \exp(-j2\pi r/n), \ldots, \exp(-j2\pi(n-1)r/n))^T \tag{5.11b}$$
$$r = 0,1,\ldots,n-1$$

The sequence of eigenvalues $\psi_0, \psi_1, \ldots, \psi_{n-1}$ is the Discrete Fourier Transform of the first row of the matrix C_n and the eigenvectors are independent of the elements of C_n. Now define the matrices

$$U_n \triangleq \{\underline{u}_0 | \underline{u}_1 | \ldots | \underline{u}_{n-1}\} \tag{5.12a}$$

$$\Psi_n \triangleq \text{diag}(\psi_0, \psi_1, \ldots, \psi_{n-1}) \tag{5.12b}$$

The matrix U_n is a unitary matrix, so $U_n^* = \text{conj}[U_n^T] = U_n^{-1}$. And C_n is unitarily similar to the diagonal matrix Ψ_n, that is C_n is a normal matrix [31 pp. 201-202].

$$C_n = U_n \Psi_n U_n^* \tag{5.13a}$$

$$C_n^{-1} = U_n \Psi_n^{-1} U_n^* \tag{5.13b}$$

C_n^{-1} will exist if and only if all the eigenvalues are non-zero.

5.2.2 Eigenvalue Eigenvector Decomposition of R

Let R(n) be the first row of the matrix R ,then

$$R(n) = \delta(n) + A_1\delta((n) \bmod P_1) \ , \ n = 0,1,\ldots,L-1 \qquad (5.14)$$

$$= \delta(n) + A_1 \sum_{l=0}^{L_1-1} \delta(n-lP_1) \ , \ L_1 = \frac{L}{P_1}$$

The sequence of eigenvalues $\psi(m)$ of R is given by

$$\psi(m) = \sum_{n=0}^{L-1} R(n).\exp(-j2\pi nm/L) \qquad (5.15)$$

$$= \sum_{n=0}^{L-1} \delta(n).\exp(-j2\pi nm/L) +$$

$$A_1 \sum_{n=0}^{L-1} \sum_{l=0}^{L_1-1} \delta(n-lP_1).\exp(-j2\pi nm/L)$$

$$= \begin{cases} 1 + A_1L_1 \ , \ m = 0,L_1,2L_1,\ldots,(P_1-1)L_1 \\ 1 \quad , \ o.w \end{cases}$$

Let $\Psi_L = \mathrm{diag}(\psi(0),\psi(1),\ldots,\psi(L-1))$, be the diagonal matrix of the eigenvalues of R and U_L the unitary matrix of eigenvectors of R. Then

$$R = U_L\Psi_L U_L^* \qquad (5.16)$$

and since all eigenvalues are non zero

$$R^{-1} = U_L \Psi_L^{-1} U_L^* \tag{5.17}$$

5.2.3 The Optimum Detector

We had derived the log-likelihhod ratio $z(\underline{y}|\beta)$ in eq. 5.6b. Substituting for $|R|$ and R^{-1} in eq. 5.6b and using the fact that $U_L U_L^* = I$ we obtain

$$z(\underline{y}|\beta) = \tfrac{1}{2}\underline{y}^T U_L (I - \Psi_L^{-1}) U_L^* \underline{y} - \tfrac{1}{2}\ln|\Psi_L| \tag{5.18a}$$

$$\text{where } |\Psi_L| = \text{Det } \Psi_L = \text{Det } R = (1 + A_1 L_1)^{P_1} \tag{5.18b}$$

Denote the diagonal matrix $I - \Psi_L^{-1}$ by θ_L and let $\theta(m)$ denote the sequence of the diagonal entries of θ_L, $\theta(m)$ is then simply given by

$$\theta(m) = 1 - \frac{1}{\Psi(m)}$$

$$= \begin{cases} A_1 L_1/(1+A_1 L_1) , & m = 0, L_1, \ldots, (P_1-1)L_1 \\ 0 \quad \text{o.w.} \end{cases} \tag{5.19}$$

For brevity define $c_1 \triangleq A_1 L_1/(1+A_1 L_1)$

So now $z(\underline{y}|\beta)$ is given by

$$z(\underline{y}|\beta) = \tfrac{1}{2}\underline{y}^T U_L \theta_L U_L^* \underline{y} - \tfrac{1}{2}\ln|\Psi_L| \tag{5.20}$$

Now there are two options available to us 1) Calculate the vectors $\underline{y}^T U_L$ and $U_L^* \underline{y}$ first or 2) Calculate the matrix $U_L \theta_L U_L^*$ first. We will consider both options, the first option gives us better insight and the second leads to a

practical detector structure.

5.2.3.1 Optimum Detector in the Frequency Domain

Define the row vector $\underline{Y}$ as follows

$$(\frac{1}{L})^{1/2}\underline{Y} \triangleq \underline{y}^T U_L \tag{5.21a}$$

it follows that

$$(\frac{1}{L})^{1/2}\underline{Y}^* = U_L^*\underline{y} \tag{5.21b}$$

The row vector $\underline{Y}$ is simply the DFT of $\underline{y}$ and with $\underline{y}$ real, $\underline{Y}^*$ is the conjugate transpose of $\underline{Y}$. So $z(\underline{y}|\beta)$ is equivalent to the statisitc $z(\underline{Y}|\beta)$ given by

$$z(\underline{Y}|\beta) = \frac{1}{2L}\cdot\underline{Y}\theta_L\underline{Y}^* - \frac{1}{2}\ln|\Psi_L| \tag{5.22}$$

If we assume that the period P_i and the power level A_i are known an equivalent detection statistic is $\phi(\underline{Y})$

$$\phi(\underline{Y}|\beta) \triangleq \frac{1}{2L}\cdot\underline{Y}\theta_L\underline{Y}^* \tag{5.23}$$

Since θ_L is a diagonal matrix, we may simplify the above equation as follows, let Y(m) be the mth element of $\underline{Y}$ then

$$\phi(\underline{Y}|\beta) = \frac{1}{2L}\sum_{m=0}^{L-1}\theta(m)|Y(m)|^2 \tag{5.24a}$$

$$= \sum_{m=0}^{L-1}|\gamma(m)Y(m)|^2 \tag{5.24b}$$

where $\gamma(m) \triangleq (\frac{1}{2L}\theta(m))^{1/2}$ (5.24c)

Detection based on $\Phi(\underline{Y}|\beta)$ is similar to an energy detector, we will call it a " frequency selective energy detector " or FSED. In fact $\gamma(m)$ defines a digital comb filter [34 p. 241]. A block diagram of the above detector is given in fig. 5.1. We now examine the sequence Y(m) under both the noise alone and the signal + noise hypotheses.

$$H_0 : y(i) = n(i) , \ i = 0,1,\ldots,L-1 \quad \& \ Y(m) = N(m) , \ m = 0,1,\ldots,L-1 \tag{5.26a}$$

$$H_1 : y(i) = p_1(i) + n(i) , \ i = 0,1,\ldots L-1 \quad \& \ Y(m) = P_1(m) + N(m) , \ m = 0,1,\ldots,L-1 \tag{5.26b}$$

Where N(m) is the L point DFT of the observed noise sequence and $P_1(m)$ is the L point DFT of the PRS $p_1(i)$. Define $\tilde{p}_1(i)$ to be one period of PRS $p_1(i)$.

$$\tilde{p}_1(i) = \begin{cases} p_1(i) , & i = 0,1,\ldots,P_1-1 \\ 0 , & \text{o.w.} \end{cases} \tag{5.27}$$

then

$$P_1(m) = \sum_{i=0}^{L-1} p_1(i).\exp(-j2\pi im/L) \tag{5.28}$$

$$= \sum_{n=0}^{L_1-1} \sum_{i=nP_1}^{(n+1)P_1-1} \tilde{p}_1(i-nP_1).\exp(-j2\pi im/L)$$

and using the substitution $s = i-nP_1$, we get

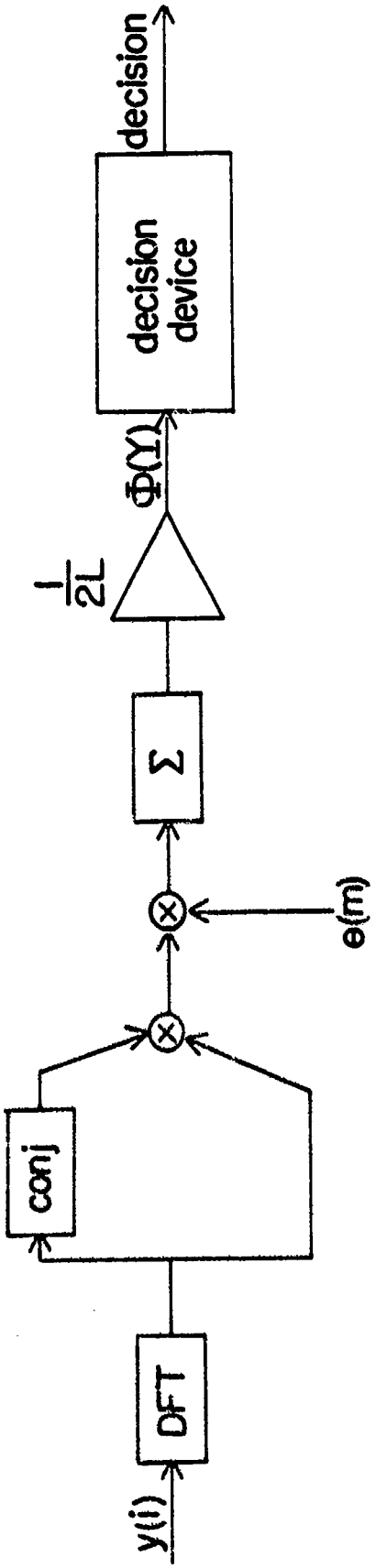

Fig. 5.1 Block diagram of the Frequency Selective Energy Detector.

$$= \sum_{n=0}^{L_1-1} \sum_{s=0}^{P_1-1} \tilde{p}_1(s).\exp(-j2\pi(s+nP_1)m/L)$$

$$= \sum_{s=0}^{P_1-1} \tilde{p}_1(s).\exp(-j2\pi sm/L).\sum_{n=0}^{L_1-1} \exp(-j2\pi nm/L_1)$$

$$\text{now} \sum_{n=0}^{L_1-1} \exp(-j2\pi nm/L_1) = \begin{cases} L_1 & , m = 0,L_1,\ldots,(P_1-1)L_1 \\ 0 & , \text{o.w.} \end{cases}$$

So

$$P_1(m) = \begin{cases} L_1 \sum_{s=0}^{P_1-1} \tilde{p}_1(s).\exp(-j2\pi sm/L) & , m=0,L_1,\ldots,(P_1-1)L_1 \\ 0 & , \text{o.w.} \end{cases} \qquad (5.29)$$

The above shows that under H_1, $Y(m)$ has signal components only for $m=0,L_1,\ldots,(P_1-1)L_1$. This is intuitively pleasing because $\theta(m)$ is non-zero for precisely the above m's. So the frequency selective energy detector rejects the "out of band noise."

5.2.3.2 Optimum Detector in the Time Domain

Now we first calculate the matrix $U_L\theta_L U_L^*$. This will lead to a time domain solution for the detector. Let $Q \triangleq U_L\theta_L U_L^*$; then because θ_L is diagonal Q is circulant. So the matrix Q may be determined in terms of its first row Q(n), in fact, the first row is just the inverse DFT of the sequence $\theta(m)$.

$$Q(n) = \frac{1}{L}\sum_{m=0}^{L-1}\theta(m).\exp(j2\pi nm/L) \qquad (5.30)$$

$$= (c_1/L).\sum_{m=0}^{L-1}\sum_{r=0}^{P_1-1}\delta(m-rL_1).\exp(j2\pi nm/L)$$

$$= (c_1/L).\sum_{r=0}^{P_1-1}\exp(j2\pi nr/L_1)$$

$$= \begin{cases} c_1P_1/L\ , & n = 0,P_1,\ldots,(L_1-1)P_1 \\ 0\ , & \text{o.w.} \end{cases}$$

So $z(\underline{y}|\beta)$ is given by

$$z(\underline{y}|\beta) = \frac{1}{2}\underline{y}^T Q\underline{y} - \frac{1}{2}\ln|\Psi_L| \qquad (5.31a)$$

$$= \left(\frac{c_1P_1}{2L}\right).\sum_{j=0}^{P_1-1}\left(\sum_{k=0}^{L_1-1}y(j+kP_1)\right)^2 - \frac{1}{2}\ln|\Psi_L| \qquad (5.31b)$$

If we assume that the signal power and period are known then an equivalent detection statistic is $\phi(\underline{y})$ giver by

$$\phi(\underline{y}|\beta) = \left(\frac{c_1P_1}{2L}\right).\sum_{j=0}^{P_1-1}\left(\sum_{k=0}^{L_1-1}y(j+kP_1)\right)^2 \qquad (5.32)$$

We call the detector that uses $\phi(\underline{y}|\beta)$ as the detection statistic the circulating average energy detector (CAED) or the periodic averaging energy detector. Fig. 5.2a is a block diagram of the generic signal processor that produces $\phi(\underline{y}|\beta)$ with the parameters P_1, L_1 and A_1. The "analog shift register" is initially set to zero, once the desired number

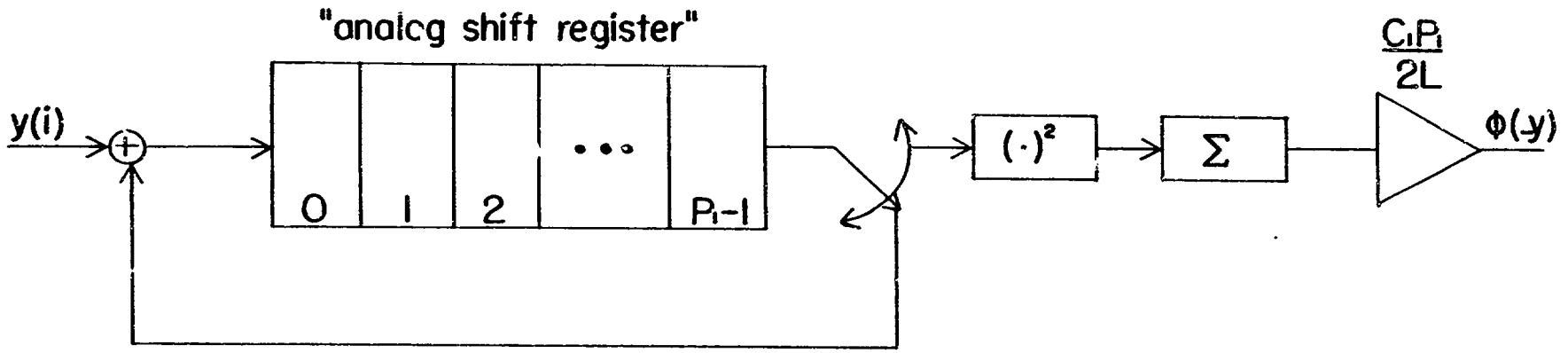

Fig. 5.2a Block diagram of the Circulating Average Energy Detector Signal Processor with Paramaters P_1, L_1, A_1.

of periods (L_1) have been measured the switch feeds the output of the "analog shift registor" into the squarer. In future we will call this signal processor the CAEDSP with the appropriate parameter values denoted in brackets. Fig. 5.2b is a block diagram of the above CAED.

5.2.4 Performance Evaluation of the Optimum Detector

First of all note that $\phi(\underline{y}|\beta)$ and $\Phi(\underline{Y}|\beta)$ are the same random variable, hence decisions based on $\phi(\underline{y}|\beta)$ are equivalent to decisions based on $\Phi(\underline{Y}|\beta)$ and they result in identical performance. In this section we derive the probability density function for $\phi(\underline{y}|\beta)$ and $z(\underline{y}|\beta)$ and compare the performance of the optimum detector with that of the total energy detector.

5.2.4.1 Derivation of the p.d.f. of $\phi(y)$ and $z(y|\beta)$

Let $\alpha(j) = +\left(\frac{c_1 P_1}{2L}\right)^{1/2} \cdot \sum_{k=0}^{L_1-1} y(j+kP_1)$, then $\alpha(j)$ is normal. The statistics of $\alpha(j)$ are derived below

$$E[\alpha(j)|H_k] = 0 \ , \ k = 0,1 \tag{5.33a}$$

$$E[\alpha^2(j)|H_0] = \left(\frac{c_1 P_1}{2L}\right) \cdot \sum_{k=0}^{L_1-1} \sum_{s=0}^{L_1-1} E[y(j+kP_1)y(j+sP_1)|H_0] \tag{5.33b}$$

$$= \left(\frac{c_1 P_1}{2L}\right) \cdot \sum_{k=0}^{L_1-1} \sum_{s=0}^{L_1-1} \delta((k-s)P_1)$$

$$= c_1 P_1 L_1 / 2L = c_1/2 \triangleq \sigma_0^2$$

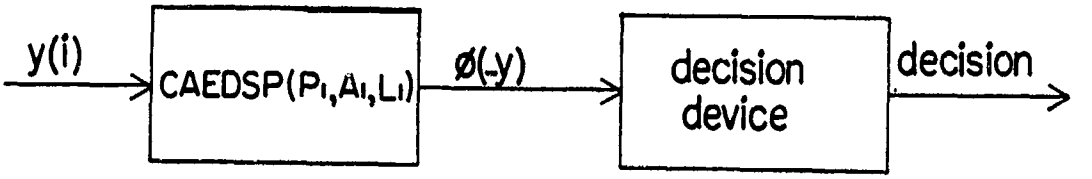

Fig. 5.2b Block diagram of the Circulating Average Energy Detector.

$$E[\alpha^2(j)|H_1] = \left(\frac{c_1 P_1}{2L}\right).\sum_{k=0}^{L_1-1}\sum_{s=0}^{L_1-1} E[y(j+kP_1)y(j+sP_1)|H_1] \quad (5.33c)$$

$$= \left(\frac{c_1 P_1}{2L}\right).\sum_{k=0}^{L_1-1}\sum_{s=0}^{L_1-1} E[n(j+kP_1)n(j+sP_1) + \tilde{p}_1^2(j)]$$

$$= \left(\frac{c_1 P_1}{2L}\right).(L_1 + A_1 L_1^2)$$

$$= (c_1/2).(1 + A_1 L_1) = A_1 L_1/2 \triangleq \sigma_1^2$$

So we have

$$f(\alpha(j)|H_k) = (\frac{1}{2\pi})^{1/2}.(\frac{1}{\sigma_k}).\exp(-\frac{\alpha^2(j)}{2\sigma_k^2}) \quad , \quad k=0,1 \qquad (5.34)$$

Now let $\gamma(j) = \alpha^2(j)$, then it follows that

$$f(\gamma(j)|H_k) = \begin{cases} (\frac{1}{2\pi\gamma(j)\sigma_k^2})^{1/2}.\exp(-\frac{\gamma(j)}{2\sigma_k^2}) & , \ \gamma(j)>0 \\ 0 \quad , \ \text{o.w.} \end{cases} \qquad (5.35)$$

which is a gamma density function with one degree of freedom. Now the $\gamma(j)$'s are independent and identically distributed under both hypotheses. Since $\phi(\underline{y}|\beta) = \sum_{j=0}^{P_1-1} \gamma(j)$, $\phi(\underline{y}|\beta)$ also has a gamma density but with P_1 degrees of freedom.

$$f(\phi|H_k) = \begin{cases} \frac{\phi^{(P_1/2)-1}}{(2\sigma_k^2)^{P_1/2}.\Gamma(P_1/2)}.\exp(-\frac{\phi}{2\sigma_k^2}) & , \ \phi > 0 \\ 0 \quad , \ \text{o.w.} \end{cases} \qquad (5.36)$$

Where $\Gamma(.)$ is the gamma function [35 pp. 255-263]. Now $z(\underline{y}|\beta) = \frac{1}{2}\phi(\underline{y}|\beta) - \frac{1}{2}.\ln|\Psi_L|$, substituting for $|\Psi_L|$ gives $z(\underline{y}|\beta) = \frac{1}{2}\phi(\underline{y}|\beta) - (P_1/2).\ln(1+A_1L_1)$. If we let $b_1 \triangleq (P_1/2).\ln(1+A_1L_1)$ then it follows that

$$f(z|H_k) = \begin{cases} \frac{(z+b_1)^{(P_1/2)-1}}{(2\sigma_k^2)^{P_1/2}.\Gamma(P_1/2)}.\exp(-\frac{z+b_1}{2\sigma_k^2}) & , \ z>-b_1 \\ 0 \quad , \ \text{o.w.} \end{cases} \qquad (5.37)$$

If u is a threshold level for z, the probabilities of

detection and false alarm are given by

$$P_D = \int_u^\infty f(z|H_1)dz$$

$$= \int_u^\infty \frac{(z+b_1)^{(P_1/2)-1}}{(2\sigma_1^2)^{P_1/2}.\Gamma(P_1/2)}.\exp(-\frac{z+b_1}{2\sigma_1^2})dz \qquad (5.38a)$$

using the substitution $w = z+b_1$, we obtain

$$P_D = \int_{u+b_1}^\infty \frac{w^{(P_1/2)-1}}{(2\sigma_1^2)^{P_1/2}.\Gamma(P_1/2)}.\exp(-\frac{w}{2\sigma_1^2})dw \qquad (5.38b)$$

$$= \Gamma(\frac{P_1}{2}, \frac{u+b_1}{2\sigma_1^2})/\Gamma(P_1/2) \qquad (5.38c)$$

$$= 1 - \gamma(\frac{P_1}{2}, \frac{u+b_1}{2\sigma_1^2})/\Gamma(P_1/2) \qquad (5.38d)$$

Similarly

$$P_{FA} = \Gamma(\frac{P_1}{2}, \frac{u+b_1}{2\sigma_0^2})/\Gamma(P_1/2) \qquad (5.39a)$$

$$= 1 - \gamma(\frac{P_1}{2}, \frac{u+b_1}{2\sigma_0^2})/\Gamma(P_1/2) \qquad (5.39b)$$

$\Gamma(.,.)$ and $\gamma(.,.)$ are the incomplete gamma functions defined as [35 pp. 255-263]

$$\Gamma(\alpha,x) = \int_x^\infty t^{\alpha-1}.\exp(-t)dt \qquad (5.40a)$$

$$\gamma(\alpha,x) = \int_0^x t^{\alpha-1}.\exp(-t)dt \qquad (5.40b)$$

5.2.4.2 R.O.C. Curves and Comparison with Energy Detector

The energy detector is a sub-optimum detector, it would be optimum if the signal samples were independent. That is, it ignores the signal periodicity. So the energy detector is based on the following observation statistics

$$H_0 = y_i \sim N(0,1) \text{ i.i.d.} \tag{5.41a}$$

$$H_1' = y_i \sim N(0,1+A_1) \text{ i.i.d.} \tag{5.41b}$$

and

$$f(\underline{y}|H_0) = (\frac{1}{2\pi})^{L/2}.\exp(-\underline{y}^T\underline{y}/2) \tag{5.42a}$$

$$f(\underline{y}|H_1') = (\frac{1}{2\pi})^{L/2}.(\frac{1}{1+A_1})^{L/2}.\exp(-\frac{1}{2(1+A_1)}.\underline{y}^T\underline{y}) \tag{5.42b}$$

The likelihood ratio $\ell_{ed}(\underline{y})$ and the log-likelihood ratio $z_{ed}(\underline{y})$ are given by

$$\ell_{ed}(\underline{y}|A_1) = (\frac{1}{1+A_1})^{L/2}.\exp(-\frac{A_1}{2(1+A_1)}.\underline{y}^T\underline{y}) \tag{5.43a}$$

$$z_{ed}(\underline{y}|A_1) = \frac{A_1}{2(1+A_1)}.\sum_{i=0}^{L-1} y^2(i) - (L/2).\ln(1+A_1) \tag{5.43b}$$

$\sum_{i=0}^{L-1} y^2(i)$ is the total energy in the observation. Assuming signal power is known an equivalent detection statistic is $\eta(\underline{y})$ given by

$$\eta(\underline{y}) = \frac{A_1}{2(1+A_1)}.\sum_{i=0}^{L-1} y^2(i) \tag{5.44}$$

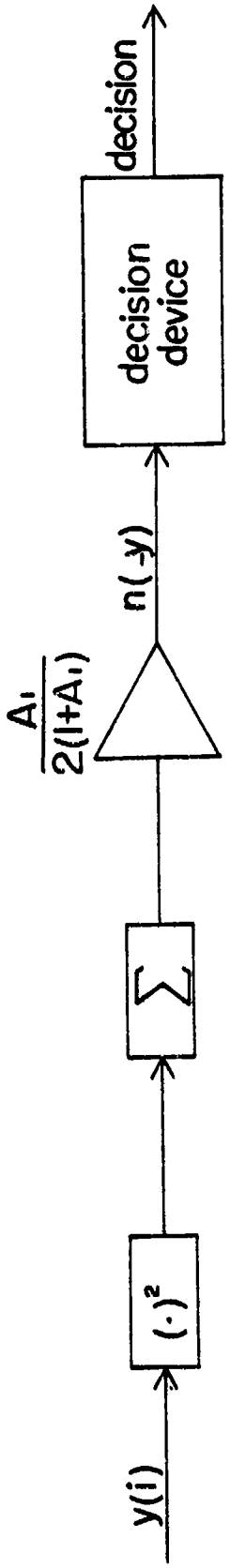

Fig. 5.3 Block diagram of the Energy Detector.

A block diagram for the energy detector is given in fig. 5.3. Under H_0, $\eta(\underline{y})$ and $z_{ed}(\underline{y})$ have gamma density functions. If we let $b_2 \triangleq (L/2).\ln(1+A_1)$, and with $\sigma_0^2=1$ we have

$$f(\eta|H_0) = \begin{cases} \dfrac{\eta^{(L/2)-1}}{(2\sigma_0^2)^{L/2}.\Gamma(L/2)}.\exp(-\dfrac{\eta}{2\sigma_0}) & , \eta > 0 \\ 0 & , \text{ o.w.} \end{cases} \qquad (5.45a)$$

$$f(z_{ed}|H_0) = \begin{cases} \dfrac{(z_{ed}+b_2)^{(L/2)-1}}{(2\sigma_0^2)^{L/2}.\Gamma(L/2)}.\exp(-\dfrac{z_{ed}+b_2}{2\sigma_0^2}) & , z_{ed} > -b_2 \\ 0 & , \text{ o.w.} \end{cases} \qquad (5.45b)$$

If eq. 5.41b were true, then under H_1', $\eta(\underline{y})$ and $z_{ed}(\underline{y})$ would also have density functions similar to eqs. 5.45a and 5.45b respectively; with σ_0^2 replaced by $\sigma_1^2=1+A_1$. If we assume that eq. 5.4b is true, then the density function of $\eta(\underline{y})$ and $z_{ed}(\underline{y})$ cannot easily be found because the terms in the summations of eq. 5.43b and 5.44 are not independent. However, it is still possible to compute some relevant statistics of $\eta(\underline{y})$ and $z_{ed}(\underline{y})$ under H_1 and the assumption that eq. 5.4b is true.

In fig. 5.4a the R.O.C. curves for the CAED are given for several signal power levels. Noise is assumed N(0,1). We assume L=1000, the signal periods range from 21 to 30 inclusive. The number of periods measured in an observation is the number of integer periods in a sample size of 1000. We have plotted the average probability of detection vs. the probability of false alarm. The average detection probability is obtained by finding the detection probability for each signal period for a given false alarm probability and then calculating the average of the detection probabilities. For comparison purposes in fig. 5.4b the R.O.C. curves for the ED are also given. The R.O.C.

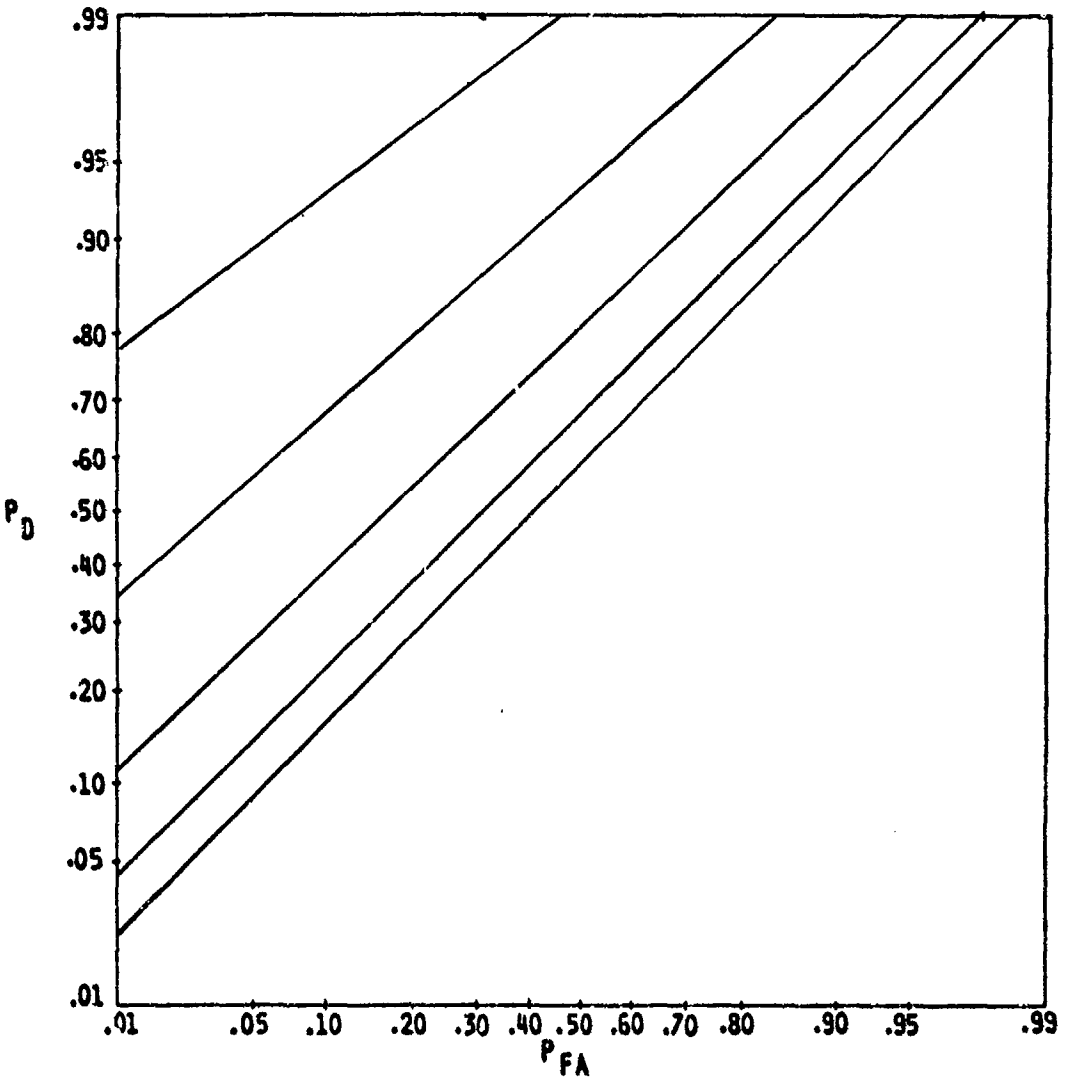

Fig. 5.4a Averaged R.O.C. curves for the CAED for signal power levels of .002, .004, .008, .016, .032.

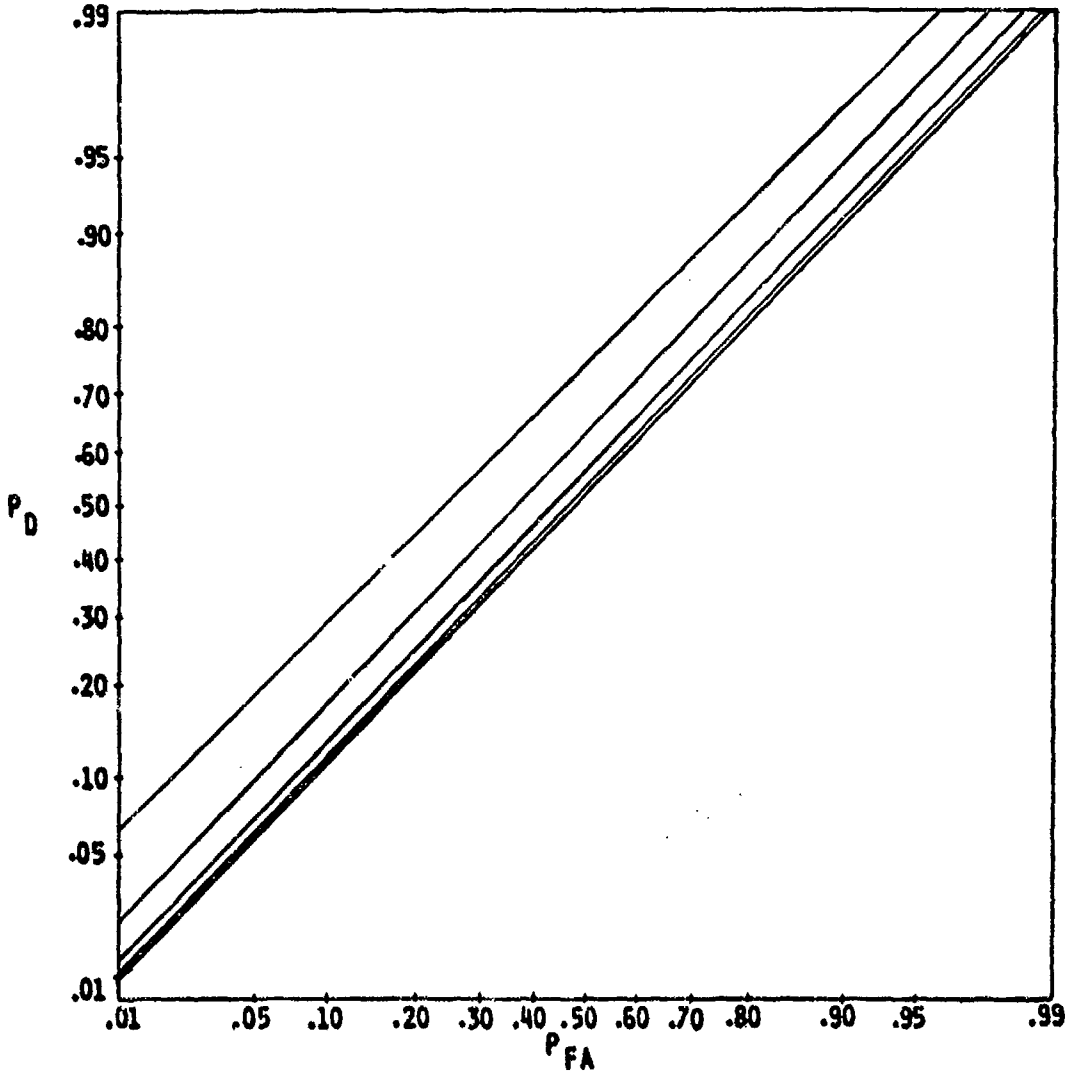

Fig. 5.4b R.O.C. curves for the ED with the same signal and noise statistics as in fig. 5.4a.

curves are obtained using Monte Carlo simulation methods. The details of the simulation are given in Appendix A.

Analytically we can compare the performance of the two detectors using the concept of normal detectability. As given in Chapter II the definition of normal detectability is valid for simple gaussian hypotheses. Here we assume the gamma densities of eqs. 5.36 and 5.44 are approximately gaussian. This will allow us to obtain approximate performance figures. The expression for normal detectabilty 'd' is repeated below

$$d \triangleq \frac{[\ E(z|H_1) - E(z|H_0)\ ]^2}{var(z)} \tag{5.46}$$

As defined d is a measure of the output SNR. We will look at both d and $d' = (d)^{1/2}$. For simple gaussian hypotheses var(z) is the same under each hypothesis. This is clearly not the case here. However if we assume that signal power is small then we can use the approximation $var(z|H_1) \approx var(z|H_0)$ [16]. Because ϕ differs from z by a constant we need only calculate $E[\phi|H_k]$, $k = 0,1$ and $var(\phi)$, similarly with the energy detector. For the normalized gamma density function f(x) the first and second moments are given by

$$f(x) = \frac{x^{p-1}}{\Gamma(p)}.\exp(-x) \ , \ 0 \leq x \leq \infty \tag{5.47a}$$

$$E(x) = \int_0^\infty \frac{x^p}{\Gamma(p)}.\exp(-x)dx = p \tag{5.47b}$$

$$E(x^2) = \int_0^\infty \frac{x^{p+1}}{\Gamma(p)}.\exp(-x)dx = p^2+p \tag{5.47c}$$

The first and second moments of the CAED detection statistic ϕ are now easily obtained.

$$E(\phi|H_k) = \int_0^\infty \phi.f(\phi|H_k)d\phi \tag{5.48a}$$

$$= \int_0^\infty (\frac{\phi}{2\sigma_k^2})^{P_1/2}.\frac{1}{\Gamma(P_1/2)}.\exp(-\frac{\phi}{2\sigma_k^2})d\phi$$

using the substitution $x = \frac{\phi}{2\sigma_k^2}$, we obtain

$$E(\phi|H_k) = 2\sigma_k^2.\int_0^\infty \frac{x^{P_1/2}}{\Gamma(P_1/2)}.\exp(-x)dx \tag{5.48b}$$

$$= \sigma_k^2 P_1$$

$$E(\phi^2|H_k) = \int_0^\infty \phi^2 f(\phi|H_k)d\phi \tag{5.48c}$$

$$= 2\sigma_k^2\int_0^\infty (\frac{\phi}{2\sigma_k^2})^{(P_1/2)+1}.\frac{1}{\Gamma(P_1/2)}.\exp(-\frac{\phi}{2\sigma_k^2})d\phi$$

using the same substitution as above we obtain

$$E(\phi^2|H_k) = (2\sigma_k^2)^2.\int_0^\infty \frac{x^{(P_1/2)+1}}{\Gamma(P_1/2)}.\exp(-x)dx \tag{5.48d}$$

$$= (2\sigma_k^2)^2.(\frac{P_1}{2} + \frac{P_1^2}{4})$$

and $var(\phi|H_k) = (2\sigma_k^2)^2.P_1/2$

From the above we can easily write the statistics under H_0 and H_1

$$E(\phi|H_0) = \sigma_0^2.P_1 \tag{5.49a}$$

$$= c_1 P_1/2$$

$$E(\phi|H_1) = \sigma_1^2.P_1 \qquad (5.49b)$$

$$= c_1P_1.(1+A_1L_1)/2$$

$$var(\phi|H_0) = (2\sigma_0^2)^2.P_1/2 \qquad (5.49c)$$

$$=c_1^2.P_1/2$$

$$var(\phi|H_1) = (2\sigma_1^2)^2.P_1/2 \qquad (5.49d)$$

$$= c_1^2.P_1(1+A_1L_1)^2/2$$

We can now obtain an expression for d by substituting the above in eq. 5.46

$$d_\phi = \frac{[c_1P_1(1+A_1L_1) - c_1P_1]^2}{2c_1^2P_1} \qquad (5.50)$$

$$= A_1^2L.L_1/2$$

Going through a similar set of calculations for the energy detector, we find

$$E(\eta|H_1) = A_1L/2 \qquad (5.51a)$$

$$E(\eta|H_0) = A_1\frac{L}{2}.\frac{1}{(1+A_1)} \qquad (5.51b)$$

$$var(\eta|H_0) = A_1^2\frac{L}{2}.\frac{1}{(1+A_1)^2} \qquad (5.51c)$$

$$d_\eta = A_1^2.L/2 \qquad (5.52)$$

For fixed performance , i.e. $d_\eta = d_\phi$ and with

A_η = input SNR for the ED and A_ϕ = input SNR for the CAED we have

$$A_\eta^2 \cdot \frac{L}{2} = A_\phi^2 \cdot \frac{L}{2} \cdot L_1 \tag{5.53}$$

or

$$\frac{A_\eta}{A_\phi} = L_1^{1/2} \tag{5.54}$$

Comparing d for the CAED and the ED for fixed input SNR we obtain

$$\frac{d_\phi}{d_\eta} = L_1 \tag{5.55}$$

The CAED outperforms the ED by $10\log L_1$ dB.; for our case L_1 ranges from 33 for P_1=30 to 47 for P_1=21 so the CAED performance is approximately 15.2 dB to 16.8 dB better than the ED performance. For fixed input SNR the CAED performance goes up linearly with L_1. This approximate result is in reasonable agreement with the simulation results. (Reminder : L_1 is the number of periods "looked at" in one observation.)

5.2.5 Detection of PRS's With Unknown Period

A related problem of interest and in some sense analogous to the classical "Detection of one of M Orthogonal signals" problem is the problem of detecting a PRS in noise where the period is one of M possible periods. The observation under the two hypotheses H_0 and H_1 is

$$H_0 : y(i) = n(i) \sim N(0,1) \text{ i.i.d.} \tag{5.56a}$$

$$H_1 : y(i) = p(i) + n(i) \ , \ \underline{p} \ \& \ \underline{n} \text{ independent} \qquad (5.56b)$$

where p(i) is a PRS as described in Sect. 5.1 with period P and where P is an element of the set $\Omega=\{P_1,P_2,\ldots,P_M\}$. We assume that $P=P_k$ with probability $Pr(P_k)$. We let the number of samples in the observation equal L. We define L_k as follows

$$L_k \triangleq \lfloor L/P_k \rfloor \qquad (5.57)$$

where $\lfloor x \rfloor$ = largest integer no larger than x. So that L_k is the number of integer periods of PRS with period P_k in an observation L samples long. We assume for simplicity that all sequences have the same power level A. We define the log-likelihood ratio given PRS with period P_k as follows

$$z(\underline{y}|P_k) = \frac{c_k}{2L_k}.\sum_{j=0}^{P_k-1}\left(\sum_{r=0}^{L_k-1} y(j+rP_k)\right)^2 - \frac{P_k}{2}.\ln(1+AL_k) \qquad (5.58)$$

where $c_k \triangleq \dfrac{AL_k}{1+AL_k}$

In all cases the optimum detection statistic is the "average likelihood ratio" Following from the Bayes-Birdsall Theorem, let $\underline{\beta}$ be a vector of signal parameters with known joint distribution and density $f(\underline{\beta})$, let $\underline{y}$ be the observation and $f(\underline{\beta}|\underline{y})$ be the a-posteriori density of $\underline{\beta}$, then

$$\ell(\underline{y}) = \ell(\underline{y}|\underline{\beta}).\frac{f(\underline{\beta})}{f(\underline{\beta}|\underline{y})} \qquad (5.59a)$$

it follows that

$$\ell(\underline{y})f(\underline{\beta}|\underline{y}) = \ell(\underline{y}|\underline{\beta})f(\underline{\beta}) \qquad (5.59b)$$

Integrating both sides with respect to $\underline{\beta}$

$$\ell(\underline{y}) = \int \ell(\underline{y}|\underline{\beta}) f(\underline{\beta}) d\underline{\beta} \tag{5.60}$$

For one of M periods we obtain

$$\ell(\underline{y}) = \sum_{k=1}^{M} \ell(\underline{y}|P_k).Pr(P_k) \tag{5.61}$$

If we assume P_k equally likely to be any member of Ω we obtain

$$\ell(\underline{y}) = \frac{1}{M} \sum_{k=1}^{M} \ell(\underline{y}|P_k) \tag{5.62a}$$

$$= \frac{1}{M} \sum_{k=1}^{M} \exp(z(\underline{y}|P_k)) \tag{5.62b}$$

$$z(\underline{y}) = \ln\left(\sum_{k=1}^{M} \exp(z(\underline{y}|P_k))\right) - \ln M \tag{5.62c}$$

A block diagram of the optimum detector is given in fig. 5.5. The R.O.C. curves are given in fig. 5.6., for Ω = {21,22,...,30} and L=1000. Noise as usual is assumed N(0,1) i.i.d.

Next we compare the performance of the above detector with that of the estimator-detector. The estimator-detector calculates $z(\underline{y}|P_i)$ for all $P_i \in \Omega$ and bases its decision on $\max_{P_i \in \Omega} z(\underline{y}|P_i)$. The block diagram for the estimator-detector is given in fig. 5.7 and the R.O.C. curves in fig. 5.8. For comparison purposes the R.O.C. curves for the energy detector are also given in fig 5.9. From the R.O.C. curves

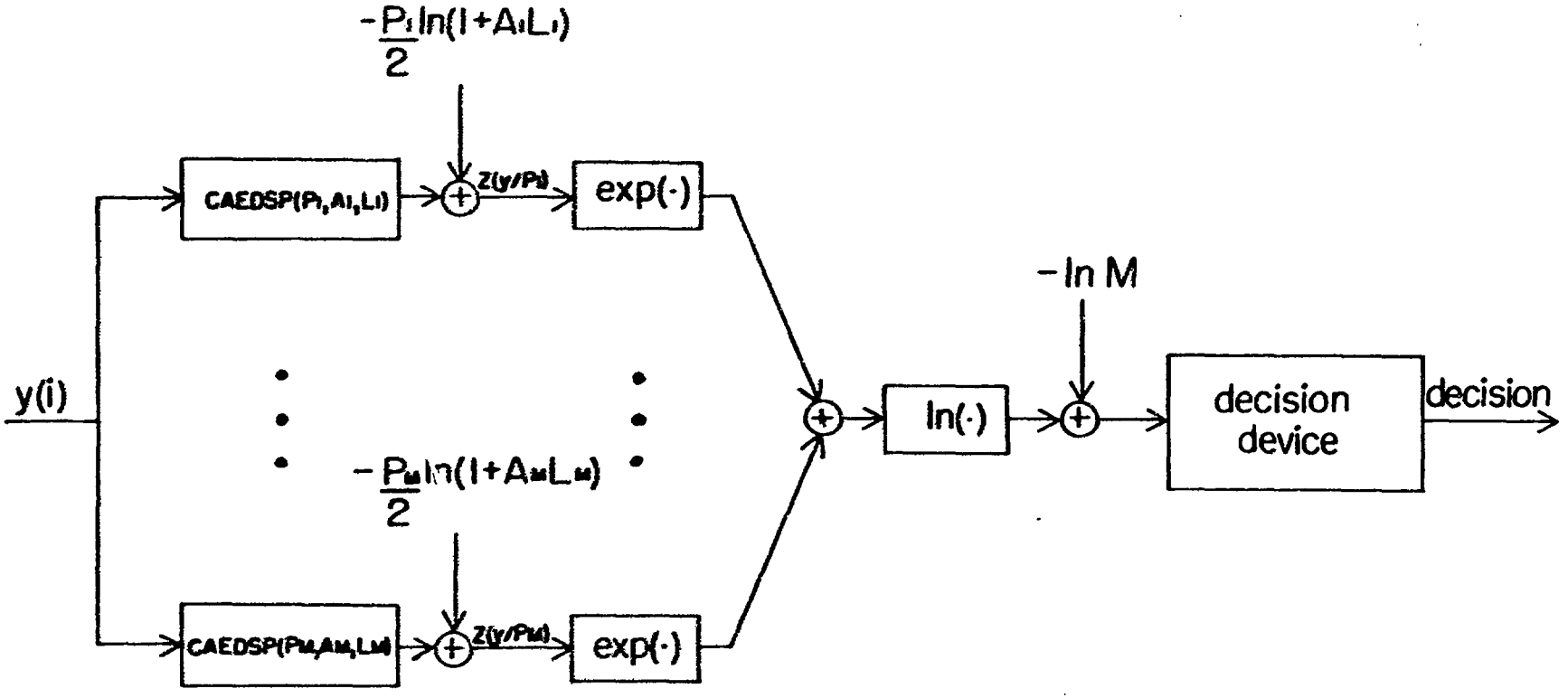

Fig. 5.5 Block diagram of the optimum detector when the signal period is equally likely to be one of M periods.

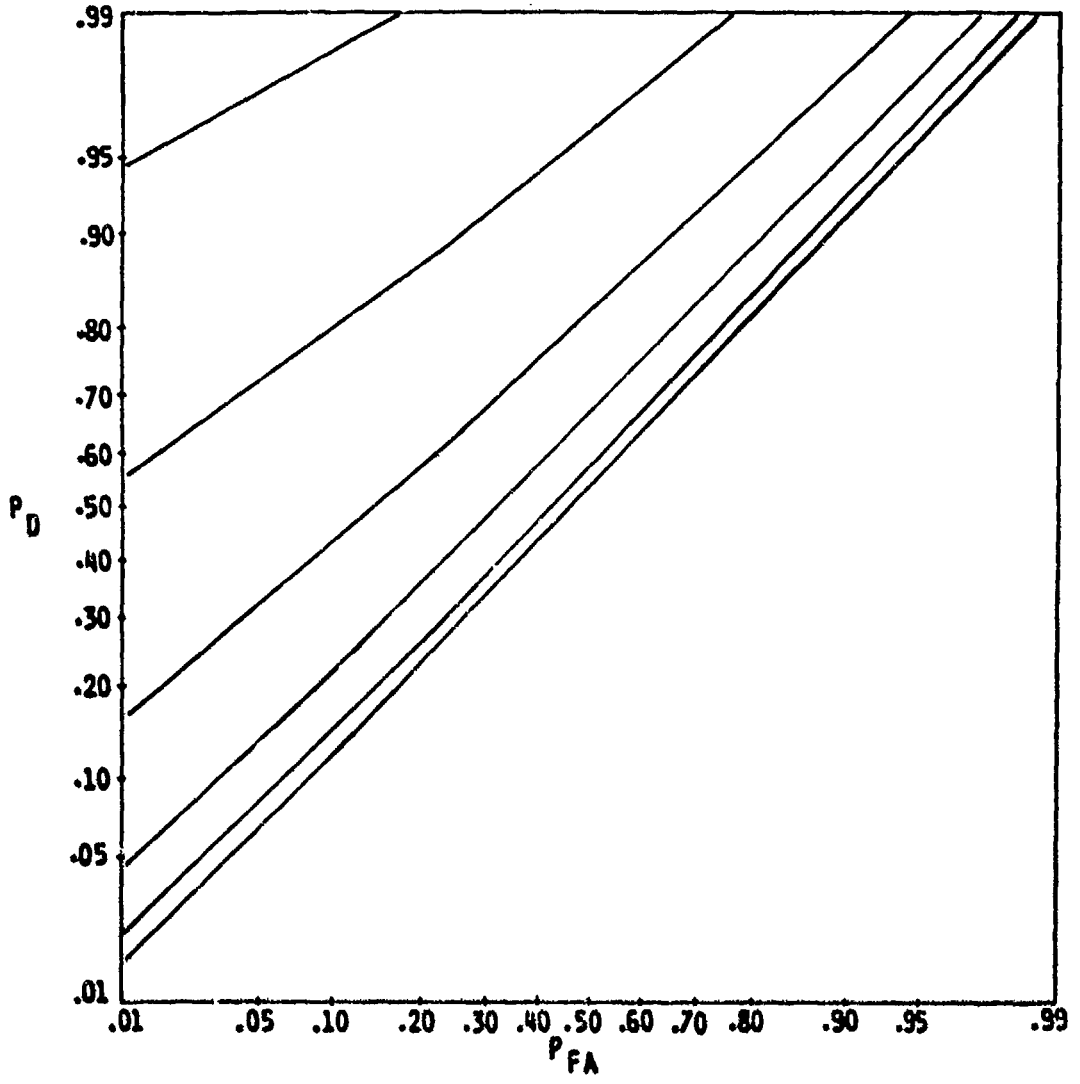

Fig. 5.6 Averaged R.O.C. curves for the optimum detector of fig. 5.5 with M=10 and signal powers of .002, .004, .008, .016, .032 and .064.

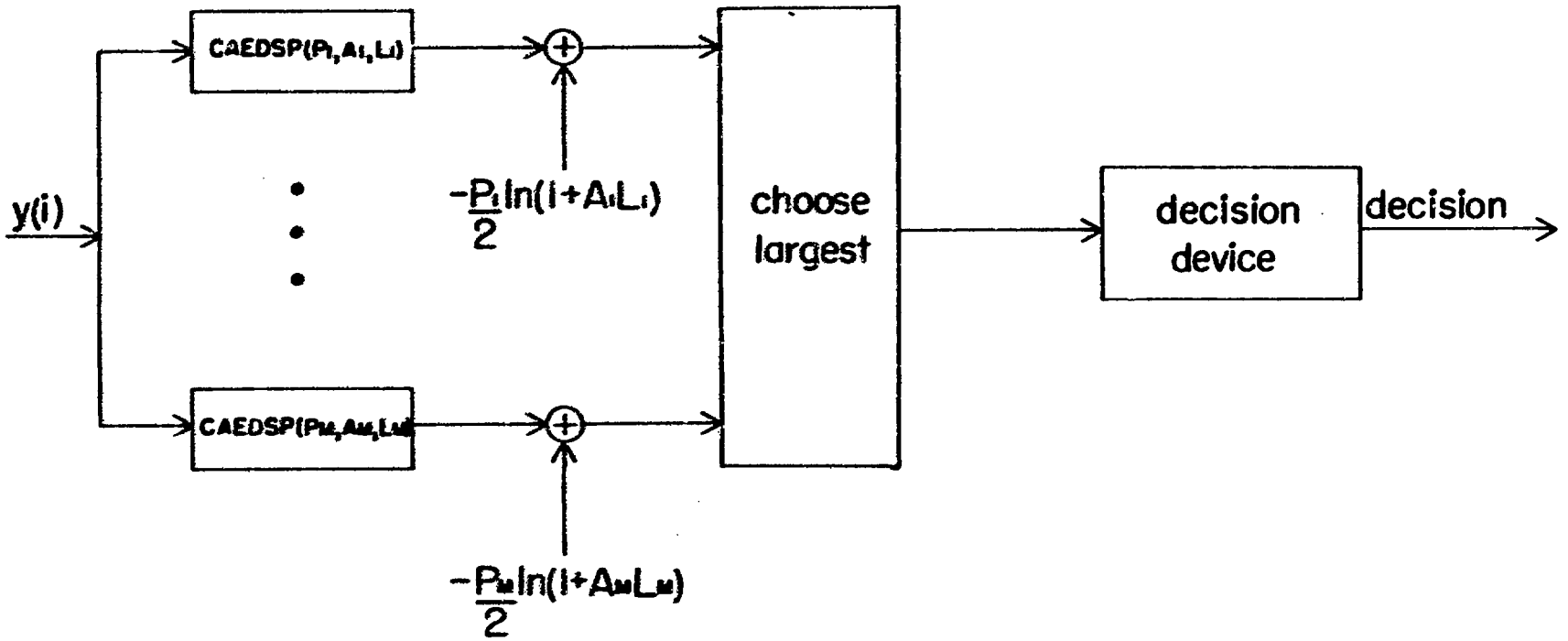

Fig. 5.7 Block diagram of the estimator-detector when the signal period is equally likely to be one of M periods.

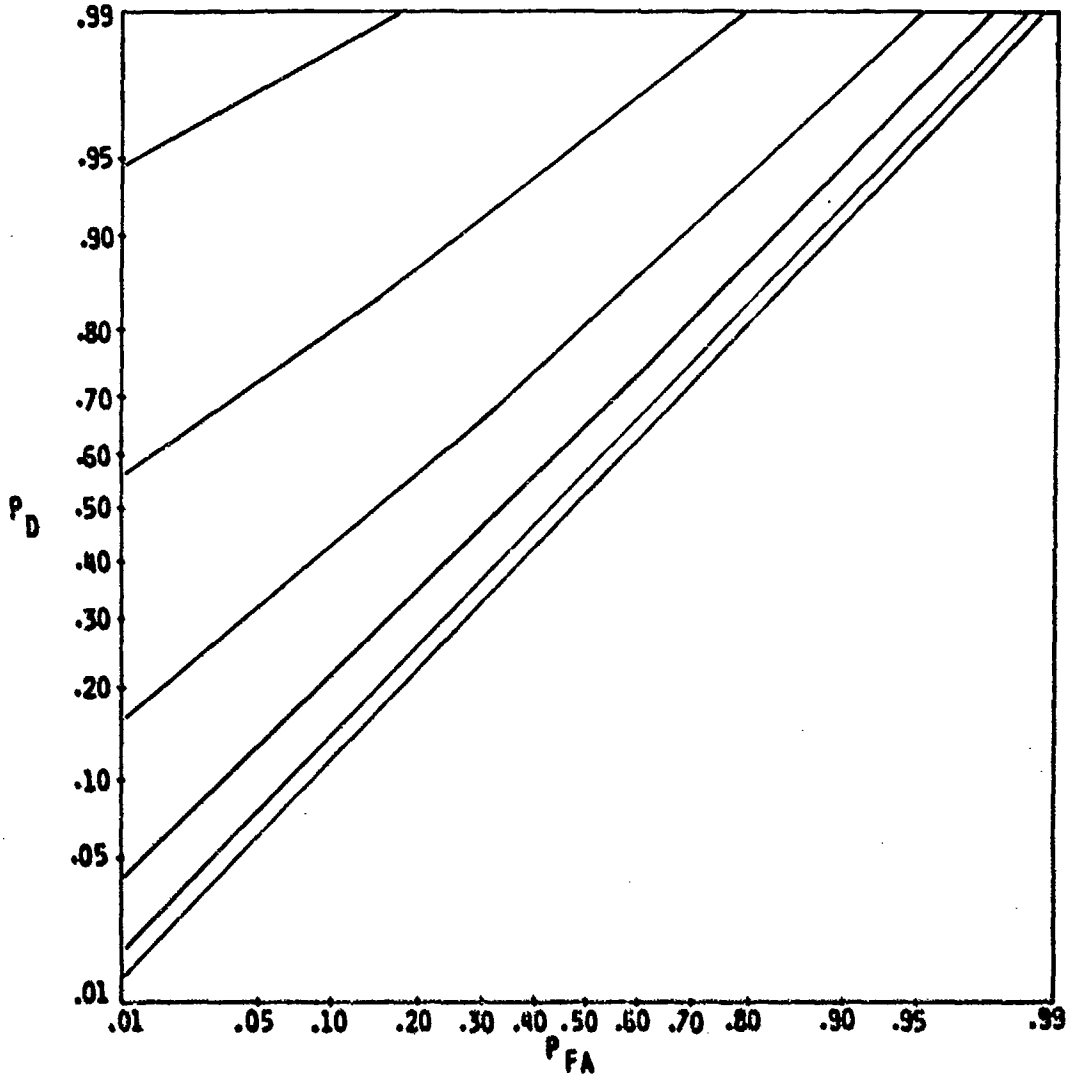

Fig. 5.8 Averaged R.O.C. curves for the estimator-detector of fig. 5.7 with M=10 and signal powers of .002, .004, .008, .016, .032 and .064.

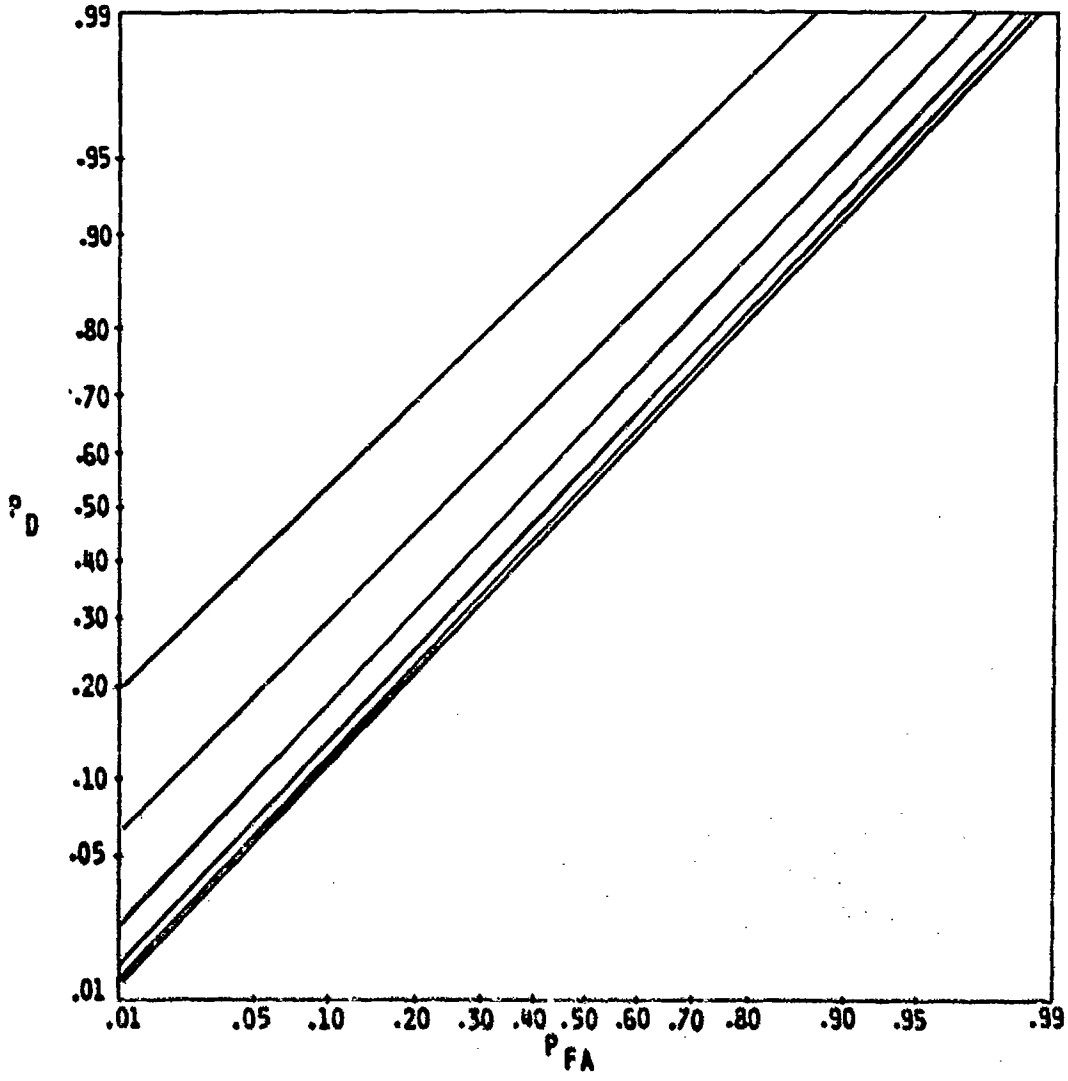

Fig. 5.9 R.O.C. curves for the energy detector with signal powers of .002, .004, .008, .016, .032 and .064.

for the optimum detector and the estimator-detector we see that the optimum (average likelihood ratio) detector and the estimator detector have essentially the same performance. Monte Carlo methods were used for generating the R.O.C. curves.

Note that the P_i for which $z(\underline{y}|P_i)$ is maximum, is the maximum likelihood estimate of the period of the PRS. Plots of Pr(Error in Estimation of period) vs. signal power are given in fig. 5.10. We now look at $z(\underline{y}|P_i)$ in more detail.

$$z(\underline{y}|P_i) = \frac{1}{2}\cdot\frac{AL_i}{1+AL_i}\cdot\frac{1}{L_i}\cdot\sum_{j=0}^{P_i-1}\left(\sum_{k=0}^{L_i-1} y(j+kP_i)\right)^2 - \frac{P_i}{2}\cdot\ln(1+AL_i) \tag{5.63a}$$

$$= \frac{1}{2}\cdot\frac{A}{A+\frac{1}{L_i}}\cdot\frac{1}{L_i}\cdot\sum_{j=0}^{P_i-1}\sum_{k=0}^{L_i-1} y(j+kP_i)\cdot\sum_{m=0}^{L_i-1} y(j+mP_i) - \frac{P_i}{2}\cdot\ln(1+AL_i) \tag{5.63b}$$

but $\frac{A}{A+\frac{1}{L_i}}\cdot\frac{1}{L_i}\cdot\sum_{m=0}^{L_i-1} y(j+mP_i)$ is the m.m.s.e. estimate of $p_i(j)$ [15 pp. 58-59], the jth sequence sample under the assumption that the sequence period is P_i; and where $0 \le j \le P_i-1$. We define $\hat{p}_i(j)$ as

$$\hat{p}_i(j) \triangleq \frac{A}{A+\frac{1}{L_i}}\cdot\frac{1}{L_i}\cdot\sum_{m=0}^{L_i-1} y(j+mP_i) \tag{5.64}$$

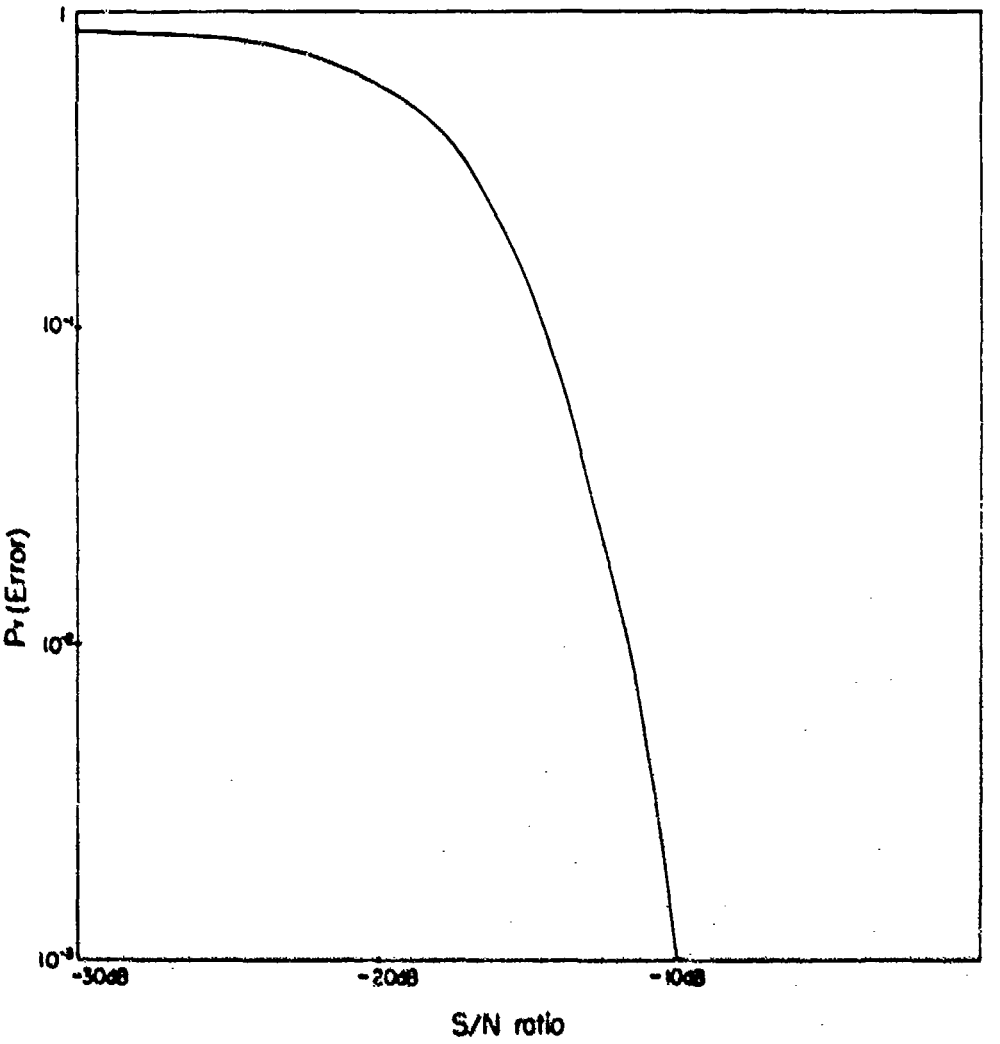

Fig. 5.10 Average Probability of Error in estimating signal period vs. S/N ratio.

Then it follows that

$$z(\underline{y}|P_i) = \frac{1}{2}.\sum_{j=0}^{P_i-1}\sum_{k=0}^{L_i-1} y(j+kP_i).\hat{p}_i(j) - \frac{P_i}{2}.\ln(1 + AL_i) \quad (5.65a)$$

or

$$z(\underline{y}|P_i) = \frac{1}{2}\underline{y}^T.\hat{\underline{p}}_i - \frac{P_i}{2}.\ln(1 + AL_i) \quad (5.65b)$$

where $\hat{\underline{p}}_i$ is the estimated PRS waveform under the assumption that the PRS period is P_i. The detection statistic may now be written as

$$\max_{P_i} z(\underline{y}|P_i) = \max_{P_i} \{ \frac{1}{2}.\underline{y}^T.\hat{\underline{p}}_i - \frac{P_i}{2}.\ln(1 + A.L_i) \} \quad (5.66)$$

Because of the simplicity of the structure of the estimator-detector (no exponential non-linearity) and no loss of performance compared to the optimum detector, the estimator-detector is the preferred realization of the optimum detector in this case. The advantage of the estimator-detector over the energy detector are 1) Better performance 2) The ability to simultaneously estimate the signal period.

The problem of estimating signal period (or frequency) is an interesting problem in its own right [36,37]. The above development focused on a periodic random sequence. We now outline the development for deterministic but unknown periodic sequences. This development differs from the previous in that it is non-Bayesian; the signals are "unknown", not random vectors.

Assume the observation consists of L samples. The statistics of the observation are

$$H_0 : y(i) = n(i) \sim N(0,1) \text{ i.i.d.} \tag{5.67a}$$

$$H_1 : y(i) = n(i) + p_k(i) \tag{5.67b}$$

where $p_k(i)$ is a periodic sequence of period P_k, $P_k \in \Omega = \{P_1, P_2, \ldots, P_M\}$. We assume that the period P_k is unknown. Let $L_k = \lfloor L/P_k \rfloor$ and define $\tilde{p}_k(i)$ as follows

$$\tilde{p}_k = \begin{cases} p_k(i) , & i=0,1,\ldots,P_k-1 \\ 0 , & \text{o.w.} \end{cases} \tag{5.68}$$

If the sequence $\underline{p}_k$ is known then the optimum estimate of the period follows from forming the M log-likelihood ratios $z(\underline{y}|p_k)$, $k=1,2,\ldots,M$ and choosing the largest.

$$f(\underline{y}|p_k) = \left(\frac{1}{2\pi}\right)^{P_k L_k} . \exp\left(-\frac{1}{2}(\underline{y}-\underline{p}_k)^T . (\underline{y}-\underline{p}_k)\right) \tag{5.69a}$$

$$f(\underline{y}|H_0) = \left(\frac{1}{2\pi}\right)^{P_k L_k} . \exp\left(-\frac{1}{2}\underline{y}^T . \underline{y}\right) \tag{5.69b}$$

and

$$z(\underline{y}|p_k) = (\underline{y} - \tfrac{1}{2}\underline{p}_k)^T \underline{p}_k \tag{5.70}$$

However as the sequences $\underline{p}_k$ are not known we follow custom and first form a maximum likelihood estimate of the M possible sequences based on the observation, and then use these estimates in eq. 5.70 and then choose the maximum. We can rewrite $z(\underline{y}|p_k)$ as follows

$$z(\underline{y}|p_k) = \sum_{i=0}^{L_k P_k - 1} (y(i) - \tfrac{1}{2}p_k(i)) . p_k(i) \tag{5.71a}$$

$$= \sum_{j=0}^{P_k-1} \left(\sum_{r=0}^{L_k-1} (y(j+rP_k) - \frac{1}{2}.\tilde{p}_k(j)) \right).\tilde{p}_k(j) \qquad (5.71b)$$

Differentiating eq. 5.71b with respect to each $\tilde{p}_k(j)$ and setting the result to zero we obtain

$$\frac{\partial z(\underline{y}|p_k)}{\partial \tilde{p}_k(j)} = \sum_{r=0}^{L_k-1} (y(j+rP_k) - \tilde{p}_k(j)) = 0 \qquad (5.72)$$

$$\text{for } j = 0,1,\ldots,P_k-1$$

or

$$\hat{\tilde{p}}_k(j) = \frac{1}{L_k}.\sum_{r=0}^{L_k-1} y(j+rP_k) \qquad (5.73)$$

$\hat{\tilde{p}}_k(j)$ is the maximum-likelihood estimate of $\tilde{p}_k(j)$. The sequence $\hat{p}_k$ extends $\hat{\tilde{p}}_k$ periodically

$$\hat{p}_k(i) = \begin{cases} \sum_{r=0}^{L_k-1} \hat{\tilde{p}}_k(i-rP_k) \;, & i=0,1,\ldots,L-1 \\ 0 \quad , \text{ o.w.} \end{cases} \qquad (5.74)$$

Based on the estimated sequences we form the M statistics $\hat{z}(\underline{y}|p_k)$ defined as

$$\hat{z}(\underline{y}|p_k) \triangleq (\underline{y} - \frac{1}{2}.\hat{\underline{p}}_k)^T.\hat{\underline{p}}_k \qquad (5.75)$$

The estimated period is then the one that corresponds to

$\max_{p_k} \hat{z}(\underline{y}|p_k)$. The block diagram of the estimator-estimator is given in fig. 5.11.

5.3 Detection of two or more PRS's in Noise

In this section we generalize the results obtained in Sect. 5.2. We first examine the problem of detecting 2 or more PRS's with known periods. Next we examine the problem of the detection of k of M PRS's in noise. Finally we develop the equations for the most general problem that fits into the framework established here, in this case we allow signal and noise to be complex with the noise not necessarily white and successive signal samples not necessarily independent.

5.3.1. Detection of 2 or more PRS's of Known Periods.

In this case the signal consists of the sum of N PRS's ($N \geq 2$) of known periods $P_1, P_2, \ldots, P_N$. The number of samples in the observation is chosen so that L=L.C.M. $\{P_1, P_2, \ldots, P_N\}$ or some integer multiple of the L.C.M. This insures that each PRS has an integer number of periods in the observation. We define L_k as the number of periods in the observation of PRS with period P_k i.e. $L_k = L/P_k$

The observation under the two hypotheses H_0 and H_1 is

$$H_0 : y(i) = n(i) \sim N(0,1) \text{ i.i.d. , } i=0,1,\ldots,L-1 \quad (5.76a)$$

$$H_1 : y(i) = n(i) + \sum_{k=1}^{N} p_k(i) \text{ , } i=0,1,\ldots,L-1 \quad (5.76b)$$

Where $p_k(i)$ has period P_k and $p_k(i) \sim N(0, A_k)$. Noise is assumed independent of the PRS's and the PRS's are assumed independent of each other. We let $R = E(\underline{y}.\underline{y}^T|H_1)$ and write

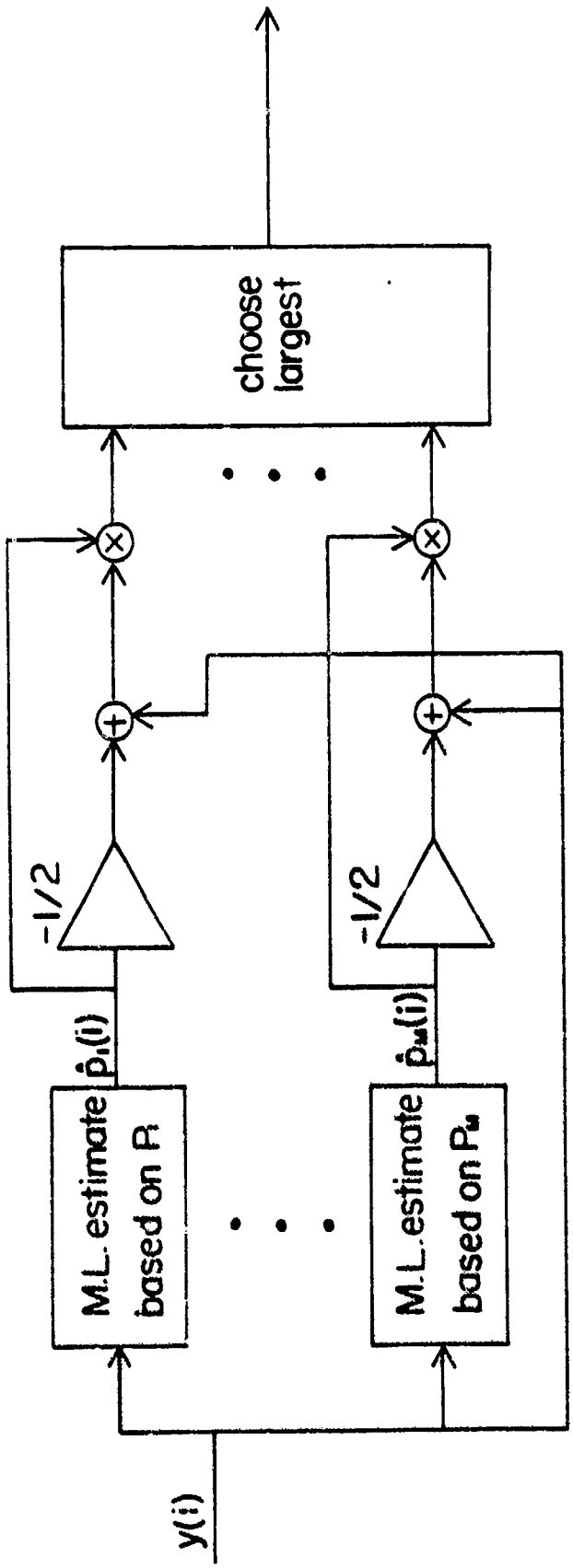

Fig. 5.11 Block diagram of the estimator-estimator.

the density function of the observation under the hypotheses H_0 and H_1 as follows

$$f(\underline{y}|H_0) = (\frac{1}{2\pi})^{L/2}.\exp(-\frac{1}{2}.\underline{y}^T\underline{y}) \tag{5.77a}$$

$$f(\underline{y}|H_1) = (\frac{1}{2\pi})^{L/2}.(\frac{1}{|R|})^{1/2}.\exp(-\frac{1}{2}.\underline{y}^T R^{-1}\underline{y}) \tag{5.77b}$$

The likelihood and the log-likelihood ratios follow

$$\ell(\underline{y}) = (\frac{1}{|R|})^{1/2}.\exp(\frac{1}{2}.\underline{y}^T(I-R^{-1})\underline{y}) \tag{5.78a}$$

$$z(\underline{y}) = \frac{1}{2}.\underline{y}^T(I-R^{-1})\underline{y} - \frac{1}{2}.\ln|R| \tag{5.78b}$$

As before the key to the simplification of the equations for $\ell(\underline{y})$ and $z(\underline{y})$ lies in the eigenvalue-eigenvector decomposition of R. First we write R as

$$R = E(\underline{y}.\underline{y}^T|H_1) \tag{5.79}$$

$$= R_n + \sum_{k=1}^{N} R_k$$

Where R_n is the noise autocorrelation and is the LxL identity matrix, R_k is the autocorrelation matrix of PRS p_k and is circulant. The above decomposition follows from the independence of the noise and the PRS's. It follows that R is also circulant. In fact

$$R = I_L + \sum_{k=1}^{N} A_k\{\delta(|i-j| \bmod P_k)\} \quad i,j=0,1,\ldots,L-1 \tag{5.80}$$

The first row of R, R(n) is given by

$$R(n) = \delta(n) + \sum_{k=1}^{N} A_k \sum_{l=0}^{L_k-1} \delta(n-lP_k) \quad , \quad n=0,1,\ldots,L-1 \qquad (5.81)$$

$\psi(m)$, the eigenvalue sequence of R is given by

$$\psi(m) = \sum_{n=0}^{L-1} R(n).\exp(-j2\pi nm/L) \qquad (5.82a)$$

$$= \begin{cases} 1 + \sum_{k=1}^{N} A_k L_k \ , & m=0 \\ 1 + A_k L_k \ , & m=L_k, 2L_k, \ldots, (P_k-1)L_k \\ & k=1,2,\ldots,N \\ 1 \ , & \text{o.w.} \end{cases} \qquad (5.82b)$$

Let $\Psi = \text{diag}(\psi(0),\psi(1),\ldots,\psi(L-1))$ be the diagonal matrix of eigenvalues of R and U_L be the unitary matrix of eigenvectors of R, then

$$R = U_L \Psi U_L^* \qquad (5.83)$$

and since all eigenvalues are non-zero

$$R^{-1} = U_L \Psi^{-1} U_L^* \qquad (5.84)$$

also

$$|R| = |\Psi| \qquad (5.85a)$$

$$= (1 + \sum_{k=1}^{N} A_k L_k) . \prod_{k=1}^{N} (1+A_k L_k)^{P_k-1}$$

$$= \frac{(1 + \sum_{k=1}^{N} A_k L_k)}{\prod_{k=1}^{N} (1 + A_k L_k)} \cdot \prod_{k=1}^{N} (1 + A_k L_k)^{P_k} \qquad (5.85b)$$

Substituting for R^{-1} and $|R|$ from eq. 5.84 and eq. 5.85 in eq. 5.78b, we obtain

$$z(\underline{y}) = \tfrac{1}{2}\underline{y}^T U_L (I - \Psi^{-1}) U_L^* \underline{y} - \sum_{k=1}^{N} \frac{P_k}{2} \cdot \ln(1 + A_k L_k)$$

$$- \tfrac{1}{2} \ln \frac{(1 + \sum_{k=1}^{N} A_k L_k)}{\prod_{k=1}^{N} (1 + A_k L_k)} \qquad (5.86)$$

We define $\theta \triangleq I - \Psi^{-1}$. θ is a diagonal matrix and the elements along the diagonal are given by $\theta(m) = 1 - \frac{1}{\psi(m)}$, so

$$\theta(m) = \begin{cases} \dfrac{\sum_{k=1}^{N} A_k L_k}{1 + \sum_{k=1}^{N} A_k L_k}, & m=0 \\ \dfrac{A_k L_k}{1 + A_k L_k}, & m = L_k, 2L_k, \ldots, (P_k - 1)L_k \\ & k = 1, 2, \ldots, N \\ 0, & \text{o.w.} \end{cases} \qquad (5.87)$$

Now define c_0 and c_k as follows

$$-c_0 \triangleq \frac{\sum_{k=1}^{N} A_k L_k}{1 + \sum_{k=1}^{N} A_k L_k} - \sum_{k=1}^{N} \frac{A_k L_k}{1 + A_k L_k} \tag{5.88}$$

$$c_k \triangleq \frac{A_k L_k}{1 + A_k L_k} \tag{5.89}$$

We may now rewrite $\theta(m)$ as follows

$$\theta(m) = \sum_{k=0}^{N} \theta_k(m) \tag{5.90}$$

where

$$\theta_k(m) = \begin{cases} -c_0 \delta(m) & , \quad k=0 \\ c_k \cdot \sum_{r=0}^{P_k - 1} \delta(m - rL_k) & , \quad k=1,2,\ldots N \end{cases} \tag{5.91}$$

Now let $Q \triangleq U_L \theta U_L^*$ and decompose θ as done for $\theta(m)$ so that $\theta \triangleq \sum_{k=0}^{N} \theta_k$. The diagonal elements of θ_k are given by $\theta_k(m)$. Define $Q_k \triangleq U_L \theta_k U_L^*$ so that $Q = \sum_{k=0}^{N} Q_k$. By definition the matrices Q_k and hence Q are circulant, so we may obtain Q in terms of its first row. Let the first row of Q be $Q(n)$, then

$$Q(n) = Q_0(n) + Q_1(n) + \ldots + Q_N(n) \tag{5.92}$$

and

$$Q_0(n) = -\frac{c_0}{L} \quad \text{all } n \tag{5.93a}$$

$$Q_k(n) = \begin{cases} \frac{c_k P_k}{L} & , n=0,P_k,2P_k,\ldots,(L_k-1).P_k \\ 0 & \text{o.w.} \end{cases} \tag{5.93b}$$

It follows that

$$z(\underline{y}) = \frac{1}{2}\underline{y}^T\left(\sum_{k=0}^{N} Q_k\right)\underline{y} - \sum_{k=1}^{N} \frac{P_k}{2}.\ln(1 + A_k L_k)$$

$$- \frac{1}{2}\ln \frac{\left(1 + \sum_{k=1}^{N} A_k L_k\right)}{\prod_{k=1}^{N}(1 + A_k L_k)} \tag{5.94a}$$

$$= -\frac{c_0}{2L}.\left(\sum_{n=0}^{L-1} y(n)\right)^2 + \sum_{k=1}^{N} \frac{c_k P_k}{2L}.\sum_{j=0}^{P_k-1}\left(\sum_{r=0}^{L_k-1} y(j+rP_k)\right)^2$$

$$- \sum_{k=1}^{N} \frac{P_k}{2}.\ln(1 + A_k L_k) - \frac{1}{2}\ln \frac{\left(1 + \sum_{k=1}^{N} A_k L_k\right)}{\prod_{k=1}^{N}(1 + A_k L_k)} \tag{5.94b}$$

The above reduces to

$$z(\underline{y}) = \sum_{k=1}^{N} z(\underline{y}|P_k) - \frac{c_0}{2L}\left(\sum_{n=0}^{L-1} y(n)\right)^2$$

$$- \frac{1}{2}\ln \frac{(1 + \sum_{k=1}^{N} A_k L_k)}{\prod_{k=1}^{N} (1 + A_k L_k)} \qquad (5.95)$$

The last term in eq. 5.95 does not depend on the reception, in fact it is a constant and maybe ignored if we assume we know the power levels A_k's. The second term in eq. 5.95 is a D.C. correction term. It is at D.C. (zero frequency) that all the PRS's interact. The R.O.C. curves for detectors based on $z(\underline{y})$ are given in fig. 5.12, for N=2, P_1=21, P_2=29 and L=609. Experimentally we have shown that decisions based on $\sum_{k=1}^{N} z(\underline{y}|P_k)$ are essentially equivalent to decisions based on $z(\underline{y})$. We call the detector that bases its decisions on $\sum_{k=1}^{N} z(\underline{y}|P_k)$ the sum-detector. R.O.C. curves for the sum-detector are given in fig. 5.13, the signal and noise statistics used in generating fig. 5.13 are the same as those used for generating fig. 5.12. For comparison purposes the R.O.C. curves obtained using an energy detector are given in fig. 5.14. Since the conditional log-likelihood ratios $z(\underline{y}|P_k)$ are not independent, it is not easy to derive the density function for $z(\underline{y})$. However, we can calculate the statistics of $z(\underline{y})$ necessary to obtain an approximate expression for the normal detectability d. The details of the calculation are tedious and are given in Appendix B. In calculating the statistics we assume that N=2 and that both the PRS's have the same power A/2 and that P_1=P_2. We obtain the following

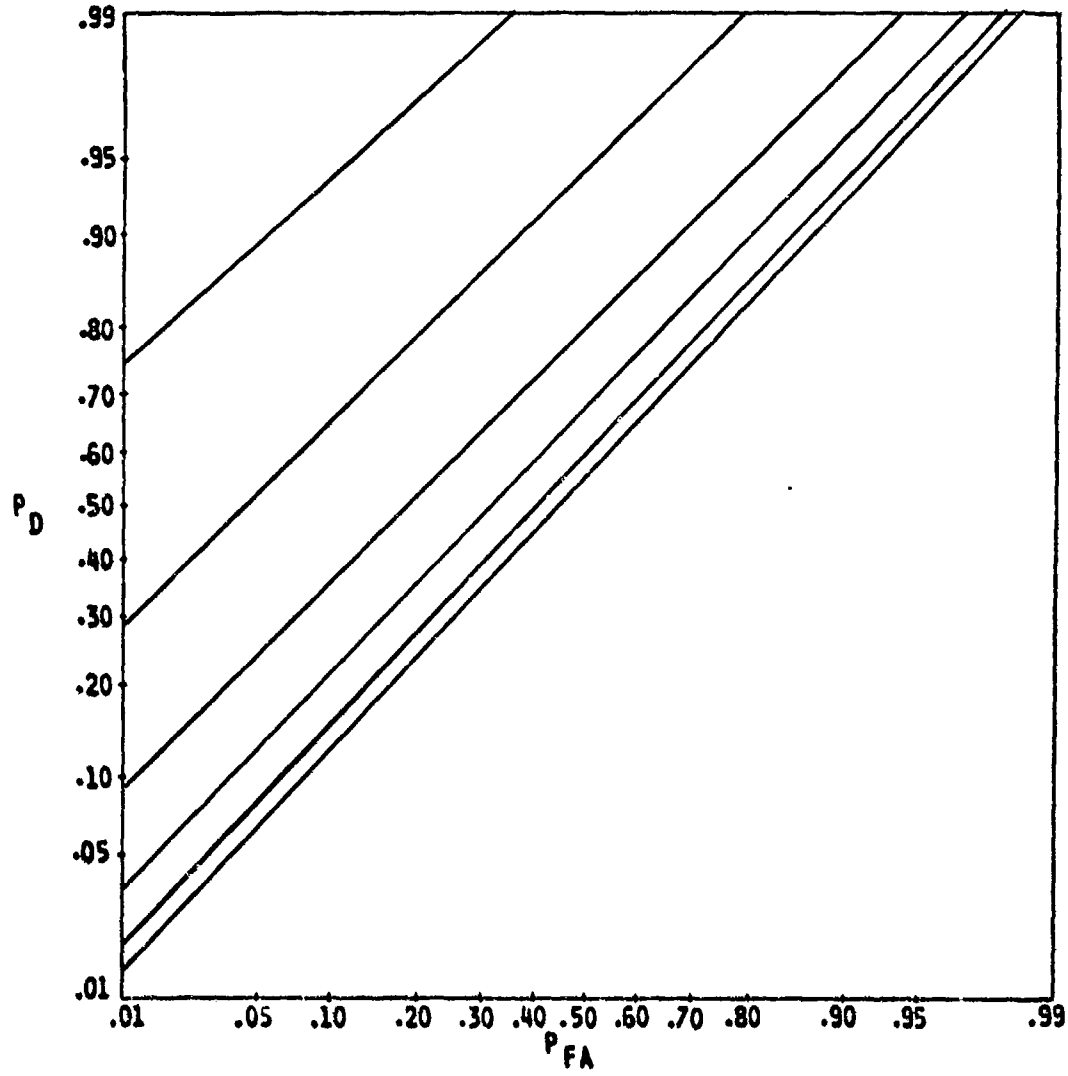

Fig. 5.12 R.O.C. curves for the optimum detector for 2 PRS's of known period in noise with P_1=21, P_2=29 and L=609. Each PRS has identical power levels of .001, .002, .004, .008, .016 and .032.

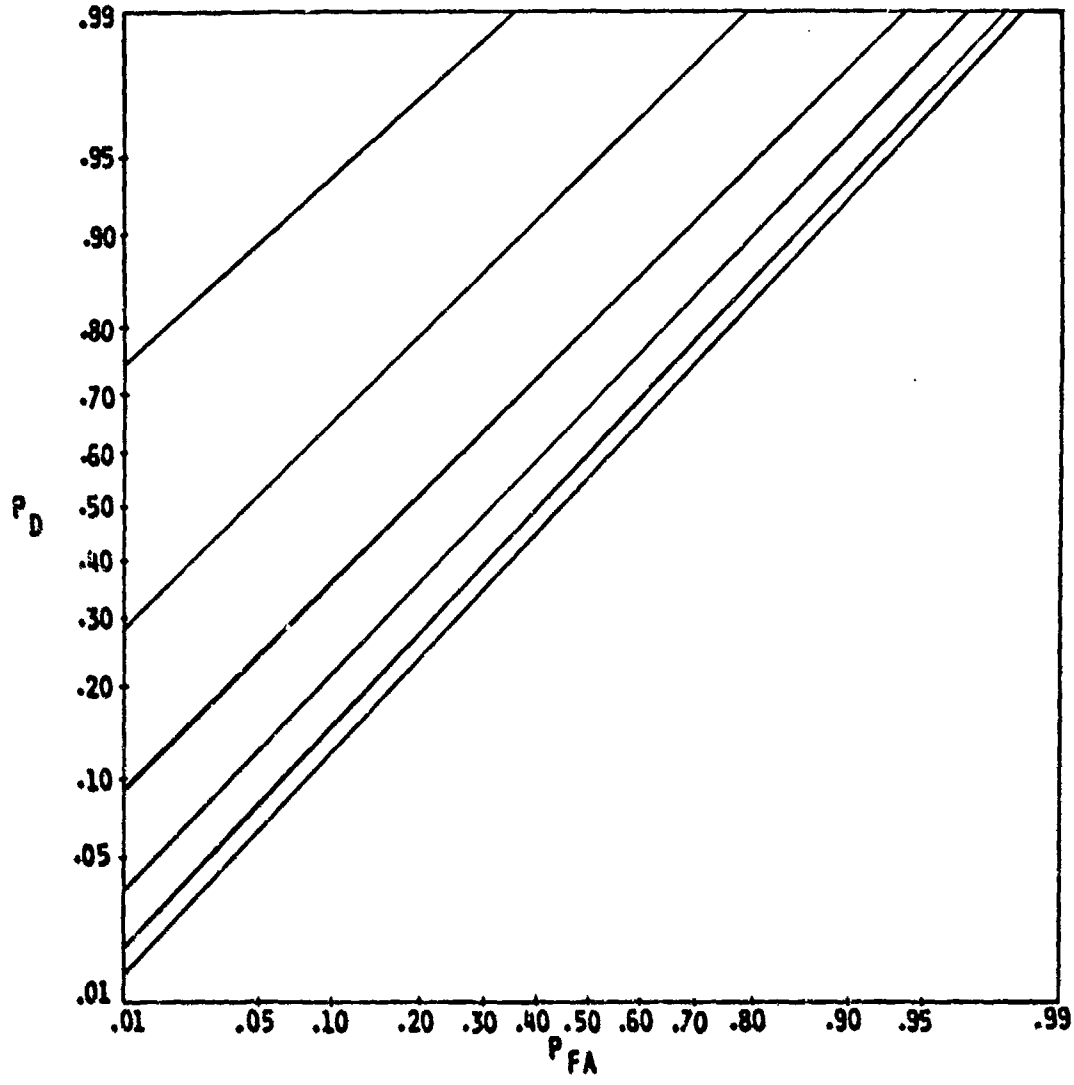

Fig. 5.13 R.O.C. curves for the sum-detector with the same signal and noise statistics as in fig. 5.12.

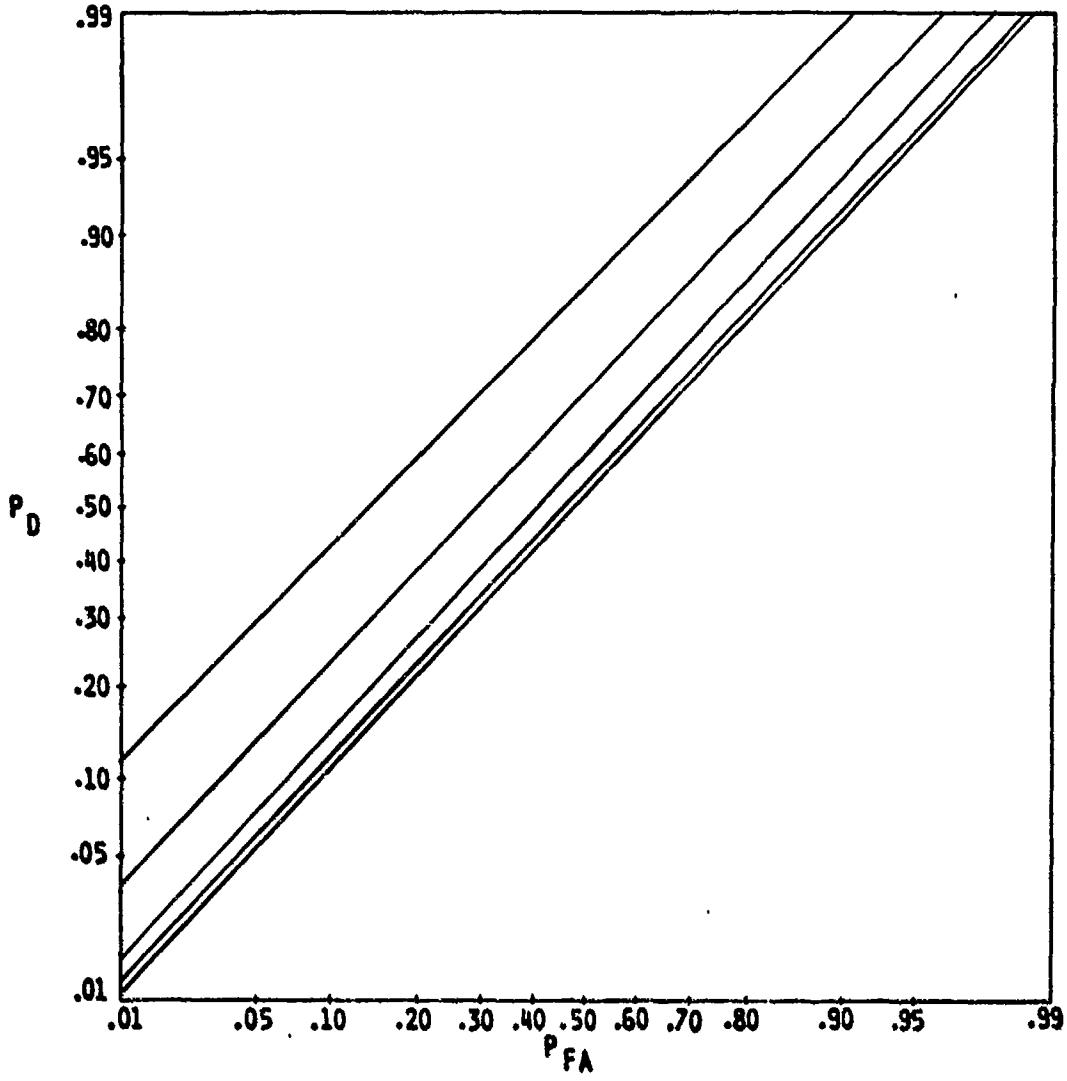

Fig. 5.14 R.O.C. curves for the energy detector with the same signal periods as in figs. 5.12 & 5.13 and signal power levels of .002, .004, .008, .016 and .032.

expression for d

$$d \simeq A^2 L(1 + L_1 + L_2)/2 \tag{5.96}$$

In the preceding development the observation size was fixed at some integer multiple of the L.C.M. of $\{P_1,\ldots,P_N\}$. This places a restriction on the observer. In the following this restriction is relaxed. The number of samples in the observation, L , is now arbitrary. It follows that there are $L_k = \lfloor L/P_k \rfloor$ integer periods, of PRS with period P_k in the observation. The observation under the two hypotheses is

$$H_0 : y(i) = n(i) \sim N(0,1) \text{ i.i.d.} \tag{5.97a}$$

$$H_1 : y(i) = n(i) + \sum_{k=1}^{N} p_k(i) \tag{5.97b}$$

The LxL autocorelation matrix $R=E(\underline{y}.\underline{y}^T|H_1)$ is no longer circulant. The key to obtaining the equations for the optimum detector was the eigenvalue-eigenvector decomposition of the circulant matrix R and R^{-1}. For the present situation where the number of samples in the observation is not divisible by all the periods, we will call R the expunged circulant matrix. A simple well defined procedure for the eigenvalue-eigenvector decomposition of the expunged circulant matrix does not exist. Also a straight forward procedure for finding the inverse of the expunged circulant matrix (if the inverse exists) does not exist. Using the optimum detector of eq. 5.94 as a guideline we hypothesize that the following detector will have near optimum performance. We base our decisions on $\bar{z}(\underline{y})$ where

$$\tilde{z}(\underline{y}) \triangleq \sum_{k=1}^{N} \tilde{z}(\underline{y}|P_k) - \frac{\tilde{c}_0}{2L}\left(\sum_{n=0}^{L-1} y(n)\right)^2$$

$$- \frac{1}{2}\ln \frac{\left(1 + \sum_{k=1}^{N} A_k |\_L/P_k\_|\right)}{\prod_{k=1}^{N} \left(1 + A_k |\_L/P_k\_|\right)} \qquad (5.98)$$

where

$$\tilde{z}(\underline{y}|P_k) = \frac{\tilde{c}_k}{2} \cdot \frac{1}{|\_L/P_k\_|} \cdot \sum_{j=0}^{P_k-1} \left(\sum_{r=0}^{|\_L/P_k\_|-1} y(j+rP_k)\right)^2$$

$$- \frac{P_k}{2} \cdot \ln(1 + A_k |\_L/P_k\_|) \qquad (5.99a)$$

$$-\tilde{c}_0 \triangleq \frac{\sum_{k=1}^{N} A_k |\_L/P_k\_|}{1 + \sum_{k=1}^{N} A_k |\_L/P_k\_|} - \sum_{k=1}^{N} \frac{A_k |\_L/P_k\_|}{1 + A_k |\_L/P_k\_|} \qquad (5.99b)$$

$$\tilde{c}_k \triangleq \frac{A_k |\_L/P_k\_|}{1 + A_k |\_L/P_k\_|} \qquad (5.99c)$$

For each PRS, the above detector utilizes the maximum number of integer periods available, this is in contrast to the optimum detector which would also utilize the "left over" samples. We will soon show that when L is large the performance of the above sub-optimum detector is nearly the same as that of the optimum detector. If we write L_k for $|\_L/P_k\_|$ the form for $\tilde{z}(\underline{y})$ reduces to

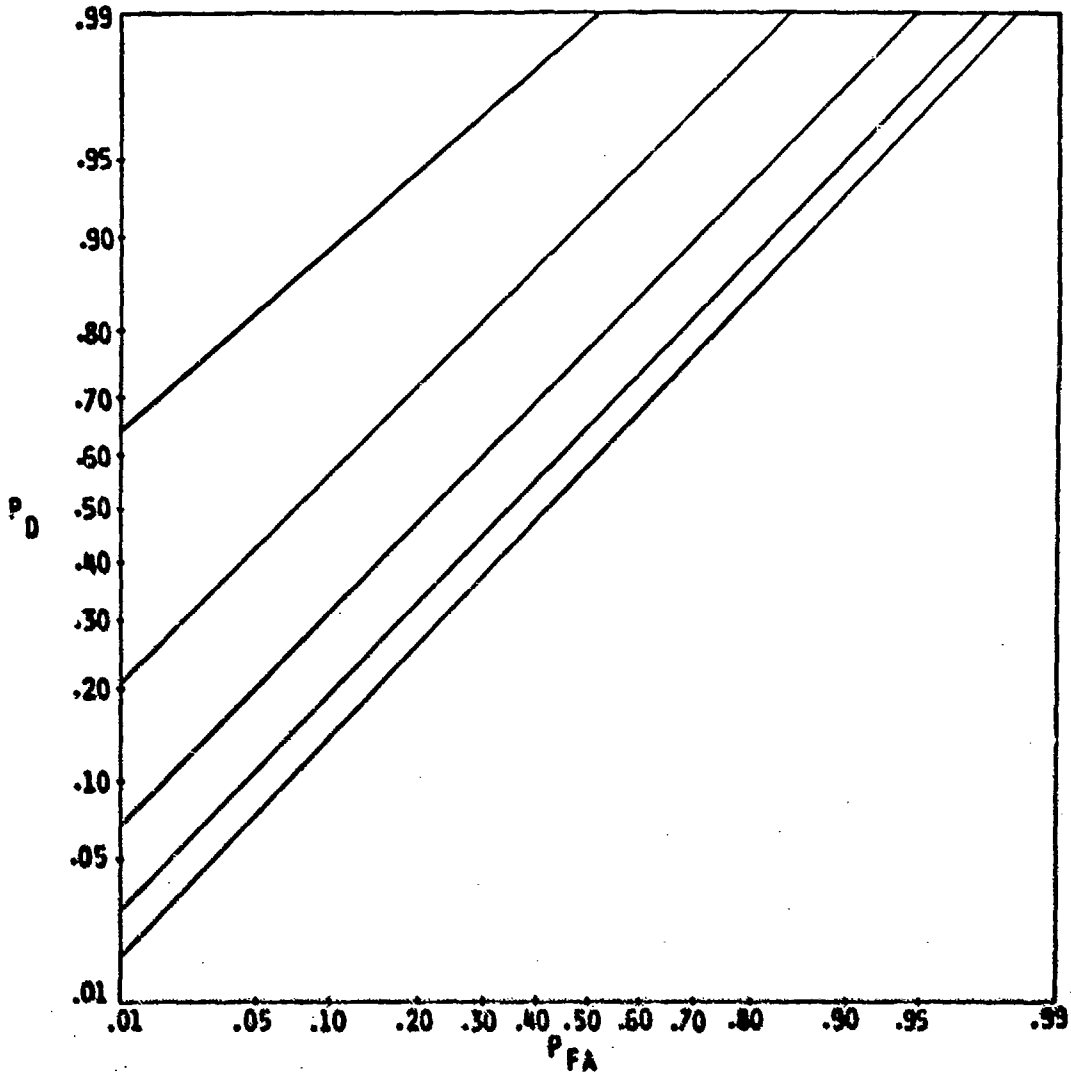

Fig. 5.15 Averaged R.O.C. curves for the quasi optimum detector for N=2, each PRS has identical power levels of .001, .002, .004, .008 and .016.

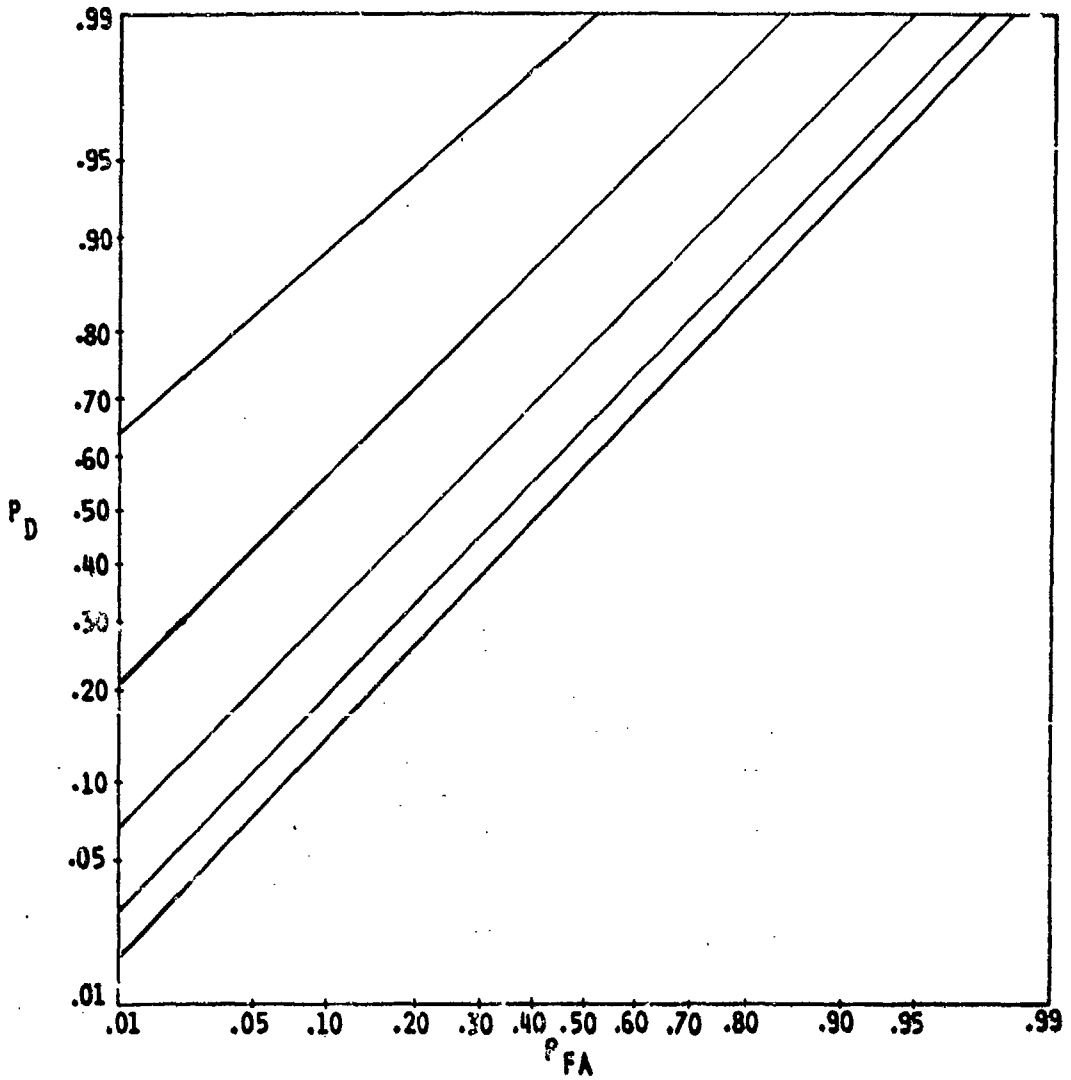

Fig. 5.16 Averaged R.O.C. curves for the quasi sum detector for N=2, with the signal and noise statistics used in fig. 5.15.

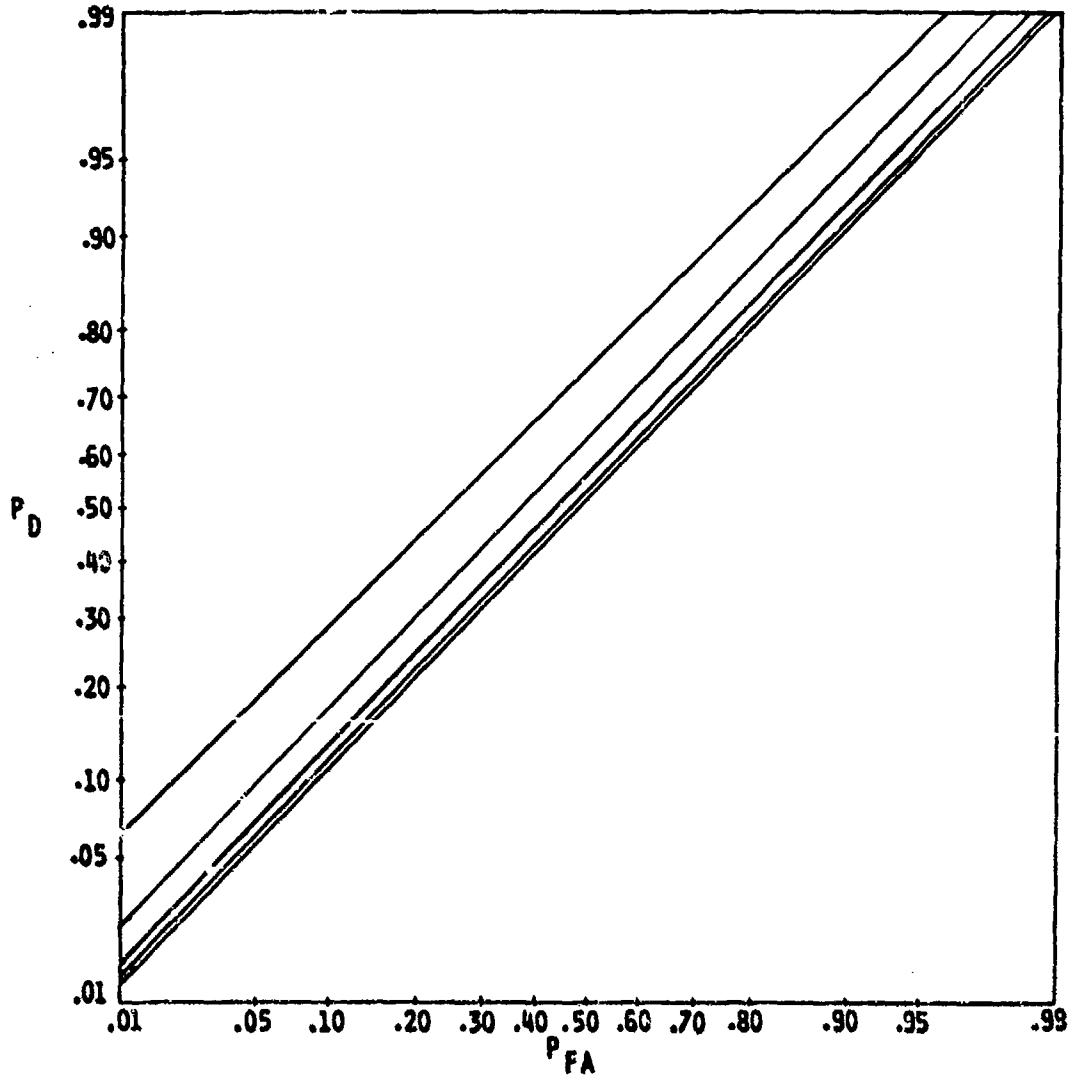

Fig. 5.17 R.O.C. curves for the energy detector with the same signal and noise statistics as used in figs. 5.15 & 5.16.

that obtained in eq. 5.94. We call the detector that bases its decisions on $\tilde{z}(\underline{y})$ the quasi optimum detector. R.O.C. curves for the quasi optimum detector, for N=2, are given in fig. 5.15. We let L=1000, P_1 is fixed at 21 P_2 is allowed to vary from 22 to 30 and the R.O.C. is the average R.O.C. We call the detector that bases its decision on $\sum_{k=1}^{N} \tilde{z}(\underline{y}|P_k)$ the quasi sum detector. The R.O.C. curves for the quasi sum detector are given in fig. 5.16. It is seen that the performance of the quasi sum detector is essentially equivalent to that of the quasi optimum detector. For comparison purposes the R.O.C. curves obtained using an energy detector are given in fig. 5.17.

An approximate expression for the normal detectability, $\tilde{d}$, for the quasi-optimum detector is given in eq. 5.100. It is assumed that N=2 and that both the PRS's have the same power level A/2 and that $P_1 \approx P_2$.

$$\tilde{d} \approx \frac{A^2 L}{2}(1 + L_1 + L_2) \tag{5.100}$$

The normal detectability, d_{opt}, for the optimum detector is then approximately upper bounded by

$$d_{opt} \lesssim \frac{A^2 L}{2}(1 + L_1 + 1 + L_2 + 1) \tag{5.101}$$

So we have

$$\frac{\tilde{d}}{d_{opt}} \approx (1 + L_1 + L_2)/(3 + L_1 + L_2) \tag{5.102a}$$

in the limit L and hence L_1 and L_2 become large

$$\frac{\tilde{d}}{d_{opt}} \simeq 1 \qquad (5.102b)$$

For the energy detector we had (eq. 5.52) $d_{ed}=A^2L/2$. We compare the input SNRs for fixed performance and obtain

$$\frac{\tilde{A}}{A} = (1 + L_1 + L_2)^{1/2} \qquad (5.103a)$$

Comparing the output SNR for fixed input SNR we obtain

$$\frac{\tilde{d}}{d_{ed}} = 1 + L_1 + L_2 \qquad (5.103b)$$

The above results are analogous to the results obtained in eq 5.54 and eq. 5.55 and are in good agreement with the simulation results.

5.3.2 Detection of k of M PRS's in Noise

This is a generalization of the detection of one of M PRS's problem considered in Sect. 5.2.5. Now we consider the signal to be the sum of k independent PRS's, where the k PRS's belong to a set of M independent PRS's. We assume that it is not known a priori which k of the M PRS's make up the signal. This implies there are $N = \binom{M}{k}$ possible sets of signals. Even for moderate M and k the signal set becomes quite large. As we will show the optimum detector for this situation has a fairly elaborate and complex structure. This fact will provide us with the motivation for searching for detectors which have performance close to that of the optimum detector and yet have much simpler structure.

As usual we will assume there are L samples in the observation, where L is large and arbitrary. The observation under the hypotheses H_0 and H_1 is

$$H_0 : y(i) = n(i) \sim N(0,1) \text{ i.i.d.} \qquad (5.104a)$$

$$H_1 : y(i) = n(i) + s_r(i) \text{ , } \underline{s} \text{ \& } \underline{n} \text{ independent} \qquad (5.105b)$$

Where $\underline{s}_r \in S = \{\underline{s}_1, \underline{s}_2, \ldots, \underline{s}_N\}$. Each of the elements of S is the sum of k PRS's belonging to $\Omega = \{\underline{p}_1, \underline{p}_2, \ldots, \underline{p}_M\}$. The optimum detection statistic, as in Sect. 5.2.5 is the average likelihood ratio. Since L is not necessarily composite we will instead use the average of the conditional quasi-likelihood ratios as the "optimum" detecton statistic. Assuming that each of the elements of S is equally likely to be the signal we obtain

$$\tilde{\ell}(\underline{y}) = \frac{1}{N} \sum_{r=1}^{N} \exp(\tilde{z}(\underline{y}|\underline{s}_r) \qquad (5.105a)$$

$$\tilde{z}(\underline{y}) = \ln(\sum_{r=1}^{N} \exp(\tilde{z}(\underline{y}|\underline{s}_r)) - \ln N \qquad (5.105b)$$

To develop the structure of the quasi-optimum detector we need to expand $\tilde{z}(\underline{y}|\underline{s}_r)$. Assume $\underline{s}_r$ consists of PRS's of periods $P_{r1}, P_{r2}, \ldots, P_{rk}$, where the PRS with period P_{r1} has power A_{r1}. Now we can write $\tilde{z}(\underline{y}|\underline{s}_r)$ in the style of eq. 5.97

$$\tilde{z}(\underline{y}|\underline{s}_r) = \tilde{z}(\underline{y}|P_{r1},P_{r2},\ldots,P_{rk})$$

$$= \sum_{l=1}^{k} \tilde{z}(\underline{y}|P_{rl}) - \frac{\tilde{c}_{or}}{2L}.\left(\sum_{n=0}^{L-1} y(n)\right)^2$$

$$- \frac{1}{2}\ln \frac{\left(1 + \sum_{l=1}^{k} A_{rl}L_{rl}\right)}{\prod_{l=1}^{k}(1 + A_{rl}L_{rl})} \qquad (5.106)$$

where

$$L_{rl} \triangleq \lfloor L/P_{rl} \rfloor \qquad (5.107)$$

$$-\tilde{c}_{or} \triangleq \frac{\sum_{l=1}^{k} A_{rl}L_{rl}}{1 + \sum_{l=1}^{k} A_{rl}L_{rl}} - \sum_{l=1}^{k} \frac{A_{rl}L_{rl}}{1 + A_{rl}L_{rl}} \qquad (5.108)$$

$$\tilde{z}(\underline{y}|P_{rl}) = \frac{\tilde{c}_{rl}}{2L_{rl}}.\sum_{j=0}^{P_{rl}-1}\left(\sum_{s=0}^{L_{rl}-1} y(j+sP_{rl})\right)^2$$

$$- \frac{P_{rl}}{2}.\ln(1 + A_{rl}L_{rl}) \qquad (5.109)$$

and

$$\tilde{c}_{rl} \triangleq \frac{A_{rl}L_{rl}}{1 + A_{rl}L_{rl}} \qquad (5.110)$$

The detector first calculates the M conditional quasi log-

likelihood ratios $\tilde{z}(\underline{y}|P_1),\ldots,\tilde{z}(\underline{y}|P_M)$. Then it forms $\binom{M}{k}$ sums of $\tilde{z}(\underline{y}|P_i)$ in groups of k and finally adds the previously calculated terms to the sums to obtain $\tilde{z}(\underline{y}|\underline{s}_r)$. The terms $\tilde{z}(\underline{y}|\underline{s}_1),\ldots,\tilde{z}(\underline{y}|\underline{s}_N)$ are exponentiated and averaged to obtain $\tilde{\ell}(\underline{y})$.

The estimator-detector bases its decisions on $\max_{\underline{s}_r \epsilon S} \tilde{z}(\underline{y}|\underline{s}_r)$. The structure of this detector is not much simpler. In fact it also caculates $N = \binom{M}{k}$ terms and bases its decision on them.

In Sect. 5.3.1 we had seen that basing decisions on $\sum_{k=1}^{N} \tilde{z}(\underline{y}|P_k)$ was essentially equivalent to basing decisions on $\tilde{z}(\underline{y})$. The next detector we try bases its decisions on $\max_{r=1,\ldots,N} \sum_{i=1}^{k} \tilde{z}(\underline{y}|P_{r,i})$. But this is the same as basing the decision on the sum of the k largest $\tilde{z}(\underline{y}|P_i)$, i=1,...,M. This detector has a much simpler structure than the previous two. We call this detector the max-detector. Choosing the k largest $\tilde{z}(\underline{y}|P_i)$ also immediately forms an estimate of the periods of the k PRS's in the signal.

The R.O.C. curves for the quasi-optimum detector, the estimator-detector and the max-detector are given in figs. 5.18, 5.19 & 5.20 respectively. We let M=10, k=2 and $\Omega=\{21,22,\ldots,30\}$. We see that the performance of the max-detector is nearly identical to the performance of the estimator-detector but slightly poorer than the performance of the quasi-optimum detector.

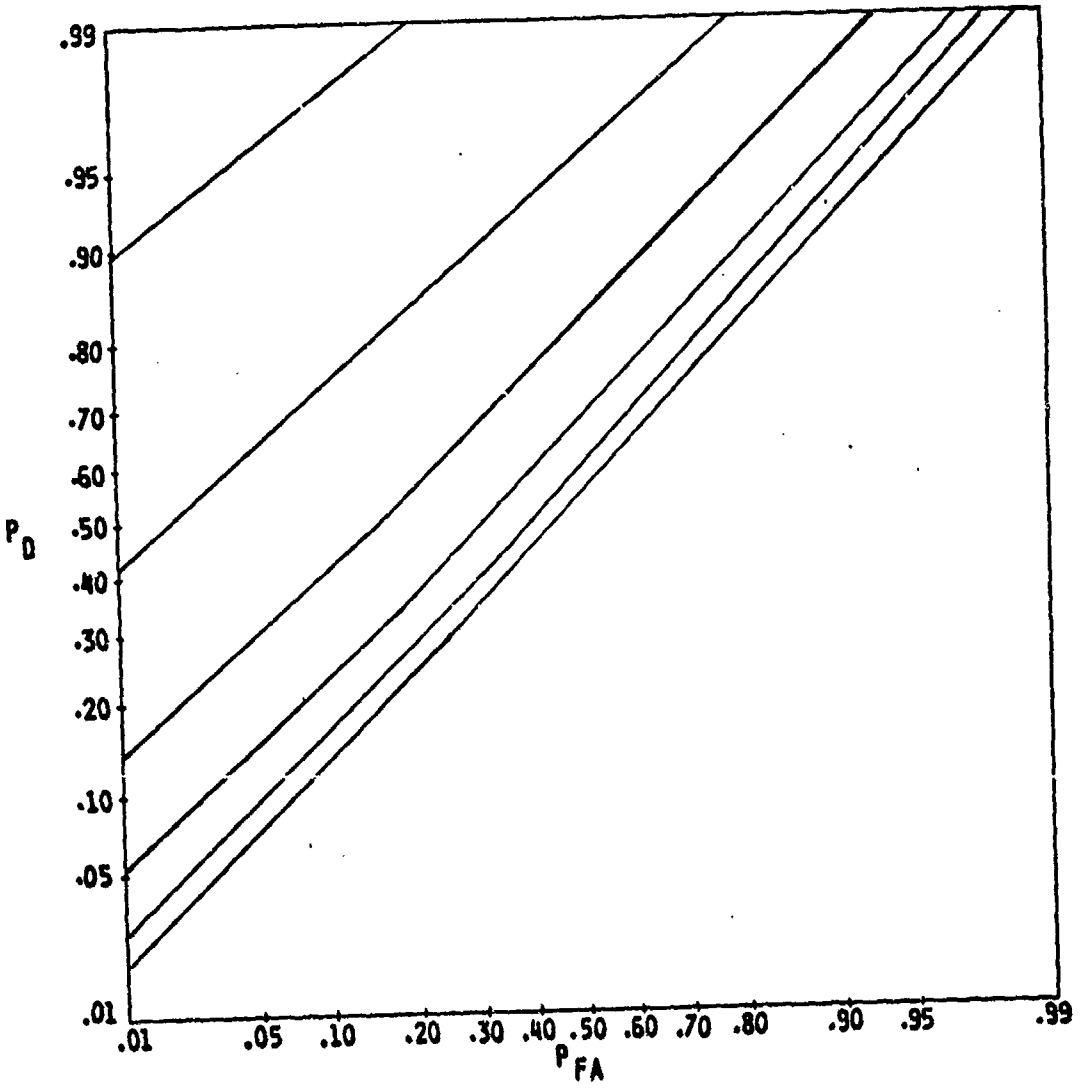

Fig. 5.18 Averaged R.O.C. curves for the quasi optimum detector for M=10 and k=2, each PRS has identical power levels of .001, .002, .004 .008, .016 and .032.

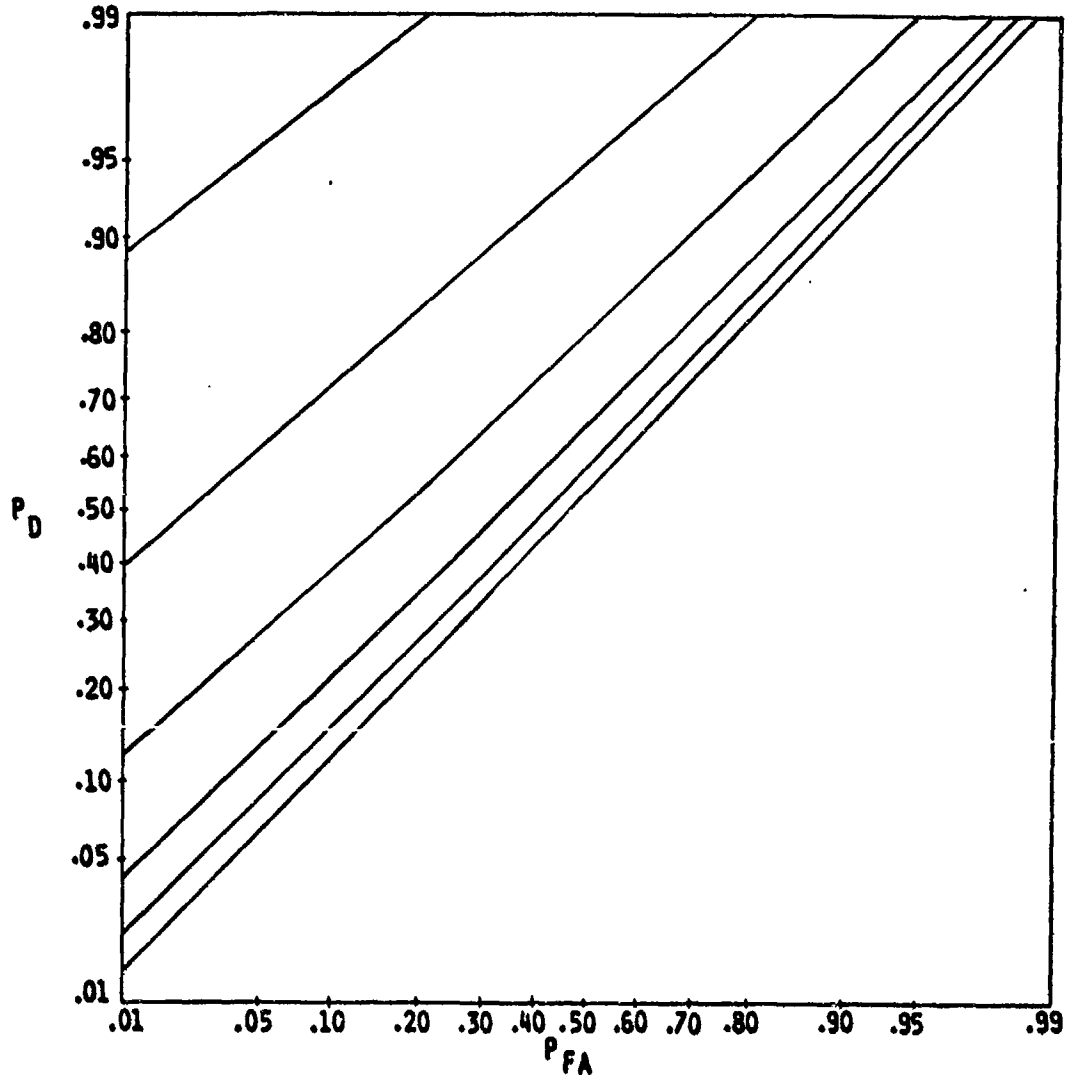

Fig 5.19 Averaged R.O.C. curves for the estimator detector for M=10 and k=2 with the same signal and noise statistics as in fig. 5.18.

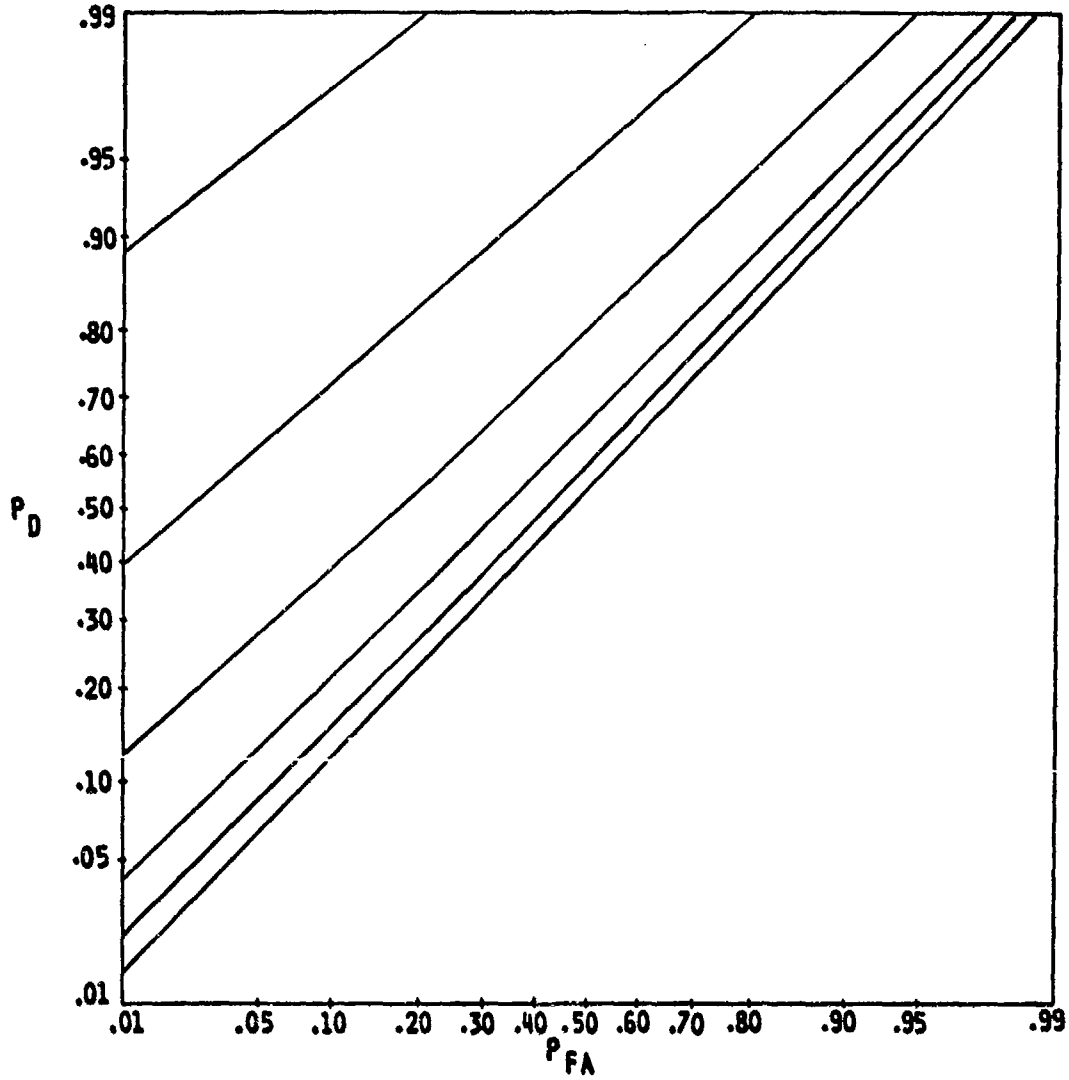

Fig 5.20 Averaged R.O.C. curves for the max detector for M=10 and k=2 with the same signal and noise statistics as in figs. 5.18 & 5.19.

5.3.3 Detection of Arbitrary PRS in non White Gaussian Noise

To complete the discussion on the detection of PRS's, we examine the situation where the signal is complex and successive signal samples are not independent, we also assume that the additive noise is not necessarily white. We assume that the signal is at least wide sense stationary and that its autocorrelation matrix is circulant. Signal and noise are still assumed to be mutually independent. We will derive the equations and give conditions under which they are valid without going in great detail. We assume there are L samples in the observation, where L is some integer multiple of the signal period. Let R_n be the noise autocorrelation matrix and R_s be the signal autocorrelation matrix. The observation statistics under hypotheses H_0 and H_1 are

$$f(\underline{y}|H_0) = (\tfrac{1}{2\pi})^{L/2}.|R_n|^{-1/2}.\exp(-\tfrac{1}{2}\underline{y}^*R_n^{-1}\underline{y}) \qquad (5.111a)$$

$$f(\underline{y}|H_1) = (\tfrac{1}{2\pi})^{L/2}.|R_n+R_s|^{-1/2}.\exp(-\tfrac{1}{2}\underline{y}^*(R_n+R_s)^{-1}\underline{y}) \qquad (5.111b)$$

From the above we may write down the likelihood ratio and the log-likelihood ratio

$$\ell(\underline{y}) = |R_n|^{1/2}.|R_n+R_s|^{-1/2}.\exp(\tfrac{1}{2}\underline{y}^*(R_n^{-1} - (R_n+R_s)^{-1})\underline{y}) \qquad (5.112a)$$

$$z(\underline{y}) = \tfrac{1}{2}.\underline{y}^*(R_n^{-1} - (R_n+R_s)^{-1})\underline{y} - \tfrac{1}{2}\ln\frac{|R_n+R_s|}{|R_n|} \qquad (5.112b)$$

In the above equations we have assumed that the appropriate inverses exist. R_s is circulant due to the signal being periodic. If the noise is white R_n will be the identity matrix and hence trivially circulant and also invertible. If the noise is not white R_n will be circulant if the associated autocorrelation sequence $R_n(k)$ satisfies the

following condition

$$R_n(n) = R_n^*(L-n) \tag{5.113a}$$

or

$$R_n(n) = R_n(L+n) \tag{5.113b}$$

In other words, if the noise is not white we require that the noise and the noise autocorrelation be periodic, and the number of samples in the observation L either be the noise period or some integer multiple of the noise period. With R_n and R_s circulant we have

$$R_n = U_L \Psi_n U_L^* \tag{5.114a}$$

$$R_s = U_L \Psi_s U_L^* \tag{5.114b}$$

$$R_n + R_s = U_L (\Psi_n + \Psi_s) U_L^* \tag{5.114c}$$

$$R_n^{-1} = U_L \Psi_n^{-1} U_L^* \tag{5.114d}$$

$$(R_n + R_s)^{-1} = U_L (\Psi_n + \Psi_s)^{-1} U_L^* \tag{5.114e}$$

where Ψ_n and Ψ_s are diagonal matrices and the diagonal elements are given by $\psi_n(m)$ and $\psi_s(m)$ respectively

$$\psi_n(m) = \sum_{k=0}^{L-1} R_n(k).\exp(-\, j2\pi km/L) \tag{5.115a}$$

$$\psi_s(m) = \sum_{k=0}^{L-1} R_s(k).\exp(-\, j2\pi km/L) \tag{5.115b}$$

Now for R_n^{-1} to exist we require that $\psi_n(m) > 0$ for all m, this means that $R_n(k)$ can not have a period smaller than L. Whenever $\psi_n(m) > 0$ for all m both R_n^{-1} and $(R_n+R_s)^{-1}$ will exist. Substituting for R_n^{-1} and $(R_n+R_s)^{-1}$ in eq. 5.112b we obtain

$$z(\underline{y}) = \tfrac{1}{2}\underline{y}^* U_L(\Psi_n^{-1} - (\Psi_n+\Psi_s)^{-1})U_L^*\underline{y} - \tfrac{1}{2}\ln\frac{|\Psi_n+\Psi_s|}{|\Psi_n|} \qquad (5.116)$$

now

$$\underline{y}^* U_L = L^{-1/2}.(\overline{Y}(0),\overline{Y}(-1),\ldots,\overline{Y}(-L+1)) \qquad (5.117a)$$

where $\overline{Y}$ is the complex conjugate of Y also

$$U_L^*\underline{y} = L^{-1/2}.(Y(0),Y(-1),\ldots,Y(-L+1))^T \qquad (5.117b)$$

Now let $\Psi_n^{-1} - (\Psi_n+\Psi_s)^{-1} \triangleq \theta$, θ is a diagonal matrix and let the diagonal entries be $\theta(m)$ then $z(\underline{y})$ is given by

$$z(\underline{y}) = \frac{1}{2L}\sum_{m=0}^{L-1}\theta(m)|Y(-m)|^2 - \tfrac{1}{2}\ln\frac{|\Psi_n+\Psi_s|}{|\Psi_n|} \qquad (5.118a)$$

$$= \frac{1}{2L}\sum_{m=0}^{L-1}\theta(m)|Y(L-m)|^2 - \tfrac{1}{2}\ln\frac{|\Psi_n+\Psi_s|}{|\Psi_n|} \qquad (5.118b)$$

The above detector may easily be generalized for all the cases discussed in the earlier sections using procedures similar to the ones used earlier. The above analysis holds for white noise if we replace R_n, R_n^{-1}, Ψ_n and Ψ_n^{-1} by the LxL identity matrix.

5.4 The Abstract Problem Revisited

In Sect. 5.1 we had developed the analogy between the exact problem developed in Chapter III and the detection of two independent PRS's $p_1(n)$ and $p_2(n)$ with relatively prime periods P_1 and P_2 respectively and an observation interval of $L=P_1.P_2$ samples. Using this analogy and the results established in Sects. 5.2 & 5.3 we will answer the questions asked at the begining of this chapter and establish some guidelines for the exact problem.

For the two PRS problem we considered two detection philosophies 1) Consider the $L=P_1.P_2$ samples to be independent. 2) Consider the L samples as having been generated from P_1+P_2 independent samples. According to the first philosophy the optimum detector was the energy detector, the second philosophy led to the circular averaging energy detector (frequency selective energy detector) as the optimum detector. The performance of the CAED/FSED was shown to be considerably better than that of the ED (figs. 5.14 & 5.15 and eqs. 5.102 & 5.103). This suggests that the detector for the original problem have M+N degrees of freedom; that is, it should consider the MN peaks in the ambiguity diagram as having been generated from M+N independent sets of doppler and delay parameters. As an example let M=9 and N=7, i.e. we have 9 paths to one receiver and 7 paths to the other receiver. The crosscorrelation of the receptions at the two receivers will have 63 peaks. Treating the 63 peaks as being generated from 16 independent parameter sets rather than as 63 independent entities results in a performance improvement of the order of 12dB (obtained by substituting for L_1 and L_2 in eq. 5.103b).

The near optimum performance of the estimator-detector and the max-detector (figs. 5.18, 5.19 & 5.20) suggests that the estimates of the path parameters (differential doppler and delay) be used to locate the the MN peaks in the

crosscorrelation or the ambiguity diagram. Differential doppler and delay estimation is a topic of on-going research interest and is outside the scope of this thesis.

CHAPTER VI

SUMMARY AND CONCLUSIONS

The object of this thesis was to form guidelines and rules of thumb for an experimenter faced with the problem of detecting a moving acoustic source, where sound is assumed to propagate over a multipath channel. Source signals were received at two remote receivers; the Bivariate Normalized Crosscorrelation (BNC) function (and the associated ambiguity function) of the receptions at the two receivers was used as the observation for the detector. It was assumed that there were M paths to one receiver and N paths to the other receiver and that the observation times were long enough for the path pairs to be resolved.

The exact multipath channel problem is difficult to solve, as was shown in Chapter III, so most researchers asssume that the propagation is by a single path channel. Detectors based on the single path channel model, when the propagation is by multipath, are by definition sub-optimum because they do not utilize all the information available about the source in the receptions. Our approach was novel in the sense that we chose to retain the multipath channel assumption. Based on this we formulated two solvable abstract problems for further study. The abstract problems were chosen to be sufficiently close to reality so that their study would provide useful information about the real problem. This also provided a framework for maximizing the information available to the detector about the source.

In Chapter IV we studied the "Extended M-Orthogonal Signals" problem. This provided us a method for combining

the information, available in the ambiguity plane, for detection purposes. We also showed that it was necessary to localize a quarter to a half of the peaks in the ambiguity plane for acceptable detection performance.

The ambiguity diagram consists of MN peaks due to the signal. The MN peaks are generated by M+N independent sets of doppler and delay parameters. In Chapter V we addressed the question; Should the detector treat the MN peaks as independent entities or as being generated from M+N independent parameter sets? In other words, should the detector have MN degrees of freedom or M+N degrees of freedom? To answer this question we used Periodic Random Sequences (PRS's). It was shown that a detector with M+N degrees of freedom had better detection performance than a detector with MN degrees of freedom. Also the results of Chapter V suggest that the M+N sets of doppler and delay parameters be estimated and the estimates be used to localize the peaks in the ambiguity diagram.

Putting the results of Chapter IV and Chapter V together we can form the following guidelines:

1) Use observation (or integration) times that are long enough so that when the BNC function is formed path pairs can be resolved.

2) Estimate the M+N sets of doppler and delay paramters.

3) Use the estimates to form the differential doppler and differential delay values, and use these values to localize the peaks on the ambiguity diagram.

4) Use the Extended M-Orthogonal Signals technique to combine the peak values in the ambiguity diagram.

Acceptable detection performance is obtained if at least a quarter to a half of the peaks have been correctly localized.

The Extended M-Orthogonal signals formulation is based

on the classical M-Orthogonal signals problem, however it is a new formulation. The theory developed for the detection and estimation of Periodic Random Sequences is based on well known results of detection and estimation theory but this formulation is believed to be new. This has application wherever the signals exhibit periodic or cyclic behavior (engine noise, cyclic codes etc.).

Further work is needed in passive estimation of doppler and delay parameters assuming multipath propagation. This could form the basis for a Doctoral Thesis. Given the estimates of the doppler and delay parameters, localization of the peaks in the ambiguity plane could form the basis for a masters project. To test the validity of the guidelines established in the thesis (and their refinement) experimental work needs to be done.

APPENDICES

APPENDIX A

MONTE CARLO SIMULATION METHODS

The R.O.C. curves and the scatter plots in Chapter V were generated using Monte Carlo simulations. In this Appendix we use the example of one PRS in noise to briefly outline the simulation methods.

Assume that the observation interval is L samples long. Let the PRS period be P_1 and the PRS power level be A_1. For convenience we let $L=L_1P_1$, where L_1 is the number of integer periods of the PRS in the observation. We repeat the equation for $z(\underline{y})$, the detection statistic, in modified form below

$$z(\underline{y}) = K_1 \sum_{j=0}^{P_1-1} \Big(\sum_{k=0}^{L_1-1} y(j+kP_1) \Big)^2 - K_2 \qquad \text{(A1)}$$

K_1 and K_2 are constants that do not depend on the reception and can be pre-calculated.

The probabilities of detection and false alarm were calculated on the basis of 2,000 independent trials under both H_1 and H_0. Let us assume that the vectors $\underline{v}_0$ and $\underline{v}_1$ each contain 2,000 independent outcomes of $z(\underline{y})$ under H_0 and H_1 respectively. Two 25 bin histograms HG_0 and HG_1 were formed using the data from $\underline{v}_0$ and $\underline{v}_1$ respectively. The 25 bins for both the histograms were "uniformly spaced" between min $\underline{v}_1$ and max $\underline{v}_0$. Data points from $\underline{v}_0$ smaller than min $\underline{v}_1$ were put in the first bin of HG_0. Data points from $\underline{v}_1$ larger than max $\underline{v}_0$ were put in the last bin of HG_1. With the 25 bin histograms available it is fairly straightforward to calculate 25 points on the R.O.C. curve.

Now we describe the generation of the vectors $\underline{v}_0$ and $\underline{v}_1$. A uniform random number generator that generated independent variates in the range [0,1) ($U \sim (0,1)$) with a

period of $2^{23}-1$ was available. The Box-Muller method [38] was used to generate zero mean unit variance gaussian ($N\sim(0,1)$) random variates. Given M i.i.d. $U \sim (0,1)$ random variates the Box-Muller method gives a simple and efficient procedure for generating M i.i.d. $N \sim (0,1)$ random variates (where M is even). The elements of $\underline{v}_0$ were generated as follows

Step 1 : Generate L uniform random variates if L is even L+1 if L is odd.

Step 2 : Use the Box-Muller method to get L $N \sim (0,1)$ random variates.

Step 3 : Perform the signal processing indicated in eq. A1 to get an element of $\underline{v}_0$.

Step 4 : Repeat steps 1 through 3 until $\underline{v}_0$ contains 2,000 elements.

The elements of $\underline{v}_1$ were generated as follows:

Step 1 : Generate L uniform random variates if L is even, L+1 if L is odd.

Step 2 : Use the Box-Muller method to get L $N \sim (0,1)$ random variates and store in a vector.

Step 3 : Generate P_1 uniform random variates if P_1 is even, P_1+1 if P_1 is odd.

Step 4 : Use the Box-Muller method to get P_1 $N \sim (0,1)$ random variates.

Step 5 : Multiply the P_1 $N \sim (0,1)$ random variates by $(A_1)^{1/2}$.

Step 6 : Periodically extend the P_1 random variates in Step 5 L_1 times and store in a vector.

Step 7 : Add the vectors of Step 2 and Step 6 element by element.

Step 8 : Perform the signal processing indicated in eq. A1 to get an element of $\underline{v}_1$.

Step 9 : Repeat steps 1 through 8 until $\underline{v}_1$ contains 2,000 elements.

The above procedures give an idea of the simulation methods used for the more complicated problems.

APPENDIX B

DERIVATION OF THE NORMAL DETECTABILITY OF THE FSED

In this appendix an expression for the normal detectability of the FSED (CAED) is derived. We assume that the signal consisists of two PRS's with periods P_1 and P_2. We let the observation be L samples long, where $L=P_1.P_2$. We define $L_k=L/P_k$ to be the number of periods in the obsesrvation of the PRS with period P_k. We further assume that $P_1 \simeq P_2$. The normal detectability is defined as

$$d = \frac{[E_1(z) - E_0(z)]^2}{var(z)} \tag{B1}$$

We will use the variance of z under H_0 in eq. B1. Expresssions for $z(\underline{y})$ for the situation described above are given in eqs. 5.78b, 5.86, 5.94 and 5.95. Using eqs. 5.87, 5.88, 5.89, 5.90 and 5.91 an alternative expression for $z(\underline{y})$ is obtained

$$z(\underline{y}) = (2L)^{-1} \sum_{m=0}^{L-1} \theta(m)|Y(m)|^2 - \frac{1}{2} \ln|\Psi| \tag{B2}$$

The last term in eq. B2 does not affect the value of d and will be carried through as a constant, "K". Y(m) is the L point DFT of the observation

$$H_0 : Y(m) = N(m) \tag{B3a}$$

$$H_1 : Y(m) = N(m) + P_1(m) + P_2(m) \tag{B3b}$$

where N(m), $P_1(m)$ and $P_2(m)$ are the DFT's of the noise, PRS with period P_1 and PRS with period P_2 respectively. $\theta(m)$ is defined as (see eqs. 5.90 and 5.91)

$$\theta(m) = -c_0\delta(m) + c_1 \sum_{r=0}^{P_1-1} \delta(m-rL_1) + c_2 \sum_{r=0}^{P_2-1} \delta(m-rL_2) \qquad (B4)$$

Now

$$E_0(z) = (2L)^{-1} \sum_{m=0}^{L-1} \theta(m) E_0(|Y(m)|^2 - K \qquad (B5)$$

Expanding Y(m) we obtain

$$E_0(|Y(m)|^2) = \sum_{k=0}^{L-1} \sum_{l=0}^{L-1} En(k)n(l).\exp(j2\pi m(l-k)/L) \qquad (B6a)$$

$$= \sum_{k=0}^{L-1} \sum_{l=0}^{L-1} \delta(k-l).\exp(j2\pi m(l-k)/L) \qquad (B6b)$$

$$= L \qquad (B7)$$

So

$$E_0(z) = (2L)^{-1} \sum_{m=0}^{L-1} L.\theta(m) - K \qquad (B8)$$

but

$$\sum_{m=0}^{L-1} \theta(m) = -c_0 + c_1P_1 + c_2P_2 \qquad (B9)$$

it follows that

$$E_0(z) = \frac{1}{2} (-c_0 + c_1P_1 + c_2P_2) - K \qquad (B10)$$

Now we calculate the expectation of $z(\underline{y})$ under H_1.

$$E_1(z) = (2L)^{-1} \sum_{m=0}^{L-1} \theta(m) E_1(|Y(m)|^2) - K \qquad (B11)$$

the expectation within the summation can be written as

$$E_1(|Y(m)|^2) = E(|N(m) + P_1(m) + P_2(m)|^2)$$

$$= E(|N(m)|^2 + |P_1(m)|^2 + |P_2(m)|^2 \qquad (B12)$$

$$+ 2\mathrm{Re}(N(m)P_1^*(m) + N(m)P_2^*(m) + P_1(m)P_2^*(m)))$$

Since the PRS's and noise are mutually independent and zero mean the above reduces to

$$E_1(|Y(m)|^2) = E(|N(m)|^2) + E(|P_1|^2) + E(|P_2(m)|^2) \qquad (B13)$$

We already know $E(|N(m)|^2)$, we only need to find $E(|P_1(m)|^2)$, $E(|P_2(m)|^2)$ will have a similar expression. Now

$$P_1(m) = \sum_{l=0}^{L-1} p_1(l).\exp(-j2\pi lm/L)$$

$$= \sum_{k=0}^{L_1-1} \sum_{s=0}^{P_1-1} \tilde{p}_1(s).\exp(-j2\pi sm/L).\exp(-j2\pi km/L_1) \qquad (B14)$$

where $\tilde{p}_1(s)$ is one period of $p_1(l)$. Eq. B14 simplifies to

$$P_1(m) = L_1 \sum_{s=0}^{P_1-1} \tilde{p}_1(s).\exp(-j2\pi sv/P_1) \qquad (B15)$$

$$m = vL_1 \ , \ v = 0,1,\ldots,P_1-1$$

It follows that

$$|P_1(m)|^2 = L_1^2 \sum_{s=0}^{P_1-1}\sum_{k=0}^{P_1-1} \tilde{p}_1(s)\tilde{p}_1(k).\exp(j2\pi v(k-s)/P_1)$$

$$m = vL_1 \ , \ v = 0,1,\ldots,P_1-1 \qquad (B16)$$

and

$$E|P_1(m)|^2 = L_1^2 \sum_{s=0}^{P_1-1}\sum_{k=0}^{P_1-1} E\tilde{p}_1(s)\tilde{p}_1(k).\exp(j2\pi v(k-s)/P_1)$$

$$= A_1L_1^2 \sum_{s=0}^{P_1-1}\sum_{k=0}^{P_1-1} \delta(k-s).\exp(j2\pi v(k-s)/P_1) \qquad (B17)$$

$$m = vL_1 \ , \ v = 0,1,\ldots,P_1-1$$

The above simplifies to

$$E(|P_1(m)|^2) = A_1L_1^2P_1 \sum_{v=0}^{P_1-1} \delta(m-vL_1) \qquad (B18)$$

similarly we have

$$E(|P_1(m)|^2) = A_2L_2^2P_2 \sum_{v=0}^{P_2-1} \delta(m-vL_2) \qquad (B19)$$

So

$$E(|Y(M)|^2) = L + A_1 L_1^2 P_1 \sum_{v=0}^{P_1-1} \delta(m-vL_1)$$

$$+ A_2 L_2^2 P_2 \sum_{v=0}^{P_2-1} \delta(m-vL_2) \qquad \text{(B20)}$$

Now

$$\sum_{m=0}^{L-1} \theta(m) E_1(|Y(m)|^2) = \sum_{m=0}^{L-1} L\theta(m) + A_1 L_1^2 P_1 \sum_{m=0}^{L-1} \sum_{v=0}^{P_1-1} \theta(m)\delta(m-vL_1)$$

$$+ A_2 L_2^2 P_2 \sum_{m=0}^{L-1} \sum_{v=0}^{P_2-1} \theta(m)\delta(m-vL_2) \qquad \text{(B21)}$$

We will consider each of the terms in eq. B21 separately

$$1) \sum_{m=0}^{L-1} L\theta(m) = L(-c_0 + c_1 P_1 + c_2 P_2) \qquad \text{(B22)}$$

$$2) \; A_1 L_1^2 P_1 \sum_{m=0}^{L-1} \sum_{v=0}^{P_1-1} \theta(m)\delta(m-vL_1)$$

$$= A_1 L_1^2 P_1 \sum_{v=0}^{P_1-1} \theta(vL_1) \qquad \text{(B23)}$$

$$= A_1 L_1^2 P_1 \sum_{v=0}^{P_1-1} (-c_0 \delta(vL_1) + c_1 \sum_{r=0}^{P_1-1} \delta((v-r)L_1)$$

$$+ c_2 \sum_{r=0}^{P_2-1} \delta(vL_1 - rL_2))$$

$$= A_1 L_1^2 P_1 (-c_0 + c_1 P_1 + c_2)$$

Similarly

$$3)\ A_2 L_2^2 P_2 \sum_{m=0}^{L-1} \sum_{v=0}^{P_2-1} \theta(m)\delta(m - vL_2)$$

$$= A_2 L_2^2 (-c_0 + c_1 + c_2 P_2) \qquad \text{(B24)}$$

It follows that

$$E_1(z) = \tfrac{1}{2}.(-c_0 + c_1 P_1 + c_2 P_2) + (2L)^{-1}.A_1 L_1^2 P_1 (-c_0 + c_1 P_1 + c_2)$$

$$+ (2L)^{-1}.A_2 L_2^2 P_2 (-c_0 + c_1 + c_2 P_2) - K$$

$$= \tfrac{1}{2}\ (-c_0 + c_1 P_1 + c_2 P_2 + A_1 L_1 (-c_0 + c_1 P_1 + c_2)$$

$$+ A_2 L_2 (-c_0 + c_1 + c_2 P_2)) - K \qquad \text{(B25)}$$

We can now write an expression for the difference in the expectations of z under H_1 and H_0

$$E_1(z) - E_0(z) = \frac{1}{2}\,(A_1L_1(c_2-c_0) + A_2L_2(c_1-c_0) + c_1A_1L + c_2A_2L) \tag{B26}$$

Now we find the variance of z under H_0

$$\mathrm{var}_0(z) = E_0(z)^2 - (E_0z)^2 \tag{B27}$$

For z^2 we have the following expression

$$z^2 = (2L)^{-2} \sum_{m=0}^{L-1} \sum_{n=0}^{L-1} \theta(m)\theta(n)|Y(m)|^2|Y(n)|^2 - \frac{K}{L} \sum_{m=0}^{L-1} \theta(m)|Y(m)|^2 + K^2 \tag{B28}$$

$E_0(z)^2$ is then given by

$$E_0(z)^2 = (2L)^{-2} \sum_{m=0}^{L-1} \sum_{n=0}^{L-1} \theta(m)\theta(n)E_0|Y(m)|^2|Y(n)|^2 - \frac{K}{L} \sum_{m=0}^{L-1} \theta(m)E_0|Y(m)|^2 + K^2 \tag{B29}$$

and $(E_0z)^2$ is given by

$$(E_0 z)^2 = (2L)^{-2} \left(\sum_{m=0}^{L-1} \theta(m) E_0 |Y(m)|^2\right)^2$$

$$-\frac{K}{L} \sum_{m=0}^{L-1} \theta(m) E_0 |Y(m)|^2 + K^2 \qquad \text{(B30)}$$

So

$$\text{var}_0(z) = (2L)^{-2} \sum_{m=0}^{L-1} \sum_{n=0}^{L-1} \theta(m)\theta(n) E_0 |Y(m)|^2 |Y(n)|^2$$

$$-(2L)^{-2} \left(\sum_{m=0}^{L-1} \theta(m) E_0 |Y(m)|^2\right)^2 \qquad \text{(B31)}$$

The above expression for the variance simplifies to

$$\text{var}_0(z) = \frac{1}{2} \left((-c_0+c_1+c_2)^2 + c_1^2(L_2-1) + c_2^2(L_1-1)\right) \qquad \text{(B32)}$$

Now using the approximations that $A_1=A_2=A/2$, $P_1 \approx P_2$ and $L_1 \approx L_2$ we obtain the desired expression for d

$$d \approx A^2 L(1 + L_1 + L_2)/2 \qquad \text{(B33)}$$

REFERENCES

REFERENCES

1. Y. T. Suh, "Signal Detection in Noises of Unknown Powers Using Two Input Receivers," Ph.D. Dissertation, The University of Michigan, Ann Arbor, Michigan, 1983.

2. G. C. Carter, "Time Delay Estimation for Passive Sonar Signal Processing," IEEE Transactions on Acoustics Speech and Signal Processing, Vol. ASSP-29, No. 3, June 1981.

3. E. Weinstein and D. Kletter, "Delay and Doppler Estimation by Time Space Paritition of the Array Data," IEEE Transactions on Acoustics, Speech and Signal Processing, Vol. ASSP-31, No. 6, December 1983.

4. L. Bjorno, ed., Underwater Acoustics and Signal Processing, D. Reidel Publishing Co., Boston Massachusetts, 1981.

5. W. B. Adams, J. P. Kuhn and W. P. Whyland, "Correlator Compensation Requirements for Passive Time Delay Estimation with Moving Source or Receivers," IEEE Transactions on Acoustics, Speech and Signal Processing, Vol. ASSP-28, No. 2, April 1980.

6. E. K. Al Hussaini and S. A. Kassam, "Robust Eckart Filters for Time Delay Estimation," IEEE Transactions on Acoustics, Speech and Signal Processing, Vol. ASSP-32, No. 5, October 1984.

7. H. L. Van Trees, Detection, Estimation and Modulation Theory, Part III, John Wiley & Sons, New York, 1971.

8. S. S. Wolf and J. L. Gastwirth, "Robust Two Input Correlators," The Journal of the Acoustical Society of

America, Vol. 41, No. 5, 1967.

9. J. B. Thomas, "Nonparametric Detection," Proceedings of the IEEE, Vol. 58, No. 5, May 1970.

10. T. G. Birdsall and F. Khan, "Implications of Multipath Propagation for Two-Frequency Coherance Measurements," The Journal of the Acoustical Society of America, Vol. 78, No. 1, July 1985.

11. W. R. Hahn, "Optimum Signal Processing for Passive Sonar and Range Estimation," The Journal of the Acoustical Society of America, Vol. 58, No. 1, July 1975.

12. T. G. Birdsall and F. Khan, "Notes on Spatial Coherance Measurement," Internal Memo, Cooley Electronics Lab., University of Michigan, Ann Arbor, Michigan.

13. W. W. Peterson, T. G. Birdsall and W. C. Fox, "The Theory of Signal Detectability," IRE Transactions on Information Theory, Vol. 4, No. 2, June 1954

14. W. L. Root, "An Introduction to the Theory of the Detection of Signals in Noise," Proceedings of the IEEE, Vol. 58, No. 5, May 1970.

15. H. L. Van Trees, Detection, Estimation and Modulation Theory, Part I, John Wiley & Sons, New York, 1968.

16. I. Selin, Detection Theory, Princeton University Press, Princeton, 1965.

17. A. D. Whalen, Detection of Signals in Noise, Academic Press, New York, 1971.

18. T. G. Birdsall, The Theory of Signal Detectability: R.O.C. Curves and their Character, Technical Report No. 177, Cooley Electronics Laboratory, The Univertsity of Michigan, Ann Arbor Michigan, 1973.

19. S. L. Adams and J. W. Doubek, "Frequency Coherance and Time Coherance in Random Multipath Channels," The Journal of the Acoustical Society of America, Vol. 62, No. 2, August 1977.

20. H. M. Kwon, Digital Coding for Underwater Acoustic Multipath Channels, Technical Report No. 232, Cooley Electronics Laboratory, The University of Michigan, Ann Arbor Michigan, 1984.

21. P. M. Schultheis and E. Weinstein, "Estimation of Differential Doppler Shifts," The Journal of the Acoustical Society of America, Vol. 66, No. 5, November 1979.

22. W. B. Davenport Jr. and W. L. Root, An Introduction to the Theory of Random Signals and Noise, McGraw Hill, New York, 1958.

23. D. C. Cooper, "The Probability Density Function for the Output of a Correlator with Band Pass Input Waveforms," IEEE Transactions on Information Theory, Vol. IT-17, April 1965.

24. J. L. Brown and H. S. Piper, "Output Characteristic Function for an Analog Cross Correlator with Band Pass Inputs," IEEE Transactions on Information Theory, Vol. IT-13, No. 1, January 1967.

25. L. E. Miller and J. S. Lee, "The Probability Density Function for the Output of an Analog Crosscorrelator,"

IEEE Transactions on Information Theory, Vol. IT-20, No. 4, July 1974.

26. L. C. Andrews and C. S. Brice, "The pdf and cdf for the Sum of N Filtered Outputs of an Analog Cross Correlator with Band Pass Inputs," IEEE Transactions on Information Theory, Vol. IT-29, No. 2, March 1983.

27. L. W. Nolte and D. Jaarsma, "More on the Detection of M Orthogonal Signals," The Journal of the Acoustical Society of America, Vol. 41, No. 2, February 1967.

28. L. W. Nolte and D. Jaarsma, Detectability of Recurrence Phenomenon, Technical Report No. 179, Cooley Electronics Laboratory, The University of Michigan, Ann Arbor Michigan, May 1967.

29. J. Aitchison and J. Brown, The Log Normal Distribution, Cambridge University Press, London 1969.

30. T. G. Birdsall, Signal Detection Theory Lecture Notes, Department of Electrical Engineering and Computer Science, The University of Michigan, Ann Arbor Michigan.

31. E. D. Nering, Linear Algebra and Matrix Theory, 2nd ed., John Wiley & Sons, New York, 1970.

32. R. M. Gray, "On the Asymptotic Eigenvalue Distribution of Toeplitz Matrices," IEEE Transactions on Information Theory, Vol. IT-18, No. 6, November 1972.

33. W. A. Fuller, Introduction to Statistical Time Series, John Wiley & Sons, New York, 1976.

34. S. A. Tretter, Introduction to Discrete Time Signal

Processing," John Wiley & Sons, New York, 1976.

35. M. Abramowitz and I. A. Stegun, Handbook of Mathematical Functions, Dover Publications, New York, 1965.

36. S. M. Kay, "Accurate Frequency Estimation at Low Signal-to-Noise Ratio," IEEE Transactions on Acoustics, Speech and Signal Processing, Vol. ASSP-32, No. 3, June 1984.

37. T. J. Abatzoglou, "A Fast Maximum Likelihood Algorithm for Frequency Estimation of a Sinusoid Based on Newton's Method," IEEE Transactions on Acoustics, Speech and Signal Processing, Vol. ASSP-33, No. 1, February 1985.

38. R. Y. Rubinstein, Simulation and the Monte Carlo Method, John Wiley & Sons, New York, 1981.